

Enhancing Scalability in Bayesian Nonparametric Factor Analysis of Spatiotemporal Data

Yifan Cheng ^{*} and Cheng Li [†]

Department of Statistics and Data Science, National University of Singapore

Abstract

This manuscript puts forward novel practicable spatiotemporal Bayesian factor analysis frameworks computationally feasible for moderate to large data. Our models exhibit significantly enhanced computational scalability and storage efficiency, deliver high overall modeling performances, and possess powerful inferential capabilities for adequately predicting outcomes at future time points or new spatial locations and satisfactorily clustering spatial locations into regions with similar temporal trajectories, a frequently encountered crucial task. We integrate on top of a baseline separable factor model with temporally dependent latent factors and spatially dependent factor loadings under a probit stick breaking process (PSBP) prior a new slice sampling algorithm that permits unknown varying numbers of spatial mixture components across all factors and guarantees them to be non-increasing through the MCMC iterations, thus considerably enhancing model flexibility, efficiency, and scalability. We further introduce a novel spatial latent nearest-neighbor Gaussian process (NNGP) prior and new sequential updating algorithms for the spatially varying latent variables in the PSBP prior, thereby attaining high spatial scalability. The markedly accelerated posterior sampling and spatial prediction as well as the great modeling and inferential performances of our models are substantiated by our simulation experiments.

Contents

1	Introduction	3
2	Bayesian Spatiotemporal Gaussian Factor Model	5
2.1	Spatiotemporal Factor Model and Prior Specification	5
2.2	Spatial Clustering via Probit Stick Breaking Process on Factor Loadings	7
3	Slice Sampling for Bayesian Spatial Clustering	8
4	Spatial Scalability via Nearest-Neighbor Gaussian Process and Sequential Updates	12
4.1	Computational Burdens for a Large Spatial Covariance Matrix	12
4.2	Incorporating the Latent NNGP	13
4.3	Approximating $F(\rho)^{-1}$ and $\det(F(\rho))$	14

^{*}y.cheng@u.nus.edu

[†]stalic@nus.edu.sg

4.4	Sequentially Updating α_{jl_j} 's Under Our Spatial NNGP Prior	15
4.5	Full GP Extension of the Latent NNGP for Spatial Prediction	17
5	Spatial Prediction and Temporal Trends Clustering	18
5.1	Predictions at New Spatial Locations	18
5.2	Summarizing Spatial Clusters with Similar Temporal Trajectories	19
6	Simulation Experiments	20
6.1	Computational Efficiency and Goodness-of-Fit for Main Model Fitting	20
6.2	Efficiency, Accuracy, and Precision for Predictions at New Locations	24
6.3	Accuracy for Spatial Clustering of Temporal Trends	26
7	Discussion	27
A	Gibbs Samplers for Our Spatiotemporal Bayesian Gaussian Factor Models	30
A.1	Full Gibbs Sampling Details for Our Baseline Model in Section 2.1	32
A.2	Full Gibbs Sampling Details for Our Model in Section 2.2	34
A.3	Full Gibbs Sampling Details for Our Model in Section 3	37
B	Temporal Portion Sampling Acceleration for Evenly Dispersed Time Points	42
B.1	Temporal Part Computational Burdens When T is Large	42
B.2	Some Set-Up and Notations	43
B.3	Simple Sparse Closed-Form Representations for $H(\psi)_{T \times T}^{-1}$ and $\text{Rooti}(H)_{T \times T}$	44
B.3.1	When <code>temporal.structure</code> = 'ar1' or 'exponential'	44
B.3.2	When <code>temporal.structure</code> = 'sar1' or 'sexponential'	45
B.3.3	Attained Acceleration Outcomes Pertaining to Sampling $\Upsilon_{k \times k}$ and ψ	48
B.4	Simple Sparse Closed-Form Representations for the T Vectors H_t^+ 's of Length $T - 1$ & Repetitive Closed-Form Solutions for the T Scalars H_t^* 's	48
B.4.1	When <code>temporal.structure</code> = 'ar1' or 'exponential'	48
B.4.2	When <code>temporal.structure</code> = 'sar1' or 'sexponential'	52
B.4.3	Attained Acceleration Outcomes Pertaining to Sampling η_t 's	52
B.5	Proof of Equation (B.1)	53
C	A VAR(1) Process for the Latent Temporal Factors $\eta_{1:T}$	59
C.1	New Gibbs Sampling Steps for Temporal-Related Parameters	59
C.2	Predictions at Desired Future Time Points	61
D	Facilitating Efficient Computation for Spatial PSBP	62
E	Some Notes on Slice Sampling Adapted in Our Context	64
F	Some Further Comments Regarding the Latent NNGP	64
G	More on Predictions at Future Time Points or New Spatial Locations	65
G.1	Predicting $\hat{\mathbf{y}}_{(T+1):(T+q)}$ Given $\mathbf{y}_{1:T}$ and $[X_{(T+1):(T+q)}]_{qO_m \times p}$ (if $p \geq 1$)	65

G.2	Predicting $\hat{\mathbf{y}}(\mathbf{s}_{(m+1):(m+r)})$ Given $\mathbf{y}(\mathbf{s}_{1:m})$ and $X(\mathbf{s}_{(m+1):(m+r)})_{rTO \times p}$ (if $p \geq 1$)	
	Under Our Models in Section 2	66
G.2.1	Under Our Baseline Modeling Framework in Section 2.1	66
G.2.2	Under Our Modeling Framework in Section 2.2	68
H	Scalability Improvements Corresponding to Our 3 Novelties – A Summary of Computational Complexity and Memory	70
H.1	Flexibility, Computation, and Storage Improvements Brought About by Our Slice Sampling Approach in Section 3 with Spatial NNGP & Sequential Updates . . .	71
H.2	Posterior Sampling Computational Acceleration & Storage Alleviation and Faster Spatial Prediction Brought About by Our Spatial NNGP Prior in Section 4 . . .	72
H.3	Posterior Sampling Computational Acceleration Brought About by Our Sequential Updating Methods in Section 4.4 (with spatial NNGP)	73
H.4	An Overall Scalability Improvements Summary for Our Three Novelties	74
I	Extension to Three Non-Gaussian Observed Data Types	75

1 Introduction

One pivotal task frequently occurring in spatiotemporal applications such as infectious disease control and natural disaster prevention involves identifying spatial clusters with similar temporal trajectories and picking out the regions that may require early special attention, which requires modeling the covariance structure with dependence along both the spatial and temporal dimensions. In general, there are several primary goals a spatiotemporal model would want to accomplish regarding the statistical modeling and inference of such data. For one thing, the model should effectively characterize the major sources of variation across both dimensions while retaining spatial and temporal dimension reduction properties and hence overall interpretability to a satisfactory extent, given that one typically observes only a single trajectory of data across both space and time with no independent replicates. Additionally, the model should properly account for spatiotemporal heterogeneity and nonstationarity prevalent in various data types such as imaging data in neurosciences and geosciences, as decently addressing these aspects is crucial for better inferential performances. Furthermore, the model should entail a parsimonious structure that facilitates efficient computation on data with moderate to high spatial and temporal dimensions for practicable implementation, especially when Bayesian inference that usually involves computationally intensive posterior sampling is concerned. Last but not least, the model should possess great capabilities for computationally feasible and performance-wise adequate inferences including out-of-sample predictions at both future time points and new spatial locations as well as spatial clustering of temporal trends.

This work focuses on the Bayesian spatiotemporal latent factor model developed in Berchuck et al. (2022), which achieves the first two goals described above. Factor models can effectively reduce dimension by producing a handful of informative latent factors from a host of raw variables. Although Bayesian spatial factor analysis is not new to the literature, previous works often assumed independent replicates (Christensen and Amemiya (2002), Wall and Liu (2009),

Ren and Banerjee (2013)) and conducted dimension reduction on a large number of observation types at each spatial location. The separable factor model with temporally dependent latent factors and spatially dependent factor loadings introduced by Berchuck et al. (2022), in contrast, effectively reduces dimension both spatially and temporally, thus offering convenient interpretability. This general framework also enables clustering spatial locations into distinct groups, a commonly adopted modeling strategy to further capture spatial heterogeneity that is typically achieved by placing Bayesian mixture priors. Examples of Bayesian mixture priors, which are widely employed in recent Bayesian spatiotemporal literature, include the mixture of finite mixtures (Hu et al. 2023), the Dirichlet process (Mozdzen et al. 2022), the temporal dependent Dirichlet process (De Iorio et al. 2023), and the Indian buffet process (Yang et al. 2022). More spatially structured priors like the random spanning tree prior (Zhang et al. 2023) may also be considered to enhance the spatial contiguity of clusters. In line with these, the model proposed by Berchuck et al. (2022) incorporates clustering across spatial locations via a probit stick breaking process (PSBP) prior (Rodríguez and Dunson 2011) coupled with a spatial latent neighborhood structure from a Gaussian process with exponential correlation, thereby capturing both spatial dependence and heterogeneity.

Despite its capability and flexibility, the Bayesian spatiotemporal factor model in Berchuck et al. (2022) relies on standard Markov chain Monte Carlo (MCMC) algorithms that become prohibitively slow even when the numbers of spatial locations and time points increase to a couple hundred. This elevated computational cost is mainly attributable to the necessity, during each MCMC iteration, to sample and update various elements including the latent temporal trajectories, the factor loadings under the spatial mixture prior, and most importantly, the spatially varying latent variables across all locations linked to a Gaussian process (GP) prior. We identify within the MCMC algorithm and tackle correspondingly in the main text of this paper two principal computational burdens, both of which may arise when the number of spatial locations is large. The first stems mostly from the posterior sampling of mixture labels across all spatial locations under a PSBP prior on the factor loadings, which can incur substantial computational costs and raise intimidating storage concerns when dealing with a large number of spatial mixture components. The second results from the sampling of spatially varying latent variables in the PSBP prior, where the prime challenge lies in the notorious cubic computational complexity related to fitting Gaussian processes.

In the rejoinder to these thorny computational issues and aiming at our desired inferential capabilities, we make three key contributions to this baseline Bayesian spatiotemporal factor model. First, we follow Walker (2007) and develop a new slice sampling algorithm specifically tailored to mixture weights determined by the spatially varying latent variables in the PSBP prior, which ensures the correct conditional posterior distributions and differs from the infinite mixture algorithm presented in Berchuck et al. (2022)’s supplementary material. Under our version of slice sampling, the numbers of spatial mixture components, which do not need to be pre-specified and are permitted to vary across all factors, are ensured non-increasing through the MCMC iterations, thus leading to notably accelerated computation for model fitting and spatial prediction as well as significantly alleviated storage requirements for spatial prediction and clustering. Second, we impose the Nearest-Neighbor Gaussian Process (NNGP) prior (Datta et al. 2016) in place of the full GP prior independently on and further propose novel sequential

updating algorithms for the spatially varying latent variables. Our approach successfully attains high spatial scalability by reducing the corresponding posterior sampling computational complexity from cubic to linear in the number of locations. Under our spatial NNGP prior, the computational speed for making predictions at new locations is markedly increased as well, and storage with respect to the spatial covariance matrix and its inverse can be reduced from quadratic to linear if needed. Third, we devise and implement in our GitHub [repository](#) two critical inferential procedures—outcome predictions at new spatial locations and spatial clustering of temporal trends. We showcase in our simulation experiments the conspicuous spatial prediction computational edge over the baseline framework as well as the satisfactory spatial prediction and clustering performances of the integrated framework with our new posterior sampling scheme and spatial latent prior. It is worth noting that both aforementioned tasks are not currently supported by Berchuck et al. (2022)’s R package `spBFA`, likely due to the prohibitive storage requirements that ensue under the baseline model when the numbers of spatial mixture components and location points are large, as conducting each of the two inferential procedures needs posterior samples of either the spatially varying latent variables or the resultant mixture weights across all locations. Consequently, our improved algorithm manifests considerably superior scalability for MCMC-based posterior sampling as well as subsequent vital inferential tasks on datasets with a few hundred spatial locations and time points. Detailed scalability summaries for our novel approaches is presented in Appendix H.

The rest of this paper is organized as follows. Section 2 depicts our baseline Bayesian spatiotemporal latent factor model with prior specification. Section 3 deduces the complete data likelihood with the introduced cluster numbers and latent uniform variables for our novel slice sampling algorithm and delineates detailed new posterior sampling steps for the involved spatial clustering parameters. Section 4 derives our novel spatial latent NNGP prior and sequential updating schemes and provides theoretical justifications for the resulting great computational acceleration and high spatial scalability. Section 5 elaborates on spatial prediction and temporal trends clustering. Section 6 presents extensive simulation experiments to demonstrate the remarkably accelerated computation under and appealing comprehensive performances of our introduced new approaches regarding main model fitting and certain crucial inferential procedures. Section 7 concludes with a summary of our achievements and pointers towards potential future work. Finally, the Appendices detail full posterior sampling steps for our models, pinpoint and offer powerful acceleration solutions on equispaced time points to temporal portion computational burdens in the original MCMC algorithm, integrate a more complicated temporal structure process into our modeling frameworks, give indispensable methodology, justification, notes, comments, procedures, and summaries complementary to Sections 2 to 5, and present model extensions to accommodate some non-normal observations.

2 Bayesian Spatiotemporal Gaussian Factor Model

2.1 Spatiotemporal Factor Model and Prior Specification

We first describe the basic latent factor model for spatiotemporal data used in Berchuck et al. (2022). For a generic outcome $y_t(\mathbf{s}_{i,o})$ of type o ($o = 1, \dots, O$) observed at time t ($t = 1, \dots, T$)

and spatial location i ($i = 1, \dots, m$), we assume the separable latent factor model

$$y_t(\mathbf{s}_{i,o}) = \mathbf{x}_t(\mathbf{s}_{i,o})^\top \boldsymbol{\beta} + \sum_{j=1}^k \lambda_j(\mathbf{s}_{i,o}) \eta_{tj} + \epsilon_t(\mathbf{s}_{i,o}), \quad (2.1)$$

where $\mathbf{x}_t(\mathbf{s}_{i,o}) \in \mathbb{R}^p$ is the spatiotemporal covariate vector, $\boldsymbol{\beta} \in \mathbb{R}^p$ is the vector of coefficients, η_{tj} 's are the latent temporal factors, $\lambda_j(\mathbf{s}_{i,o})$'s are the spatial-specific factor loadings, and $\epsilon_t(\mathbf{s}_{i,o})$ is the error term. Consider the stacked quantities $\mathbf{y}_t = (y_t(\mathbf{s}_{1,1}), \dots, y_t(\mathbf{s}_{m,1}), \dots, y_t(\mathbf{s}_{1,O}), \dots, y_t(\mathbf{s}_{m,O}))^\top \in \mathbb{R}^{mO \times 1}$, $\mathbf{X}_t = (\mathbf{x}_t(\mathbf{s}_{1,1}), \dots, \mathbf{x}_t(\mathbf{s}_{m,1}), \dots, \mathbf{x}_t(\mathbf{s}_{1,O}), \dots, \mathbf{x}_t(\mathbf{s}_{m,O}))^\top \in \mathbb{R}^{mO \times p}$, $\Lambda = (\boldsymbol{\lambda}_1, \dots, \boldsymbol{\lambda}_k) \in \mathbb{R}^{mO \times k}$ with $\boldsymbol{\lambda}_j = (\lambda_j(\mathbf{s}_{1,1}), \dots, \lambda_j(\mathbf{s}_{m,1}), \dots, \lambda_j(\mathbf{s}_{1,O}), \dots, \lambda_j(\mathbf{s}_{m,O}))^\top \in \mathbb{R}^{mO \times 1}$, $\boldsymbol{\eta}_t = (\eta_{t1}, \dots, \eta_{tk})^\top \in \mathbb{R}^{k \times 1}$, and $\boldsymbol{\epsilon}_t = (\epsilon_t(\mathbf{s}_{1,1}), \dots, \epsilon_t(\mathbf{s}_{m,O}))^\top \in \mathbb{R}^{mO \times 1}$. Then (2.1) is equivalent to the matrix-form model specification

$$\mathbf{y}_t = \mathbf{X}_t \boldsymbol{\beta} + \Lambda \boldsymbol{\eta}_t + \boldsymbol{\epsilon}_t, \quad \text{for } t = 1, \dots, T. \quad (2.2)$$

We assume that the error vector is distributed as $\boldsymbol{\epsilon}_t \sim N_{mO}(\mathbf{0}, \Xi)$ independently across time $t = 1, \dots, T$, where $\Xi = \text{Diag}(\sigma^2(\mathbf{s}_{1,1}), \dots, \sigma^2(\mathbf{s}_{m,1}), \dots, \sigma^2(\mathbf{s}_{1,O}), \dots, \sigma^2(\mathbf{s}_{m,O}))$.

Concentrating on Bayesian inference, we now delineate the prior specification for this spatiotemporal latent factor model. Each error variance $\sigma^2(\mathbf{s}_{i,o})$ is assigned independent inverse gamma prior $\mathcal{IG}(a, b)$, and the coefficient vector $\boldsymbol{\beta}_{p \times 1}$ is imposed a standard conjugate normal prior $N_p(\boldsymbol{\mu}_{0\boldsymbol{\beta}}, \Sigma_{0\boldsymbol{\beta}})$ in the presence of covariates $\mathbf{x}_t(\mathbf{s}_{i,o})$'s. For the temporal latent factors $\boldsymbol{\eta}_t$'s, we consider in the main text a general Kronecker-type covariance structure on the prior $\boldsymbol{\eta} \sim N_{Tk}(\mathbf{0}, H(\psi)_{T \times T} \otimes \Upsilon)$, where $\boldsymbol{\eta} = (\boldsymbol{\eta}_1^\top, \dots, \boldsymbol{\eta}_T^\top)^\top \in \mathbb{R}^{T \times k}$, $H(\psi) \in \mathbb{R}^{T \times T}$ captures the temporal correlation structure on $\boldsymbol{\eta}_1, \dots, \boldsymbol{\eta}_T$ with tuning parameter ψ , and $\Upsilon \in \mathbb{R}^{k \times k}$ describes the covariance between the k latent components. Examples of $H(\psi)$ are the AR(1) process $[H(\psi)]_{tt'} = \psi^{|v_t - v_{t'}|}$ and the Gaussian process with exponential covariance function $[H(\psi)]_{tt'} = \exp\{-\psi|v_t - v_{t'}|\}$ for $t, t' \in \{1, \dots, T\}$, where v_t denotes the time point indexed by t and permits irregularly spaced time points. We also consider the seasonal counterparts of AR(1) and Gaussian processes with an arbitrary temporal seasonal period $d \in \mathbb{N}, d \geq 1$ for modeling the latent process $\{\boldsymbol{\eta}_t\}_{t=1}^T$. The tuning parameter ψ is given a uniform prior on a bounded interval, which lacks conjugacy and requires a Metropolis step in posterior sampling. The covariance matrix $\Upsilon_{k \times k}$ is assumed to be unstructured and assigned a conjugate inverse Wishart prior $\Upsilon \sim \mathcal{IW}(\zeta, \Omega)$. When all time points are equally spaced, a frequently encountered scenario in numerous practical applications, we can considerably accelerate the Gibbs sampling steps for temporal-related parameters $\boldsymbol{\eta}_t$'s, $\Upsilon_{k \times k}$, and ψ (to be elaborated in Appendix B) and adopt a more complicated VAR(1) model for $\{\boldsymbol{\eta}_t\}_{t=1}^T$ (see Appendix C). To encode spatial dependency information, our baseline model directly imposes a spatially correlated Gaussian process on the columns $\{\boldsymbol{\lambda}_j\}_{j=1}^k$ of the factor loadings matrix Λ , i.e., assign a normal prior with Kronecker-type covariance structure $\boldsymbol{\lambda}_j \stackrel{\text{iid}}{\sim} N_{Om}(\mathbf{0}, \kappa_{O \times O} \otimes F(\rho)_{m \times m})$ for $j \in \{1, \dots, k\}$. $\kappa \in \mathbb{R}^{O \times O}$ depicts the covariance between the O observation types and is imposed an $\mathcal{IW}(\nu, \Theta)$ prior. For a continuous spatial domain, $F(\rho)$ denotes the covariance matrix from a Gaussian process over the m spatial locations with an exponential covariance function tuning parameter ρ that can be further assigned a uniform prior. Following Berchuck et al. (2022), we can obtain the posterior distribution of all parameters under this baseline model from a Gibbs sampler.

2.2 Spatial Clustering via Probit Stick Breaking Process on Factor Loadings

To further integrate spatial clustering capabilities on top of our baseline model in Section 2.1, we opt to fully specify the factor loadings matrix $\Lambda_{mO \times k}$ so that a spatial structure can be directly imposed on the columns $\{\boldsymbol{\lambda}_j\}_{j=1}^k$ of Λ . More precisely, we assume that the factor loadings come from a spatial mixture model, under which spatially close locations share similar factor loadings. Since the Dirichlet Process (DP) is the workhorse of Bayesian nonparametric clustering, we follow Berchuck et al. (2022) and adapt the Probit Stick Breaking Process (PSBP) (Rodríguez and Dunson 2011), an extension of the stick breaking construction of the DP (Sethuraman 1994), to introduce dependency in the spatial setting.

For any given (j, i, o) , we let the latent mixture distribution $G_j^{i,o}$ follow the PSBP $((G_j^{i,o})_0, \boldsymbol{\alpha}_j^{i,o})$ process with base measure $(G_j^{i,o})_0$ and concentration parameter vector $\boldsymbol{\alpha}_j^{i,o}$, if

$$G_j^{i,o} = \sum_{l=1}^{\infty} w_{jl}(\mathbf{s}_{i,o}) \delta_{\theta_{jl}}, \text{ where}$$

$$\theta_{jl} \stackrel{\text{iid}}{\sim} (G_j^{i,o})_0, \text{ and } w_{jl}(\mathbf{s}_{i,o}) = \Phi(\alpha_{jl}(\mathbf{s}_{i,o})) \prod_{r=1}^{l-1} [1 - \Phi(\alpha_{jr}(\mathbf{s}_{i,o}))], \text{ for } l \in \mathbb{N}. \quad (2.3)$$

The above construction is indeed adequate since $\sum_{l=1}^{\infty} w_{jl}(\mathbf{s}_{i,o}) = 1$ almost surely for all (j, i, o) (Rodríguez and Dunson 2011). We can often truncate the infinite sequence at a large number of terms to obtain a finite mixture for practical implementation of posterior sampling. To make computation feasible, we consider this finite-mixture version of Equation (2.3). Let a pre-specified fixed $L \in \mathbb{N}$, $1 < L < \infty$ be the number of clusters for all factor $j \in \{1, \dots, k\}$ and let $w_{jL}(\mathbf{s}_{i,o}) = \prod_{r=1}^{L-1} [1 - \Phi(\alpha_{jr}(\mathbf{s}_{i,o}))]$ be the last mixture weight for all (j, i, o) in Equation (2.3). We then impose the PSBP in (2.3) on $\boldsymbol{\lambda}_j$'s independently across all (j, i, o) ,

$$\lambda_j(\mathbf{s}_{i,o}) = \theta_{j\xi_j(\mathbf{s}_{i,o})} \mid G_j^{i,o} \sim G_j^{i,o}, \text{ where } \xi_j(\mathbf{s}_{i,o}) \sim \text{Multinomial}(w_{j1}(\mathbf{s}_{i,o}), \dots, w_{jL}(\mathbf{s}_{i,o}))$$

such that $\mathbb{P}(\xi_j(\mathbf{s}_{i,o}) = l) = w_{jl}(\mathbf{s}_{i,o})$, for any $l = 1, \dots, L$. (2.4)

With the PSBP model delineated in (2.3) and (2.4), spatial neighborhood proximity can now be incorporated into the columns $\boldsymbol{\lambda}_j, j \in \{1, \dots, k\}$ of the factor loadings matrix $\Lambda_{mO \times k}$ by jointly modeling the latent variables $\boldsymbol{\alpha}_{jl}$'s, ordered first by observation type o and then by spatial index i , that dictate the weights w_{jl} 's. Independently across all (j, l) , we assign the prior

$$\boldsymbol{\alpha}_{jl} = (\boldsymbol{\alpha}_{jl}(\mathbf{s}_1)^{\text{T}}, \dots, \boldsymbol{\alpha}_{jl}(\mathbf{s}_m)^{\text{T}})^{\text{T}} \sim N_{mO}(\mathbf{0}, F(\rho)_{m \times m} \otimes \kappa_{O \times O}), \quad (2.5)$$

for $j = 1, \dots, k$ and $l = 1, \dots, L - 1$. In Equation (2.5), the covariance structure of $\boldsymbol{\alpha}_{jl}$'s is modeled as the Kronecker product of two matrices. Specifically, the matrix $F(\rho)$ stems from a spatial Gaussian process with an exponential covariance function parameterized by ρ , a length-scale parameter specifying the level of spatial correlation. ρ is assigned a uniform prior and requires Metropolis moves in posterior sampling. The other covariance matrix $\kappa_{O \times O}$ describes the covariance across the O observation types and is left fully unstructured, with a standard conjugate $\mathcal{IW}(\nu, \Theta)$ prior imposed. Although directly proceeding with $\boldsymbol{\alpha}_{jl}$'s posterior sampling is computationally burdensome, we can successfully tackle this issue by introducing latent normal variables $z_{jl}(\mathbf{s}_{i,o})$'s to bring about conjugacy for $\boldsymbol{\alpha}_{jl}$'s (see Appendix D).

Finally, for the atoms θ_{jl} 's in Equation (2.4), we follow Bhattacharya and Dunson (2011) to assign a multiplicative gamma process shrinkage prior

$$\begin{aligned} \theta_{jl} &\stackrel{\text{ind}}{\sim} N(0, \tau_j^{-1}), \text{ where} \\ \tau_j &= \prod_{h=1}^j \delta_h \text{ with } \delta_1 \sim \text{Gamma}(a_1, 1) \text{ and } \delta_h \sim \text{Gamma}(a_2, 1), \text{ for all } h \geq 2. \end{aligned} \quad (2.6)$$

Since the precision τ_j tends to increase over the column index j if $a_2 > 1$, we can specify a k larger than the number of supposed factors and count on this shrinkage prior to adaptively retain only the meaningful factors.

3 Slice Sampling for Bayesian Spatial Clustering

To derive a computationally feasible posterior sampling algorithm for the model (2.1) with the spatial PSBP prior depicted in Section 2.2, Berchuck et al. (2022) adopted a finite-mixture version of (2.3) with a same number of spatial mixture components $L \in \mathbb{N}$, $L > 1$ for all factors. Despite implementation conveniences, several notable issues persist regarding this approach. For one thing, pre-specifying a fixed common L is likely restrictive since the numbers of spatial mixtures are unknown and may well differ across the k latent factors. Moreover, an at least moderately large L would typically be required to guarantee satisfactory model fitting. This leads to computational inefficiency since we need to sample more spatial clustering parameters θ_{jl} 's, α_{jl} 's in each MCMC iteration and perform more complicated calculations when updating $\xi_j(\mathbf{s}_{i,o})$'s, δ_h 's, κ , and ρ . Most importantly, when both L and the number of spatial locations m are large, storage requirements for either spatial prediction at new locations or clustering of temporal trends can become highly prohibitive, as one needs to store posterior samples of θ_{jl} 's, α_{jl} 's, and \mathbf{w}_{jl} 's from all kept post-burn-in MCMC iterations. Last but not least, posterior sampling of the introduced latent variables $z_{jl}(\mathbf{s}_{i,o})$'s (Appendix D), which grows computationally demanding for a large L , is required when a common fixed L is assumed.

These concerns can be effectively addressed by assuming a varying number of clusters L_j for the j^{th} latent factor loadings λ_j and adapting pertinent slice sampling ideas in Walker (2007). Our novel algorithm follows the original version of slice sampling (Walker 2007) and essentially differs from Berchuck et al. (2022)'s flawed implementation in their supplementary material and R package `spBFA` (see Appendix E). Since we do have a spatial cluster number upper bound mO , it would indeed be reasonable to introduce unknown cluster number parameters $L_j \in \mathbb{N} \setminus \{0\}$ for all latent factors $j = 1, \dots, k$ and proceed with the corresponding finite mixture models. We opt not to adopt independent infinite mixture models specified by Equation (2.3) for all (j, i, o) , which might appear theoretically more adequate, primarily to guarantee non-increasing L_j estimates through the MCMC iterations, thus facilitating computation and easing storage requirements (Appendix H.1). We shall discuss more details in Appendix E.

Let us fix an arbitrary pair $(i, o) \in \{1, \dots, m\} \times \{1, \dots, O\}$. Consider our spatial PSBP prior (Section 2.2) under the finite-mixture version of (2.3) with L_j mixture components for the j^{th} latent factor loadings. For $t = 1, \dots, T$, the observation $y_t(\mathbf{s}_{i,o})$ has density

$$f_{\Theta}(y_t(\mathbf{s}_{i,o})) \quad (3.1)$$

$$= \sum_{l_1=1}^{L_1} \dots \sum_{l_k=1}^{L_k} \left\{ \left[\prod_{j=1}^k w_{jl_j}(\mathbf{s}_{i,o}) \right] \times f(y_t(\mathbf{s}_{i,o}) \mid \boldsymbol{\beta}, \boldsymbol{\eta}_t, \sigma^2(\mathbf{s}_{i,o}), \theta_{jl_j} \text{ for all } j = 1, \dots, k) \right\},$$

where Θ denotes the set of all parameters in our model including the newly introduced L_j 's but excluding the to-be-introduced $u_j(\mathbf{s}_{i,o})$'s. To incorporate slice sampling (Walker 2007), we further introduce latent variables $u_j(\mathbf{s}_{i,o})$, $j \in \{1, \dots, k\}$, such that

$$\begin{aligned} & f_{\Theta}(y_t(\mathbf{s}_{i,o}), u_{1:k}(\mathbf{s}_{i,o})) \\ &= \sum_{l_1=1}^{L_1} \dots \sum_{l_k=1}^{L_k} \left\{ \left[\prod_{j=1}^k \mathbb{1}_{\{u_j(\mathbf{s}_{i,o}) < w_{jl_j}(\mathbf{s}_{i,o})\}} \right] \times f(y_t(\mathbf{s}_{i,o}) \mid \boldsymbol{\beta}, \boldsymbol{\eta}_t, \sigma^2(\mathbf{s}_{i,o}), \theta_{1l_1}, \dots, \theta_{kl_k}) \right\}, \end{aligned} \quad (3.2)$$

where $\mathbb{1}_E$ denotes the indicator function of an event E . It is clear that integrating over $u_j(\mathbf{s}_{i,o})$'s in (3.2) with respect to the Lebesgue measure on the measurable space $((0, 1]^k, \mathcal{B}((0, 1]^k))$ yields (3.1). Hence, the joint density in Equation (3.2) with the corresponding marginal density in Equation (3.1) indeed exists. As $\{y_t(\mathbf{s}_{i,o}), (i, o, t) \in \{1, \dots, m\} \times \{1, \dots, O\} \times \{1, \dots, T\}\}$ constitutes our observed data, the complete data likelihood is now

$$\begin{aligned} \ell_{\text{complete}} &= \prod_{o=1}^O \prod_{i=1}^m \prod_{t=1}^T \left[\prod_{j=1}^k \mathbb{1}_{\{u_j(\mathbf{s}_{i,o}) < w_{j\xi_j(\mathbf{s}_{i,o})}(\mathbf{s}_{i,o})\}} \right] \\ &\quad \times f\left(y_t(\mathbf{s}_{i,o}) \mid \boldsymbol{\beta}, \boldsymbol{\eta}_t, \sigma^2(\mathbf{s}_{i,o}), \xi_j(\mathbf{s}_{i,o}), \theta_{j\xi_j(\mathbf{s}_{i,o})} \text{ for all } j = 1, \dots, k\right), \end{aligned} \quad (3.3)$$

where for any $(i, o, j) \in \{1, \dots, m\} \times \{1, \dots, O\} \times \{1, \dots, k\}$ and $l_j \in \{1, \dots, L_j\}$,

$$w_{jl_j}(\mathbf{s}_{i,o}) = \begin{cases} \Phi(\alpha_{jl_j}(\mathbf{s}_{i,o})) \prod_{r_j < l_j} [1 - \Phi(\alpha_{jr_j}(\mathbf{s}_{i,o}))], & \text{if } l_j \in \{1, \dots, L_j - 1\} \\ \prod_{r_j < L_j} [1 - \Phi(\alpha_{jr_j}(\mathbf{s}_{i,o}))], & \text{if } l_j = L_j \end{cases}. \quad (3.4)$$

Under this model specification, we no longer need to introduce and sample the latent normal parameters $z_{jl}(\mathbf{s}_{i,o})$'s (Section 2.2) from their full conditional distributions (Equation (D.4) in Appendix D), which requires a total of $O(kLmO)$ flops per MCMC iteration and is thus computationally inefficient for a large L . Instead, we are only required to sample the latent uniform $u_j(\mathbf{s}_{i,o})$'s from their full conditional distributions, which turns out to be rather simple. For any $(i, o, j) \in \{1, \dots, m\} \times \{1, \dots, O\} \times \{1, \dots, k\}$, the full conditional density of $u_j(\mathbf{s}_{i,o})$ is

$$f(u_j(\mathbf{s}_{i,o}) \mid \cdot) \propto \mathbb{1}_{\{u_j(\mathbf{s}_{i,o}) < w_{j\xi_j(\mathbf{s}_{i,o})}(\mathbf{s}_{i,o})\}} \sim \text{Unif}\left(0, w_{j\xi_j(\mathbf{s}_{i,o})}(\mathbf{s}_{i,o})\right). \quad (3.5)$$

The corresponding computational complexity per MCMC iteration is reduced to $O(kmO)$. We now delineate in the following the full conditional distributions and Gibbs sampling steps for other spatial clustering parameters.

The pivotal role played by the introduced parameters L_j 's and $u_j(\mathbf{s}_{i,o})$'s is reflected in the step updating L_j 's and sampling cluster labels $\xi_j(\mathbf{s}_{i,o})$'s from their full conditional distributions. Fix any arbitrary $j \in \{1, \dots, k\}$. For all $l_j \in \{1, \dots, L_j^{\text{old}}\}$ and for any (i, o) ,

$$\begin{aligned} \mathbb{P}(\xi_j(\mathbf{s}_{i,o}) = l_j \mid \cdot) &\propto \mathbb{1}_{\{w_{jl_j}(\mathbf{s}_{i,o}) > u_j(\mathbf{s}_{i,o})\}} \\ &\quad \times \prod_{t=1}^T f\left(y_t(\mathbf{s}_{i,o}) \mid \boldsymbol{\beta}, \boldsymbol{\eta}_t, \sigma^2(\mathbf{s}_{i,o}), \xi_j(\mathbf{s}_{i,o}) = l_j, \boldsymbol{\xi}_{-j}(\mathbf{s}_{i,o}), \boldsymbol{\theta}_{\boldsymbol{\xi}(\mathbf{s}_{i,o})}\right), \end{aligned} \quad (3.6)$$

where for any (i, o, j, l_j) such that $w_{jl_j}(\mathbf{s}_{i,o}) > u_j(\mathbf{s}_{i,o})$, for all $t \in \{1, \dots, T\}$,

$$\begin{aligned} & f\left(y_t(\mathbf{s}_{i,o}) \mid \boldsymbol{\beta}, \boldsymbol{\eta}_t, \sigma^2(\mathbf{s}_{i,o}), \xi_j(\mathbf{s}_{i,o}) = l_j, \boldsymbol{\xi}_{-j}(\mathbf{s}_{i,o}), \boldsymbol{\theta}_{\boldsymbol{\xi}(\mathbf{s}_{i,o})}\right) \\ &= (2\pi)^{-\frac{1}{2}} \sigma^{-1}(\mathbf{s}_{i,o}) \exp \left\{ -\frac{1}{2} \sigma^{-2}(\mathbf{s}_{i,o}) \left[y_t(\mathbf{s}_{i,o}) - \mathbf{x}_t(\mathbf{s}_{i,o})^\top \boldsymbol{\beta} - \sum_{h \neq j} \theta_{h\xi_h(\mathbf{s}_{i,o})} \eta_{th} - \theta_{jl_j} \eta_{tj} \right]^2 \right\}. \end{aligned}$$

For any $(i, o) \in \{1, \dots, m\} \times \{1, \dots, O\}$, we let

$$\begin{aligned} L_j^{i,o} &= \text{the smallest positive integer such that } \sum_{l_j=1}^{L_j^{i,o}} w_{jl_j}(\mathbf{s}_{i,o}) > 1 - u_j(\mathbf{s}_{i,o}) \\ \text{and } L_j^{\text{new}} &= \max \left\{ L_j^{i,o} : i = 1, \dots, m, o = 1, \dots, O \right\}. \end{aligned} \quad (3.7)$$

Then it is clear from Equation (3.6) that $\mathbb{P}(\xi_j(\mathbf{s}_{i,o}) = l_j \mid \cdot) = 0$ for any $l_j > L_j^{\text{new}}$. Hence, we can update the parameter estimate for $L_j \in \mathbb{N} \setminus \{0\}$ from L_j^{old} to $L_j^{\text{new}} \leq L_j^{\text{old}} < \infty$ in this MCMC iteration and only consider $l_j \in \{1, \dots, L_j^{\text{new}}\}$ to be the possible values for $\xi_j(\mathbf{s}_{i,o})$ for all (i, o) . After obtaining $\{L_j^{\text{new}} : j = 1, \dots, k\}$ by Equation (3.7) at the start of this Gibbs sampler step, we immediately update estimates for $\boldsymbol{\alpha}_{jl_j}$'s by only keeping the $mO \times 1$ vectors corresponding to $l_j \in \{1, 2, \dots, L_j^{\text{new}} - 1\}$ and discarding the ones corresponding to $l_j \in \{L_j^{\text{new}}, L_j^{\text{new}} + 1, \dots, L_j^{\text{old}} - 1\}$. We then formulate our new weights w_{jl_j} for $l_j = 1, \dots, L_j^{\text{new}}$ (as specified by Equation (3.4)) by discarding the previous w_{jl_j} estimates with $l_j \in \{L_j^{\text{new}} + 1, \dots, L_j^{\text{old}}\}$ and adjusting the $w_{jL_j^{\text{new}}}(\mathbf{s}_{i,o})$ estimates if L_j^{new} is strictly less than L_j^{old} . New cluster labels $\xi_j(\mathbf{s}_{i,o})$'s can then be sampled according to Equation (3.6) based on these new weights. Among all kept weights parameters, only the $w_{jL_j^{\text{new}}}(\mathbf{s}_{i,o})$ estimates are possibly altered (increased) in this step. Since all updated weights are ensured greater than or equal to their old values, it is indeed guaranteed that $\xi_j(\mathbf{s}_{i,o})^{\text{old}}$ is still in the support for $\xi_j(\mathbf{s}_{i,o})^{\text{new}}$ and $u_j(\mathbf{s}_{i,o}) < w_{j\xi_j^{\text{new}}}(\mathbf{s}_{i,o})(\mathbf{s}_{i,o})$ for all (j, i, o) .

Thanks to this ensured non-increasing property of posterior samples for L_j 's through the MCMC iterations, it is highly likely that we need to sample much fewer posterior parameter estimates for θ_{jl_j} 's and $\boldsymbol{\alpha}_{jl_j}$'s from their full conditional distributions given below. Hence, the computational and storage burdens with respect to θ_{jl_j} 's $\boldsymbol{\alpha}_{jl_j}$'s, and w_{jl_j} 's mentioned at the start of this section no longer exist. Spatial prediction can also be considerably accelerated, as we shall see in Appendix G.2.2, Sections 5.1 and 6.2. See Appendix H.1 for more details.

Fix any arbitrary $j \in \{1, \dots, k\}$ and $l_j \in \{1, \dots, L_j\}$. Let $\pi(\cdot \mid \tau_j)$ be the density of $N(0, \tau_j^{-1})$ in the shrinkage prior given by Equation (2.6). Then the conditional posterior of θ_{jl_j} is

$$f(\theta_{jl_j} \mid \cdot) \propto \pi(\theta_{jl_j} \mid \tau_j) \times \prod_{(i,o):\xi_j(\mathbf{s}_{i,o})=l_j} \prod_{t=1}^T f\left(y_t(\mathbf{s}_{i,o}) \mid \boldsymbol{\beta}, \boldsymbol{\eta}_t, \sigma^2(\mathbf{s}_{i,o}), \boldsymbol{\xi}(\mathbf{s}_{i,o}), \boldsymbol{\theta}_{\boldsymbol{\xi}(\mathbf{s}_{i,o})}\right). \quad (3.8)$$

If there exists at least one (i, o) pair such that $\xi_j(\mathbf{s}_{i,o}) = l_j$, then direct calculation shows that

$$\begin{aligned} \theta_{jl_j} \mid \cdot &\sim N\left(V_{\theta_{jl_j}} \mu_{\theta_{jl_j}}, V_{\theta_{jl_j}}\right), \text{ where } V_{\theta_{jl_j}} = \left[\tau_j + \sum_{(i,o):\xi_j(\mathbf{s}_{i,o})=l_j} \sigma^{-2}(\mathbf{s}_{i,o}) \sum_{t=1}^T \eta_{tj}^2 \right]^{-1} \\ \text{and } \mu_{\theta_{jl_j}} &= \sum_{(i,o):\xi_j(\mathbf{s}_{i,o})=l_j} \sigma^{-2}(\mathbf{s}_{i,o}) \sum_{t=1}^T \eta_{tj} \left[y_t(\mathbf{s}_{i,o}) - \mathbf{x}_t(\mathbf{s}_{i,o})^\top \boldsymbol{\beta} - \sum_{h \neq j} \theta_{h\xi_h(\mathbf{s}_{i,o})} \eta_{th} \right]. \end{aligned}$$

Otherwise, $\theta_{jl_j} | \cdot \sim N(0, \tau_j^{-1})$.

We do not need to sample any α_{jl_j} 's for j values with $L_j = 1$, as the corresponding $w_{j1}(\mathbf{s}_{i,o})$'s have already been set to 1 in the earlier Gibbs sampling step for $\xi_j(\mathbf{s}_{i,o})$'s. Fix any arbitrary (i, o, j) where $L_j > 1$ and fix an $l_j \in \{1, \dots, L_j - 1\}$. The only term in the complete data likelihood (3.3) possibly involving $\alpha_{jl_j}(\mathbf{s}_{i,o})$ is $\mathbb{1}_{\{u_j(\mathbf{s}_{i,o}) < w_{j\xi_j}(\mathbf{s}_{i,o})(\mathbf{s}_{i,o})\}}$. Hence for any (j, l_j) where $j \in \{1, \dots, k\}$ and $l_j \in \{1, \dots, L_j - 1\}$,

$$\alpha_{jl_j} | \cdot \sim N_{mO}(\mathbf{0}, F(\rho) \otimes \kappa) \times \prod_{i=1}^m \prod_{o=1}^O \mathbb{1}_{\{l_j > \xi_j(\mathbf{s}_{i,o}) \text{ or } u_j(\mathbf{s}_{i,o}) < w_{j\xi_j}(\mathbf{s}_{i,o})(\mathbf{s}_{i,o})\}}. \quad (3.9)$$

For any (j, i, o, l_j) with $l_j \leq \xi_j(\mathbf{s}_{i,o})$, replacing l_j by $\xi_j(\mathbf{s}_{i,o})$ in Equation (3.4) yields

$$u_j(\mathbf{s}_{i,o}) < w_{j\xi_j}(\mathbf{s}_{i,o})(\mathbf{s}_{i,o}) \iff \begin{cases} \Phi(\alpha_{jl_j}(\mathbf{s}_{i,o})) > \frac{u_j(\mathbf{s}_{i,o})}{\prod_{r_j < \xi_j(\mathbf{s}_{i,o})} [1 - \Phi(\alpha_{jr_j}(\mathbf{s}_{i,o}))]}, & \text{if } l_j = \xi_j(\mathbf{s}_{i,o}) < L_j \\ \Phi(\alpha_{jl_j}(\mathbf{s}_{i,o})) < 1 - \frac{u_j(\mathbf{s}_{i,o})}{\Phi(\alpha_{j\xi_j}(\mathbf{s}_{i,o})(\mathbf{s}_{i,o})) \prod_{r_j < \xi_j(\mathbf{s}_{i,o}), r_j \neq l_j} [1 - \Phi(\alpha_{jr_j}(\mathbf{s}_{i,o}))]}, & \text{if } l_j < \xi_j(\mathbf{s}_{i,o}) < L_j. \\ \Phi(\alpha_{jl_j}(\mathbf{s}_{i,o})) < 1 - \frac{u_j(\mathbf{s}_{i,o})}{\prod_{r_j < L_j, r_j \neq l_j} [1 - \Phi(\alpha_{jr_j}(\mathbf{s}_{i,o}))]}, & \text{if } \xi_j(\mathbf{s}_{i,o}) = L_j > l_j \end{cases}$$

Therefore,

$$\alpha_{jl_j} | \cdot \sim N_{mO}(\mathbf{0}, F(\rho) \otimes \kappa) \times \prod_{i=1}^m \prod_{o=1}^O \begin{cases} 1, & \text{if } l_j > \xi_j(\mathbf{s}_{i,o}) \\ \mathbb{1}_{\{\alpha_{jl_j}^{\text{new}}(\mathbf{s}_{i,o}) > \text{lowerBound}_{(j,l_j,i,o)}\}}, & \text{if } l_j = \xi_j(\mathbf{s}_{i,o}), \\ \mathbb{1}_{\{\alpha_{jl_j}^{\text{new}}(\mathbf{s}_{i,o}) < \text{upperBound}_{(j,l_j,i,o)}\}}, & \text{if } l_j < \xi_j(\mathbf{s}_{i,o}) \end{cases}, \quad (3.10)$$

where for any (j, l_j, i, o) ,

$$\text{lowerBound}_{(j,l_j,i,o)} = \Phi^{-1} \left(\frac{u_j(\mathbf{s}_{i,o}) \cdot \Phi(\alpha_{jl_j}^{\text{old}}(\mathbf{s}_{i,o}))}{w_{j\xi_j}(\mathbf{s}_{i,o})(\mathbf{s}_{i,o})} \right) \text{ and} \quad (3.11)$$

$$\text{upperBound}_{(j,l_j,i,o)} = \Phi^{-1} \left(1 - \frac{u_j(\mathbf{s}_{i,o}) \cdot [1 - \Phi(\alpha_{jl_j}^{\text{old}}(\mathbf{s}_{i,o}))]}{w_{j\xi_j}(\mathbf{s}_{i,o})(\mathbf{s}_{i,o})} \right). \quad (3.12)$$

These truncated multivariate normal posterior distributions of the α_{jl_j} 's can be directly sampled via multivariate rejection sampling, as implemented by for instance the `rtmvnorm` function in the R package `tmvtnorm`. After obtaining new estimates for α_{jl_j} 's ($j = 1, \dots, k, l_j = 1, \dots, L_j - 1$), we formulate posterior samples of w_{jl_j} 's ($j = 1, \dots, k, l_j = 1, \dots, L_j$) via Equation (3.4) correspondingly.

Gibbs sampling steps for the remaining three spatial-clustering-related parameter sets $\delta_h, h \in \{1, \dots, k\}$, $\kappa_{O \times O}$, and ρ are almost indistinguishable from their counterparts under our baseline model in Section 2.2. We simply replace L by L_j 's in the three full conditional densities in Equations (A.11), (A.18) and (A.19) to obtain Equations (A.24), (A.34) and (A.35).

Under our model in this section, α_{jl_j} 's are ordered first by observation type and then spatially, whereas \mathbf{u}_j 's, \mathbf{w}_{jl_j} 's, $\boldsymbol{\xi}_j$'s, $\boldsymbol{\lambda}_j$'s, and $\boldsymbol{\sigma}^2$ are ordered first spatially and then by observation type.

4 Spatial Scalability via Nearest-Neighbor Gaussian Process and Sequential Updates

Throughout this section, we consider a continuous spatial domain $\mathcal{D} \subset \mathbb{R}^d, d \in \mathbb{R}$ and our two models in Sections 2.2 and 3. For spatiotemporal data sets with large numbers of location points $m \in \mathbb{N}$ such as electroencephalography (EEG) data, direct Gibbs sampling parameter estimation without any additional spatial scalability techniques may be severely hindered due to a large spatial neighborhood structure matrix $F(\rho)_{m \times m}$ and longer loops over all spatial points when sampling $\sigma^2(\mathbf{s}_{i,o})$'s and quite a few spatial PSBP clustering related parameters. While there may not be handy acceleration solutions for the latter available currently, well-established approaches enabling efficient computation without hampering inferential capabilities much that can be nicely integrated to tackle the former indeed exist.

Treating the α_{jl_j} 's, ordered first by observation type and then spatially, as the location-specific latent spatial random effects $\mathbf{w}(\mathbf{s}_i)$'s in Datta et al. (2016) and Finley, Datta, and Banerjee (2022) and noting the specific likelihoods in our two models, we can straightforwardly apply relevant methods in a latent Nearest-Neighbor Gaussian Process (NNGP) model framework (Datta et al. 2016). After modifying the portions in our original Gibbs samplers for spatial related parameters κ, ρ , and α_{jl_j} 's with our newly introduced spatial latent NNGP prior and sequential updating approaches, we can avoid calculations of the exact $F(\rho)^{-1}, \det(F(\rho))$, sampling from $N_{mO} \left([I_{mO} + F(\rho)^{-1} \otimes \kappa^{-1}]^{-1} \mathbf{z}_{jl_j}, [I_{mO} + F(\rho)^{-1} \otimes \kappa^{-1}]^{-1} \right)$ or a truncated mO -variate normal distribution given in Equation (3.10), and storage of the entire $F(\rho), F(\rho)^{-1}$ in each MCMC iteration. Computational scalability and storage efficiency can hence be greatly enhanced (Appendices H.2 and H.3). Some further comments regarding the latent NNGP are given in Appendix F.

4.1 Computational Burdens for a Large Spatial Covariance Matrix

Without adopting any spatial scalability techniques, we have several noticeable storage and computational concerns in each MCMC iteration in our two Gibbs samplers (Appendices A.2 and A.3). For one thing, we need to store the entire $F(\rho)$ and $F(\rho)^{-1}$, yet storage in the order of $O(m^2)$ is highly burdensome for a large m . We further note that the full conditional distributions of $\kappa_{O \times O}$ (Equations (A.18) and (A.34)) involve $F(\rho)^{-1}$, and that both $F(\rho)^{-1}$ and $\det(F(\rho))$ have to be evaluated for sampling ρ via a Metropolis step, as we need to calculate $\log[f(\rho|\cdot)]$ (see Equations (A.19) and (A.35)) for both the current parameter estimate and the newly proposed value of ρ . The computational complexity for inversion and determinant calculation are both typically $O(m^3)$ for $m \times m$ matrices without any special structures, which becomes computationally prohibitive for large m . Finally, the posterior sampling for α_{jl_j} 's is also heavily affected by the high computational costs from $F(\rho)$. Under our model in Section 2.2, as deduced in Equation (D.5), for any arbitrary $(j, l) \in \{1, \dots, k\} \times \{1, \dots, L - 1\}$,

$$\alpha_{jl}|\cdot \sim N_{mO} \left([I_{mO} + F(\rho)^{-1} \otimes \kappa^{-1}]^{-1} \mathbf{z}_{jl}, [I_{mO} + F(\rho)^{-1} \otimes \kappa^{-1}]^{-1} \right).$$

We thus need to evaluate $[I_{mO} + F(\rho)^{-1} \otimes \kappa^{-1}]^{-1}$ and $\text{Chol} \left([I_{mO} + F(\rho)^{-1} \otimes \kappa^{-1}]^{-1} \right)$, the Cholesky factor of the $m \times m$ matrix, which both require $O(m^3)$ floating point operations

(flops) under standard methods. Under our model in Section 3, the full conditional distribution of α_{jl_j} for any arbitrary $j \in \{1, \dots, k\}$ and $l_j \in \{1, \dots, L_j - 1\}$ is likely a truncated multivariate normal distribution given by Equation (3.9), which can be directly sampled from by multivariate rejection sampling with $\text{Chol}(F(\rho) \otimes \kappa)$ calculated. We first draw a value from the corresponding un-truncated multivariate normal distribution $N_{mO}(\mathbf{0}, F(\rho) \otimes \kappa)$. We then keep the value if it falls within the multi-dimensional support region, and discard the value and draw a new un-truncated multivariate normal sample otherwise. As the dimension m increases, the acceptance rate often falls very low. Hence this rejection sampling for truncated multivariate normal distributions can get unbearably slow, as a large number $n_{jl_j} \in \mathbb{N}$ of draws from $N_{mO}(\mathbf{0}, F(\rho) \otimes \kappa)$ are required per sample, resulting in an overall computational complexity of $O(m^3) + O\left(\sum_{j=1}^k \sum_{l_j=1}^{L_j-1} n_{jl_j} \cdot m^2\right)$, which is likely greater than $O(m^3)$, for updating all α_{jl_j} 's.

4.2 Incorporating the Latent NNGP

We can successfully tackle these issues by deriving an approximated prior $\tilde{\pi}(\alpha_{jl_j} | \kappa, \rho) = N_{mO}(\mathbf{0}, \tilde{F}(\rho) \otimes \kappa)$ for all (j, l_j) , where $\tilde{F}(\rho)_{m \times m}^{-1}$ is sparse and can be calculated in $O(m)$ flops together with $\det(\tilde{F}(\rho))$. Fix any arbitrary (j, l_j) and consider the zero-centered O -variate Gaussian process $\alpha_{jl_j} | \kappa, \rho \sim N_{mO}(\mathbf{0}, F(\rho) \otimes \kappa)$ over the geographical domain $\mathcal{D} \subset \mathbb{R}^d, d \in \mathbb{N}$. Here, $\alpha_{jl_j} = (\alpha_{jl_j}(\mathbf{s}_1)^\top, \dots, \alpha_{jl_j}(\mathbf{s}_m)^\top)^\top$, where each $\alpha_{jl_j}(\mathbf{s}_i), i \in \{1, \dots, m\}$, conceived as a realization of the smooth latent surface $\{\alpha_{jl_j}(\mathbf{s}) | \mathbf{s} \in \mathcal{D}\}$, is an $O \times 1$ vector corresponding to the observation at location i on the O variables. We take the location reference set \mathcal{S} to be the same as the set of observed locations \mathcal{T} , i.e., let $\mathcal{S} = \mathcal{T} = \{\mathbf{s}_1, \dots, \mathbf{s}_m\} \subset \mathcal{D} \subset \mathbb{R}^d$, a simple yet effective choice that delivers superb inferences (Datta et al. 2016). Pick a positive integer $h \ll m$ and consider the Euclidean distance (Vecchia 1988). Let $N(\mathbf{s}_1) = \emptyset$ and define for each $i \in \{2, 3, \dots, m\}$ location point \mathbf{s}_i 's neighbor set $N(\mathbf{s}_i)$ as the $\min\{h, i-1\}$ nearest neighbors of \mathbf{s}_i in $\{\mathbf{s}_1, \dots, \mathbf{s}_{i-1}\}$. As shown by Datta et al. (2016), a quite small number of h (between 10 to 15 for the Euclidean instance) can already produce highly competitive performance, and both the choice of \mathcal{S} and the ordering of the locations do not matter much.

The GP prior $\alpha_{jl_j} | \kappa, \rho \sim N(\mathbf{0}, F(\rho) \otimes \kappa)$ gives the density

$$\pi(\alpha_{jl_j} | \kappa, \rho) = \pi(\alpha_{jl_j}(\mathbf{s}_1) | \kappa, \rho) \times \prod_{i=2}^m f(\alpha_{jl_j}(\mathbf{s}_i) | \alpha_{jl_j}(\mathbf{s}_{1:(i-1)}), \kappa, \rho),$$

which, under the latent NNGP prior, can be approximated by

$$\tilde{\pi}(\alpha_{jl_j} | \kappa, \rho) = \pi(\alpha_{jl_j}(\mathbf{s}_1) | \kappa, \rho) \times \prod_{i=2}^m f(\alpha_{jl_j}(\mathbf{s}_i) | \alpha_{jl_j, N(\mathbf{s}_i)}, \kappa, \rho), \quad (4.1)$$

where $\alpha_{jl_j, N(\mathbf{s}_i)}$ is at most of length hO for each $i \in \{2, 3, \dots, m\}$. It is clear that $\alpha_{jl_j}(\mathbf{s}_1) | \kappa, \rho \sim N_O(\mathbf{0}, \kappa)$. Since $\alpha_{jl_j} | \kappa, \rho \sim N_{mO}(\mathbf{0}, F(\rho) \otimes \kappa)$, by properties of conditional distributions of jointly multivariate normals, we have

$$\alpha_{jl_j}(\mathbf{s}_i) | \alpha_{jl_j, N(\mathbf{s}_i)}, \kappa, \rho \sim N_O\left(B_{\mathbf{s}_i} \alpha_{jl_j, N(\mathbf{s}_i)}, F_{\mathbf{s}_i}\right), \text{ for all } i \in \{2, \dots, m\}, \quad (4.2)$$

where the $O \times (|N(\mathbf{s}_i)| \cdot O)$ matrix $B_{\mathbf{s}_i} = F(\rho)_{\mathbf{s}_i, N(\mathbf{s}_i)} F(\rho)_{N(\mathbf{s}_i), \mathbf{s}_i}^{-1} \otimes I_{O \times O}$ and the $O \times O$ matrix $F_{\mathbf{s}_i} = \left[F(\rho)_{\mathbf{s}_i, \mathbf{s}_i} - F(\rho)_{\mathbf{s}_i, N(\mathbf{s}_i)} F(\rho)_{N(\mathbf{s}_i), \mathbf{s}_i}^{-1} F(\rho)_{N(\mathbf{s}_i), \mathbf{s}_i} \right] \otimes \kappa$ with $F(\rho)_{\mathbf{s}_i, \mathbf{s}_i} = 1, F(\rho)_{\mathbf{s}_i, N(\mathbf{s}_i)},$

$F(\rho)_{N(\mathbf{s}_i), \mathbf{s}_i}, F(\rho)_{N(\mathbf{s}_i)}$ being the corresponding $1 \times 1, 1 \times |N(\mathbf{s}_i)|, |N(\mathbf{s}_i)| \times 1, |N(\mathbf{s}_i)| \times |N(\mathbf{s}_i)|$ sub-matrices of $F(\rho)_{m \times m}$. Hence following Equation (4.1), we have

$$\tilde{\pi}(\boldsymbol{\alpha}_{j_l} | \kappa, \rho) \sim N_O(\mathbf{0}, \kappa) \times \prod_{i=2}^m N_O\left(B_{\mathbf{s}_i} \boldsymbol{\alpha}_{j_l, N(\mathbf{s}_i)}, F_{\mathbf{s}_i}\right). \quad (4.3)$$

We thus no longer need to store the entire $F(\rho)$ and only need to store the sub-matrices $F(\rho)_{\mathbf{s}_i, N(\mathbf{s}_i)}, F(\rho)_{N(\mathbf{s}_i), \mathbf{s}_i}, F(\rho)_{N(\mathbf{s}_i)}$ for each $i \in \{2, \dots, m\}$. Storage with respect to $F(\rho)$ itself can hence be reduced from $O(m^2)$ to $O(mh^2) = O(m)$, i.e., quadratic to linear in m since $|N(\mathbf{s}_i)| \leq h \ll m$ for all $i \in \{2, \dots, m\}$. It is known that Equation (4.3) is indeed the joint density from a valid stochastic process (Appendix A in Datta et al. 2016), as its corresponding construction ensures a directed acyclic graph $\mathcal{G} = \{\mathcal{S}, N_{\mathcal{S}}\}$. Also, for any $i \in \{2, \dots, m\}$, $|N(\mathbf{s}_i)| \leq h$ and $B_{\mathbf{s}_i}, F_{\mathbf{s}_i}$ can be calculated by at most $O(h^3)$ flops, which result from evaluating $F(\rho)_{N(\mathbf{s}_i)}^{-1}$.

4.3 Approximating $F(\rho)^{-1}$ and $\det(F(\rho))$

Let $F_{\mathbf{s}_1} = \kappa_{O \times O}$ and $B_{\mathbf{s}_1}^* = (1, 0, \dots, 0)_{1 \times m} \otimes I_{O \times O}$. Then by Equation (4.3),

$$\begin{aligned} \tilde{\pi}(\boldsymbol{\alpha}_{j_l} | \kappa, \rho) &\propto \frac{1}{\prod_{i=1}^m \sqrt{\det(F_{\mathbf{s}_i})}} \times \exp \left\{ -\frac{1}{2} \sum_{i=1}^m \boldsymbol{\alpha}_{j_l}^T (B_{\mathbf{s}_i}^*)^T F_{\mathbf{s}_i}^{-1} B_{\mathbf{s}_i}^* \boldsymbol{\alpha}_{j_l} \right\} \\ &= \frac{1}{\sqrt{\prod_{i=1}^m \det(F_{\mathbf{s}_i})}} \times \exp \left\{ -\frac{1}{2} \boldsymbol{\alpha}_{j_l}^T B_{\mathcal{S}}^T F_{\mathcal{S}}^{-1} B_{\mathcal{S}} \boldsymbol{\alpha}_{j_l} \right\}, \end{aligned} \quad (4.4)$$

where the $mO \times mO$ matrix $F_{\mathcal{S}} = \text{Diag}(F_{\mathbf{s}_1}, \dots, F_{\mathbf{s}_m})$ and $B_{\mathcal{S}} = \left([B_{\mathbf{s}_1}^*]^T, [B_{\mathbf{s}_2}^*]^T, \dots, [B_{\mathbf{s}_m}^*]^T \right)^T$. For each i , the $O \times mO$ matrix $B_{\mathbf{s}_i}^* = (B_{\mathbf{s}_i, 1}^*, B_{\mathbf{s}_i, 2}^*, \dots, B_{\mathbf{s}_i, m}^*)$ is sparse with at most $h + 1$ non-zero $O \times O$ blocks out of the m blocks

$$B_{\mathbf{s}_i, j}^* = \begin{cases} I_{O \times O}, & \text{if } j = i \\ -B_{\mathbf{s}_i}[\cdot, (l-1)O + 1 : lO], & \text{if } \exists l \in \{1, \dots, \min(h, i-1)\} \text{ such that } \mathbf{s}_j = N(\mathbf{s}_i)[l], \\ \mathbf{0}_{O \times O}, & \text{otherwise} \end{cases}$$

for $j \in \{1, \dots, m\}$, where $N(\mathbf{s}_i)[l]$ denotes the l^{th} point in $N(\mathbf{s}_i)$. Since for any $i \in \{2, 3, \dots, m\}$, $N(\mathbf{s}_i) \subset \{\mathbf{s}_1, \dots, \mathbf{s}_{i-1}\}$, $B_{\mathcal{S}}$ is lower triangular whose main diagonal entries are all 1. This implies that $\det(B_{\mathcal{S}}) = 1$ and that $B_{\mathcal{S}}^T F_{\mathcal{S}}^{-1} B_{\mathcal{S}}$ is invertible. Hence, we can let $\tilde{F}(\rho)^{-1} \otimes \kappa^{-1} = B_{\mathcal{S}}^T F_{\mathcal{S}}^{-1} B_{\mathcal{S}} = \sum_{i=1}^m (B_{\mathbf{s}_i}^*)^T F_{\mathbf{s}_i}^{-1} B_{\mathbf{s}_i}^*$, whose computational complexity is $O(mh^3) + O(mO^3) + O(m(h+1)^2O^3) = O(m)$ since $h \ll m$ and $O \in \mathbb{N}$ is also assumed very small. The $\tilde{F}(\rho)_{m \times m}^{-1}$ defined this way simplifies Equation (4.4) to

$$\tilde{\pi}(\boldsymbol{\alpha}_{j_l} | \kappa, \rho) \propto \left\{ \det \left(\tilde{F}(\rho) \otimes \kappa \right) \right\}^{-1/2} \times \exp \left\{ -\frac{1}{2} \boldsymbol{\alpha}_{j_l}^T [\tilde{F}(\rho)^{-1} \otimes \kappa^{-1}] \boldsymbol{\alpha}_{j_l} \right\}. \quad (4.5)$$

Hence $\tilde{\pi}(\boldsymbol{\alpha}_{j_l} | \kappa, \rho) = N_{mO}(\mathbf{0}, \tilde{F}(\rho) \otimes \kappa)$, which is our NNGP prior. As $\det(B_{\mathcal{S}}) = 1$, we have $\det(\tilde{F}(\rho) \otimes \kappa) = \det([B_{\mathcal{S}}^T F_{\mathcal{S}}^{-1} B_{\mathcal{S}}]^{-1}) = \det(F_{\mathcal{S}}) = \prod_{i=1}^m \det(F_{\mathbf{s}_i})$, which can be calculated in $O(mh^3) + O(mO^3) = O(m)$ flops. The total computational complexity calculating $\tilde{F}(\rho)^{-1} \otimes \kappa^{-1}$ and $\det(\tilde{F}(\rho) \otimes \kappa)$ is thus linear in m . A full GP with a dense precision matrix $F(\rho) \otimes \kappa$,

on the other hand, needs $O(m^3)$ flops updating the counterpart quantities $F(\rho)^{-1} \otimes \kappa^{-1}$ and $\det(F(\rho) \otimes \kappa)$ in each MCMC iteration. As such, the overall computational complexity required to update ρ and κ in each MCMC iteration has been reduced from cubic to quadratic in m (Table 6 in Appendix H.2).

We now consider elements of the precision matrix $\tilde{F}(\rho)_{m \times m}^{-1}$ defined earlier. For any pair $(i, j) \in \{1, \dots, m\}^2$ where $i < j$, let \tilde{F}_{ij}^{-1} be the (i, j) th entry of $\tilde{F}(\rho)^{-1}$. Then $\tilde{F}(\rho)^{-1} \otimes \kappa^{-1} = \sum_{l=1}^m (B_{\mathbf{s}_l}^*)^\top F_{\mathbf{s}_l}^{-1} B_{\mathbf{s}_l}^*$ implies $\tilde{F}_{ij}^{-1} \otimes \kappa^{-1} = \sum_{l=j}^m (B_{\mathbf{s}_l, i}^*)^\top F_{\mathbf{s}_l}^{-1} B_{\mathbf{s}_l, j}^*$. Hence $\tilde{F}_{ij}^{-1} \neq 0$ implies that there exists $l \in \{j, j+1, \dots, m\}$ such that $\mathbf{s}_i \in N(\mathbf{s}_l)$ and $\mathbf{s}_j \in N(\mathbf{s}_l)$ or $\mathbf{s}_j = \mathbf{s}_l$. We can thus obtain an upper bound, $m \cdot \frac{h(h+1)}{2}$, of the maximum number of pairs $(i, j), i < j$ leading to a non-zero \tilde{F}_{ij}^{-1} by looping over $l \in \{1, \dots, m\}$. Further taking the lower triangular and diagonal entries of $\tilde{F}(\rho)^{-1}$ into consideration, we get that $\tilde{F}(\rho)_{m \times m}^{-1}$ is sparse with at most $2 \times m \cdot \frac{h(h+1)}{2} + m = m \cdot [h(h+1) + 1]$ non-zero entries. Hence, although unnecessary in most cases, we do have the option of storing only the $O(m)$ non-zero entries and their indices instead of the entire $\tilde{F}(\rho)_{m \times m}^{-1}$. Our spatial NNGP's capability of reducing storage for $F(\rho)^{-1}$ from quadratic to linear in m can be tremendously useful by making model fitting feasible in situations with intimidating storage requirements.

4.4 Sequentially Updating α_{jl} 's Under Our Spatial NNGP Prior

Our aforementioned computational burdens (Section 4.1) yet to be addressed are all related to the posterior sampling of α_{jl} 's from their full conditional distributions, which cannot be completely solved by simply adopting the NNGP prior for the α_{jl} 's and replacing $F(\rho)_{m \times m}$ by $\tilde{F}(\rho)_{m \times m}$. We provide detailed reasons in the two ensuing paragraphs.

Under our model in Section 2.2, for any arbitrary $(j, l) \in \{1, \dots, k\} \times \{1, \dots, L-1\}$,

$$\alpha_{jl} | \cdot \sim N_{mO} \left(\left[I_{mO} + \tilde{F}(\rho)^{-1} \otimes \kappa^{-1} \right]^{-1} \mathbf{z}_{jl}, \left[I_{mO} + \tilde{F}(\rho)^{-1} \otimes \kappa^{-1} \right]^{-1} \right), \quad (4.6)$$

where \mathbf{z}_{jl} is the introduced latent normal vector (Appendix D). We thus need to evaluate $\text{Chol}([I_{mO} + \tilde{F}(\rho)^{-1} \otimes \kappa^{-1}]^{-1})$ and $[I_{mO} + \tilde{F}(\rho)^{-1} \otimes \kappa^{-1}]^{-1}$, which requires $O(m^3)$ flops via standard methods. Hence, directly proceeding with block updating α_{jl} 's according to Equation (4.6) for all (j, l) still requires $O(m^3) + O(k(L-1) \cdot (mO)^2) = O(m^3)$ flops in each MCMC iteration and thus incurs a high computational cost.

Under our model in Section 3, for any (j, l_j) where $j \in \{1, \dots, k\}$ and $l_j \in \{1, \dots, L_j - 1\}$,

$$\alpha_{jl_j} | \cdot \sim N_{mO} \left(\mathbf{0}, \tilde{F}(\rho) \otimes \kappa \right) \times \prod_{i=1}^m \prod_{o=1}^O \begin{cases} 1, & \text{if } l_j > \xi_j(\mathbf{s}_{i,o}) \\ \mathbb{1}_{\{\alpha_{jl_j}^{\text{new}}(\mathbf{s}_{i,o}) > \text{lowerBound}_{(j, l_j, i, o)}\}}, & \text{if } l_j = \xi_j(\mathbf{s}_{i,o}), \\ \mathbb{1}_{\{\alpha_{jl_j}^{\text{new}}(\mathbf{s}_{i,o}) < \text{upperBound}_{(j, l_j, i, o)}\}}, & \text{if } l_j < \xi_j(\mathbf{s}_{i,o}) \end{cases}, \quad (4.7)$$

where $\text{lowerBound}_{(j, l_j, i, o)}$'s and $\text{upperBound}_{(j, l_j, i, o)}$'s are given by Equations (3.11) and (3.12). We hence need to evaluate $\text{Chol}(\tilde{F}(\rho) \otimes \kappa)$, which generally requires $O(m^3)$ flops. Since finding a faster numerical algorithm to calculate $\text{Chol}(\tilde{F}(\rho) \otimes \kappa)$ is challenging and more seriously, rejection sampling from a high-dimensional truncated mO -variate normal distribution is unbearably slow for feasible computation due to a very small acceptance rate, similar computational issues as the ones pointed out at the end of Section 4.1 exist.

We propose a novel algorithm to bypass these computational burdens under both of our models by sequentially updating components of $\boldsymbol{\alpha}_{jl_j} = (\boldsymbol{\alpha}_{jl_j}(\mathbf{s}_1)^\top, \dots, \boldsymbol{\alpha}_{jl_j}(\mathbf{s}_m)^\top)^\top$ for each (j, l_j) instead, as to be elaborated below. Table 7 in Appendix H.3 presents the computational complexity required for the Gibbs sampler step updating all $\boldsymbol{\alpha}_{jl_j}$'s in each MCMC iteration, with and without our new method. Let $F_{\mathbf{s}_1} = \kappa_{O \times O}$ and $F_{\mathbf{s}_1}^{-1} B_{\mathbf{s}_1} \boldsymbol{\alpha}_{jl_j, N(\mathbf{s}_1)} = \mathbf{0}_{O \times 1}$ since $N(\mathbf{s}_1) = \emptyset$.

Under our model in Section 2.2 and NNGP prior $\tilde{\pi}(\boldsymbol{\alpha}_{jl} | \kappa, \rho) = N_{mO}(\mathbf{0}, \tilde{F}(\rho) \otimes \kappa)$ for all (j, l) , for any arbitrary fixed $(j, l, i) \in \{1, \dots, k\} \times \{1, \dots, L-1\} \times \{1, \dots, m\}$,

$$\begin{aligned} f(\boldsymbol{\alpha}_{jl}(\mathbf{s}_i) | \cdot) &\propto f(\mathbf{z}_{jl}(\mathbf{s}_i) | \boldsymbol{\alpha}_{jl}(\mathbf{s}_i)) \times f(\boldsymbol{\alpha}_{jl}(\mathbf{s}_i) | \boldsymbol{\alpha}_{jl, N(\mathbf{s}_i)}, \kappa, \rho) \times \prod_{r: \mathbf{s}_i \in N(\mathbf{s}_r)} f(\boldsymbol{\alpha}_{jl}(\mathbf{s}_r) | \boldsymbol{\alpha}_{jl, N(\mathbf{s}_r)}, \kappa, \rho) \\ &\sim N_O(V_{\mathbf{s}_i} \boldsymbol{\mu}_{jl, \mathbf{s}_i}, V_{\mathbf{s}_i}), \end{aligned} \quad (4.8)$$

where

$$\begin{aligned} V_{\mathbf{s}_i} &= \left[I_O + F_{\mathbf{s}_i}^{-1} + \sum_{r: \mathbf{s}_i \in N(\mathbf{s}_r)} B_{\mathbf{s}_r, k_r(\mathbf{s}_i)}^\top F_{\mathbf{s}_r}^{-1} B_{\mathbf{s}_r, k_r(\mathbf{s}_i)} \right]^{-1} \quad \text{and} \\ \boldsymbol{\mu}_{jl, \mathbf{s}_i} &= \mathbf{z}_{jl}(\mathbf{s}_i) + F_{\mathbf{s}_i}^{-1} B_{\mathbf{s}_i} \boldsymbol{\alpha}_{jl, N(\mathbf{s}_i)} + \sum_{r: \mathbf{s}_i \in N(\mathbf{s}_r)} B_{\mathbf{s}_r, k_r(\mathbf{s}_i)}^\top F_{\mathbf{s}_r}^{-1} \left\{ \boldsymbol{\alpha}_{jl}(\mathbf{s}_r) - \sum_{\substack{1 \leq k \leq |N(\mathbf{s}_r)| \\ k \neq k_r(\mathbf{s}_i)}} B_{\mathbf{s}_r, k} \boldsymbol{\alpha}_{jl, N(\mathbf{s}_r)[k]} \right\}. \end{aligned}$$

Under our model in Section 3 and NNGP prior $\tilde{\pi}(\boldsymbol{\alpha}_{jl_j} | \kappa, \rho) = N_{mO}(\mathbf{0}, \tilde{F}(\rho) \otimes \kappa)$ for all (j, l_j) , for any arbitrary fixed (j, l_j, i) where $j \in \{1, \dots, k\}$, $l_j \in \{1, \dots, L_j - 1\}$, and $i \in \{1, \dots, m\}$,

$$\begin{aligned} f(\boldsymbol{\alpha}_{jl_j}(\mathbf{s}_i) | \cdot) &\propto \prod_{r: r=i \text{ or } \mathbf{s}_i \in N(\mathbf{s}_r)} f(\boldsymbol{\alpha}_{jl_j}(\mathbf{s}_r) | \boldsymbol{\alpha}_{jl_j, N(\mathbf{s}_r)}, \kappa, \rho) \times \prod_{o=1}^O \mathbb{1}_{\{l_j > \xi_j(\mathbf{s}_{i,o}) \text{ or } u_j(\mathbf{s}_{i,o}) < w_j \xi_j(\mathbf{s}_{i,o})(\mathbf{s}_{i,o})\}} \\ &\sim N_O(V_{\mathbf{s}_i} \boldsymbol{\mu}_{jl_j, \mathbf{s}_i}, V_{\mathbf{s}_i}) \times \prod_{o=1}^O \mathbb{1}_{\{l_j > \xi_j(\mathbf{s}_{i,o}) \text{ or } u_j(\mathbf{s}_{i,o}) < w_j \xi_j(\mathbf{s}_{i,o})(\mathbf{s}_{i,o})\}}, \end{aligned} \quad (4.9)$$

where

$$\begin{aligned} V_{\mathbf{s}_i} &= \left[F_{\mathbf{s}_i}^{-1} + \sum_{r: \mathbf{s}_i \in N(\mathbf{s}_r)} B_{\mathbf{s}_r, k_r(\mathbf{s}_i)}^\top F_{\mathbf{s}_r}^{-1} B_{\mathbf{s}_r, k_r(\mathbf{s}_i)} \right]^{-1} \quad \text{and} \\ \boldsymbol{\mu}_{jl_j, \mathbf{s}_i} &= F_{\mathbf{s}_i}^{-1} B_{\mathbf{s}_i} \boldsymbol{\alpha}_{jl_j, N(\mathbf{s}_i)} + \sum_{r: \mathbf{s}_i \in N(\mathbf{s}_r)} B_{\mathbf{s}_r, k_r(\mathbf{s}_i)}^\top F_{\mathbf{s}_r}^{-1} \left\{ \boldsymbol{\alpha}_{jl_j}(\mathbf{s}_r) - \sum_{\substack{1 \leq k_j \leq |N(\mathbf{s}_r)| \\ k_j \neq k_r(\mathbf{s}_i)}} B_{\mathbf{s}_r, k_j} \boldsymbol{\alpha}_{jl_j, N(\mathbf{s}_r)[k_j]} \right\}. \end{aligned}$$

Full deduction details pertaining to the above are in Appendices A.2 and A.3. For each r such that $\mathbf{s}_i \in N(\mathbf{s}_r)$, $k_r(\mathbf{s}_i)$ in the expressions above refers to the positive integer less than or equal to $|N(\mathbf{s}_r)|$ such that $\mathbf{s}_i = N(\mathbf{s}_r)[k_r(\mathbf{s}_i)]$. We have written the $O \times (|N(\mathbf{s}_r)| \cdot O)$ matrix $B_{\mathbf{s}_r}$ as $(B_{\mathbf{s}_r, 1}, \dots, B_{\mathbf{s}_r, |N(\mathbf{s}_r)|})$, where each sub-matrix is $O \times O$, and written the $(|N(\mathbf{s}_r)| \cdot O) \times 1$ vector $\boldsymbol{\alpha}_{jl_j, N(\mathbf{s}_r)}$ as $(\boldsymbol{\alpha}_{jl_j, N(\mathbf{s}_r)[1]}^\top, \dots, \boldsymbol{\alpha}_{jl_j, N(\mathbf{s}_r)[|N(\mathbf{s}_r)|]}^\top)^\top$ so that $B_{\mathbf{s}_r} \boldsymbol{\alpha}_{jl_j, N(\mathbf{s}_r)} = \sum_{k_j=1}^{|N(\mathbf{s}_r)|} B_{\mathbf{s}_r, k_j} \boldsymbol{\alpha}_{jl_j, N(\mathbf{s}_r)[k_j]}$. Note also that we only need to consider $r = i + 1, \dots, m$ for each $i < m$ in order to find out the set $\{r \in \{1, \dots, m\} : \mathbf{s}_i \in N(\mathbf{s}_r)\}$.

If we exploit the Kronecker structures of the $B_{\mathbf{s}_i}$'s and $F_{\mathbf{s}_i}$'s with common second matrices $I_{O \times O}$ and $\kappa_{O \times O}$ as given in Section 4.2 and sequentially sample the elements $\boldsymbol{\alpha}_{jl_j}(\mathbf{s}_i)$, $i \in$

$\{1, \dots, m\}$, of α_{jl_j} one by one according to Equation (4.9), then the computational complexity associated with evaluating all m B_{s_i} 's, F_{s_i} 's, conditional normal variances and their Cholesky factors, all $m \sum_{j=1}^k (L_j - 1)$ conditional means and right-multiplying generated (possibly rejected) $1 \times O$ random vectors consisting of independent standard normal entries by the corresponding Cholesky factors of conditional normal variances is

$$O(mh^3) + O(m(O^3 + h)) + O\left(m \sum_{j=1}^k (L_j - 1) \cdot (hO^2 + h^2O^2)\right) + O\left(\sum_{j=1}^k \sum_{l_j=1}^{L_j-1} \sum_{i=1}^m n_{jl_j i}^* \cdot O^2\right),$$

which is also

$$O\left(m \times \sum_{j=1}^k (L_j - 1) \times (h^3 + O^3 + h^2O^2)\right) + O\left(\sum_{j=1}^k \sum_{l_j=1}^{L_j-1} \sum_{i=1}^m n_{jl_j i}^* \cdot O^2\right),$$

where $\sum_{j=1}^k (L_j - 1)$ is replaced by $k(L - 1)$ and the required number of draws $n_{jl_j i}^* \in \mathbb{N}$ per sample is replaced by 1 for all (j, l_j, i) if we adopt our model framework in Section 2.2 and proceed with Equation (4.8) instead. The corresponding overall computational complexity for updating all α_{jl} 's in each MCMC iteration is thus $O(mk(L - 1)(h^3 + O^3 + h^2O^2)) = O(m)$ if $L \ll m$ (instead of the original $O(m^3)$ without our sequential updating method). Under our model in Section 3, sequentially updating α_{jl_j} 's as above successfully replaces the unbearably slow rejection sampling from a high-dimensional truncated mO -variate normal distribution by computationally achievable low-dimensional truncated O -variate normal samplings. As the number of observation types $O \in \mathbb{N}$ is typically very small and often equals 1, the truncated O -variate normal samplings (Equation (4.9)) concerned with sequential updating would have adequate acceptance rates with small $n_{jl_j i}^*$'s. If the largest number of mixture components $\max_{j \in \{1, \dots, k\}} L_j$ is of constant order or increases only logarithmically with m as in Dirichlet processes, then given $k, h, O \ll m$ and $\sum_{j=1}^k L_j \leq k \cdot \max_{j \in \{1, \dots, k\}} L_j$, sequential updates in our Gibbs samplers can reduce the posterior sampling computational complexity for updating all α_{jl_j} 's in each MCMC iteration from $O(m^3) + O\left(\sum_{j=1}^k \sum_{l_j=1}^{L_j-1} n_{jl_j} \cdot m^2\right)$, which is likely greater than $O(m^3)$, to about linear in m (Table 7 in Appendix H.3). Compared to sampling α_{jl_j} 's according to Equation (4.6) or (4.7), sequentially updating α_{jl_j} 's not only significantly accelerates sampling per MCMC iteration but also leads to much faster overall posterior convergence and comparably good model fitting performances, as we shall see from our simulation experiments in Section 6.1.

4.5 Full GP Extension of the Latent NNGP for Spatial Prediction

One primary advantage of the NNGP is that it is a legitimate Gaussian process on the entire spatial domain $\mathcal{D} \subset \mathbb{R}^d$ after extending $\tilde{\pi}(\alpha_{jl_j}(\mathbf{s}_{1:m}) | \kappa, \rho)$ in Equation (4.1). For all $\mathbf{s} \in \mathcal{D} \setminus \mathcal{S}$, we let $N(\mathbf{s})$ consist of the h nearest neighbors of \mathbf{s} in $\mathcal{S} = \{\mathbf{s}_1, \mathbf{s}_2, \dots, \mathbf{s}_m\}$. We then specify the NNGP derived from the parent GP as

$$\begin{aligned} \alpha_{jl_j}(\mathbf{s}_{1:m}) | \kappa, \rho &\sim \pi(\alpha_{jl_j}(\mathbf{s}_1) | \kappa, \rho) \times \prod_{i=2}^m f(\alpha_{jl_j}(\mathbf{s}_i) | \alpha_{jl_j, N(\mathbf{s}_i)}, \kappa, \rho), \\ \alpha_{jl_j}(\mathbf{s}) | \alpha_{jl_j}(\mathbf{s}_{1:m}), \kappa, \rho &\stackrel{\text{ind}}{\sim} f(\alpha_{jl_j}(\mathbf{s}) | \alpha_{jl_j, N(\mathbf{s})}, \kappa, \rho), \text{ for all } \mathbf{s} \in \mathcal{D} \setminus \mathcal{S}. \end{aligned} \quad (4.10)$$

The generalized directed graph \mathcal{G} (Section 4.2) is still ensured acyclic and a well-defined NNGP process can always be constructed as above for any parent GP and any fixed reference set \mathcal{S} ; see Section 2.2 and Appendix D & E in Datta et al. (2016).

Extending to any arbitrary location $\mathbf{s} \in \mathcal{D}$ via nearest-neighbor kriging as in Equation (4.10) enables efficient hierarchical predictions at any new locations based on our posterior parameter estimates (Appendix G.2.2 and Section 5.1). As to be substantiated by our simulation experiments in Section 6.2, nearest-neighbor kriging of the spatially varying latent variables under the NNGP not only significantly reduces computational complexity (Appendices H.2 and H.4) but also delivers almost indistinguishable satisfactory performances in spatial prediction, thus making partial conditional prediction via nearest-neighbor kriging a superb alternative to full conditional prediction via Bayesian kriging under the full GP.

5 Spatial Prediction and Temporal Trends Clustering

5.1 Predictions at New Spatial Locations

Bayesian nonparametric predictions at any arbitrary future time points or new spatial locations under all three modeling frameworks in Sections 2 and 3 are straightforward. We can decompose the integral representation of the posterior predictive distribution (PPD) into several known densities and then obtain the PPD via composition sampling. Extensions to joint predictions for new time points and spatial locations can also be conveniently made. Here in the main text, we elaborate on new-location predictions under our model in Section 3, where the prior $\alpha_{jl_j} \stackrel{\text{iid}}{\sim} N_{mO}(\mathbf{0}, F(\rho)_{m \times m} \otimes \kappa_{O \times O})$ for all $j \in \{1, \dots, k\}$, $l_j \in \{1, \dots, L_j - 1\}$ is assigned. Details pertaining to the other prediction cases are given in Appendix G.

For Bayesian predictions at r ($r \in \mathbb{N}, r \geq 1$) new spatial locations $\mathbf{s}_{(m+1):(m+r)}$ given their corresponding covariates matrix $X(\mathbf{s}_{(m+1):(m+r)})_{rTO \times p}$, if any, we can write the PPD as

$$\begin{aligned} & f(\mathbf{y}(\mathbf{s}_{(m+1):(m+r)}) | \mathbf{y}(\mathbf{s}_{1:m}), X(\mathbf{s}_{(m+1):(m+r)})) \\ &= \int_{\Theta} f(\mathbf{y}(\mathbf{s}_{(m+1):(m+r)}) | \Theta, \mathbf{y}(\mathbf{s}_{1:m}), X(\mathbf{s}_{(m+1):(m+r)})) \pi(\Theta | \mathbf{y}(\mathbf{s}_{1:m})) d\Theta, \end{aligned}$$

where $\Theta = (\boldsymbol{\eta}, \boldsymbol{\beta}, \boldsymbol{\sigma}^2(\mathbf{s}_{(m+1):(m+r)}), \boldsymbol{\theta}, \boldsymbol{\xi}(\mathbf{s}_{(m+1):(m+r)}), \boldsymbol{\alpha}(\mathbf{s}_{(m+1):(m+r)}), \boldsymbol{\alpha}, \kappa, \rho)$ and $\boldsymbol{\alpha}$ denotes $\boldsymbol{\alpha}(\mathbf{s}_{1:m})$, and then partition the integral into

$$\begin{aligned} & \int_{\Theta} \underbrace{f(\mathbf{y}(\mathbf{s}_{(m+1):(m+r)}) | \boldsymbol{\theta}, \boldsymbol{\xi}(\mathbf{s}_{(m+1):(m+r)}), \boldsymbol{\eta}, \boldsymbol{\beta}, \boldsymbol{\sigma}^2(\mathbf{s}_{(m+1):(m+r)}), X(\mathbf{s}_{(m+1):(m+r)}))}_{T_1} \\ & \quad \times \underbrace{f(\boldsymbol{\xi}(\mathbf{s}_{(m+1):(m+r)}) | \boldsymbol{\alpha}(\mathbf{s}_{(m+1):(m+r)}))}_{T_2} \underbrace{f(\boldsymbol{\alpha}(\mathbf{s}_{(m+1):(m+r)}) | \boldsymbol{\alpha}, \kappa, \rho)}_{T_3} \\ & \quad \times \underbrace{\pi(\boldsymbol{\eta}, \boldsymbol{\beta}, \boldsymbol{\theta}, \boldsymbol{\alpha}, \kappa, \rho | \mathbf{y}(\mathbf{s}_{1:m}))}_{T_4} \underbrace{\pi(\boldsymbol{\sigma}^2(\mathbf{s}_{(m+1):(m+r)}))}_{T_5} d\Theta \end{aligned} \quad (5.1)$$

since the posterior density $\pi(\boldsymbol{\sigma}^2(\mathbf{s}_{(m+1):(m+r)}) | \mathbf{y}(\mathbf{s}_{1:m}))$ equals the prior $\pi(\boldsymbol{\sigma}^2(\mathbf{s}_{(m+1):(m+r)}))$. Values of both $\boldsymbol{\alpha}$ and $\boldsymbol{\alpha}(\mathbf{s}_{(m+1):(m+r)})$ already incorporate the cluster number parameters L_j for all $j \in \{1, \dots, k\}$.

In Equation (5.1), T_1 is the likelihood; T_4 is the parameters' posterior distribution obtained from the original model fit's MCMC sampler; T_5 denotes the prior density for $\boldsymbol{\sigma}^2(\mathbf{s}_{(m+1):(m+r)}) = (\sigma^2(\mathbf{s}_{m+1,1}), \dots, \sigma^2(\mathbf{s}_{m+1,O}), \dots, \sigma^2(\mathbf{s}_{m+r,1}), \dots, \sigma^2(\mathbf{s}_{m+r,O}))$ with $\sigma^2(\mathbf{s}_{m+i_r,o}) \stackrel{\text{iid}}{\sim} \mathcal{IG}(a, b)$, $i_r \in \{1, \dots, r\}$, $o \in \{1, \dots, O\}$; T_2 is the density of the multinomial distribution described in Section 2.2; and T_3 can be written as

$$f(\boldsymbol{\alpha}(\mathbf{s}_{(m+1):(m+r)}) | \boldsymbol{\alpha}(\mathbf{s}_{1:m}), \boldsymbol{\kappa}, \boldsymbol{\rho}) = \prod_{j=1}^k \prod_{l_j=1}^{L_j-1} f(\boldsymbol{\alpha}_{jl_j}(\mathbf{s}_{(m+1):(m+r)}) | \boldsymbol{\alpha}_{jl_j}(\mathbf{s}_{1:m}), \boldsymbol{\kappa}, \boldsymbol{\rho}). \quad (5.2)$$

We can thus straightforwardly predict $\boldsymbol{\alpha}(\mathbf{s}_{(m+1):(m+r)})$ conditioning on $\boldsymbol{\alpha}(\mathbf{s}_{1:m}), \boldsymbol{\kappa}, \boldsymbol{\rho}$.

In the simplest case when spatial independence is assumed and the spatial neighborhood structure matrix $F(\boldsymbol{\rho})$ is set to the identity matrix, for any (j, l_j) ,

$$f(\boldsymbol{\alpha}_{jl_j}(\mathbf{s}_{(m+1):(m+r)}) | \boldsymbol{\alpha}_{jl_j}(\mathbf{s}_{1:m}), \boldsymbol{\kappa}, \boldsymbol{\rho}) = \pi(\boldsymbol{\alpha}_{jl_j}(\mathbf{s}_{(m+1):(m+r)}) | \boldsymbol{\kappa}, \boldsymbol{\rho}) \sim N_{rO}(\mathbf{0}, I_{r \times r} \otimes \boldsymbol{\kappa}). \quad (5.3)$$

When spatial dependence is taken into consideration and the spatially extended full GP prior $\pi(\boldsymbol{\alpha}_{jl_j}(\mathbf{s}_{1:(m+r)}) | \boldsymbol{\kappa}, \boldsymbol{\rho}) = N_{(m+r)O}(\mathbf{0}, F(\boldsymbol{\rho})_{(m+r) \times (m+r)} \otimes \boldsymbol{\kappa}_{O \times O})$ for all (j, l_j) is placed, by properties of conditional distributions of jointly multivariate normals, for any (j, l_j) ,

$$\boldsymbol{\alpha}_{jl_j}(\mathbf{s}_{(m+1):(m+r)}) | \boldsymbol{\alpha}_{jl_j}(\mathbf{s}_{1:m}), \boldsymbol{\kappa}, \boldsymbol{\rho} \sim N_{rO} \left(B_{\mathbf{s}_{(m+1):(m+r)}} \boldsymbol{\alpha}_{jl_j}(\mathbf{s}_{1:m}), F_{\mathbf{s}_{(m+1):(m+r)}} \right), \quad (5.4)$$

where $B_{\mathbf{s}_{(m+1):(m+r)}} = \left\{ F(\boldsymbol{\rho})_{\mathbf{s}_{(m+1):(m+r)}, \mathbf{s}_{1:m}} [F(\boldsymbol{\rho})_{\mathbf{s}_{1:m}}]^{-1} \right\} \otimes I_{O \times O}$ is $rO \times mO$ and $F_{\mathbf{s}_{(m+1):(m+r)}} = \left\{ F(\boldsymbol{\rho})_{\mathbf{s}_{(m+1):(m+r)}} - F(\boldsymbol{\rho})_{\mathbf{s}_{(m+1):(m+r)}, \mathbf{s}_{1:m}} [F(\boldsymbol{\rho})_{\mathbf{s}_{1:m}}]^{-1} F(\boldsymbol{\rho})_{\mathbf{s}_{1:m}, \mathbf{s}_{(m+1):(m+r)}} \right\} \otimes \boldsymbol{\kappa}_{O \times O}$ is $rO \times rO$ with $F(\boldsymbol{\rho})_{\mathbf{s}_{1:m}}, F(\boldsymbol{\rho})_{\mathbf{s}_{(m+1):(m+r)}, \mathbf{s}_{1:m}}, F(\boldsymbol{\rho})_{\mathbf{s}_{1:m}, \mathbf{s}_{(m+1):(m+r)}}, F(\boldsymbol{\rho})_{\mathbf{s}_{(m+1):(m+r)}}$ being the corresponding $m \times m$, $r \times m$, $m \times r$, $r \times r$ sub-matrices of the $(m+r) \times (m+r)$ matrix $F(\boldsymbol{\rho})_{\mathbf{s}_{1:(m+r)}}$.

If the spatially extended latent NNGP prior $\tilde{\pi}(\boldsymbol{\alpha}_{jl_j}(\mathbf{s}_{1:(m+r)}) | \boldsymbol{\kappa}, \boldsymbol{\rho})$ for all (j, l_j) (Section 4.5) is placed instead, then for any fixed (j, l_j) ,

$$\begin{aligned} \tilde{f}(\boldsymbol{\alpha}_{jl_j}(\mathbf{s}_{(m+1):(m+r)}) | \boldsymbol{\alpha}_{jl_j}(\mathbf{s}_{1:m}), \boldsymbol{\kappa}, \boldsymbol{\rho}) &= \prod_{i_r=1}^r \tilde{f}(\boldsymbol{\alpha}_{jl_j}(\mathbf{s}_{(m+i_r)}) | \boldsymbol{\alpha}_{jl_j}(\mathbf{s}_{1:m}), \boldsymbol{\kappa}, \boldsymbol{\rho}) \\ &= \prod_{i_r=1}^r f(\boldsymbol{\alpha}_{jl_j}(\mathbf{s}_{(m+i_r)}) | \boldsymbol{\alpha}_{jl_j, N(\mathbf{s}_{(m+i_r)})}, \boldsymbol{\kappa}, \boldsymbol{\rho}) \sim \prod_{i_r=1}^r N_O \left(B_{\mathbf{s}_{(m+i_r)}} \boldsymbol{\alpha}_{jl_j, N(\mathbf{s}_{(m+i_r)})}, F_{\mathbf{s}_{(m+i_r)}} \right). \end{aligned} \quad (5.5)$$

For each i_r , $B_{\mathbf{s}_{(m+i_r)}} = \left\{ F(\boldsymbol{\rho})_{\mathbf{s}_{(m+i_r)}, N(\mathbf{s}_{(m+i_r)})} [F(\boldsymbol{\rho})_{N(\mathbf{s}_{(m+i_r)})}]^{-1} \right\} \otimes I_{O \times O}$ is $O \times hO$, and $F_{\mathbf{s}_{(m+i_r)}} = \left\{ F(\boldsymbol{\rho})_{\mathbf{s}_{(m+i_r)}} - F(\boldsymbol{\rho})_{\mathbf{s}_{(m+i_r)}, N(\mathbf{s}_{(m+i_r)})} [F(\boldsymbol{\rho})_{N(\mathbf{s}_{(m+i_r)})}]^{-1} F(\boldsymbol{\rho})_{N(\mathbf{s}_{(m+i_r)}), \mathbf{s}_{(m+i_r)}} \right\} \otimes \boldsymbol{\kappa}_{O \times O}$ is $O \times O$ with $F(\boldsymbol{\rho})_{\mathbf{s}_{(m+i_r)}} = 1$, $F(\boldsymbol{\rho})_{\mathbf{s}_{(m+i_r)}, N(\mathbf{s}_{(m+i_r)})}$, $F(\boldsymbol{\rho})_{N(\mathbf{s}_{(m+i_r)})}$, $F(\boldsymbol{\rho})_{N(\mathbf{s}_{(m+i_r)}), \mathbf{s}_{(m+i_r)}}$ being the corresponding 1×1 , $1 \times h$, $h \times 1$, $h \times h$ sub-matrices of $F(\boldsymbol{\rho})_{\mathbf{s}_{1:(m+r)}}$.

5.2 Summarizing Spatial Clusters with Similar Temporal Trajectories

For our spatiotemporal factor models specified in Sections 2.2 and 3, clustering information for temporal trajectories $\{\mathbf{y}_t : t = 1, \dots, T\}$ is fully encoded by the factor loadings matrix $\Lambda_{mO \times k}$. Individual clustering on each column $\boldsymbol{\lambda}_j$ of Λ is impossible since we have sacrificed individual identifiability to incorporate spatial dependency by adopting a spatial NNGP prior,

which fully specifies Λ . Nevertheless, we can indeed produce satisfactory clustering outcomes based on information contained in all k columns of Λ , as the factor loadings in their entirety are identifiable. The posterior distribution of the mixture weights $w_{jl}(\mathbf{s}_{i,o})$'s, which can be readily computed from posterior samples of the latent variables $\alpha_{jl}(\mathbf{s}_{i,o})$'s, contains pertinent spatial clustering information for λ_j 's.

Fix an arbitrary $o \in \{1, \dots, O\}$. Let $\mathbf{w}_o(\mathbf{s}_i) = \{w_{jl}(\mathbf{s}_{i,o})\}_{j=1, \dots, k, l_j=1, \dots, L_j}$ for all i , where L_j can be replaced by a common L under our model in Section 2.2. Then spatial proximity information has been encoded into $\mathbf{w}_o = [\mathbf{w}_o(\mathbf{s}_1), \dots, \mathbf{w}_o(\mathbf{s}_m)]^\top$, which is of dimension $m \times \sum_{j=1}^k L_j$. Any two locations \mathbf{s}_i and $\mathbf{s}_{i'}$ ($i, i' \in \{1, \dots, m\}$) would have similar temporal trajectories for observation type o if the two vectors $\mathbf{w}_o(\mathbf{s}_i)$ and $\mathbf{w}_o(\mathbf{s}_{i'})$ are close to each other. Therefore, we can apply k-means clustering to the $m \times \sum_{i=1}^n \sum_{j=1}^k L_j^{(t_i)}$ matrix $(\hat{\mathbf{w}}_o^{(t_1)}, \hat{\mathbf{w}}_o^{(t_2)}, \dots, \hat{\mathbf{w}}_o^{(t_n)})$, where each $L_j^{(t_i)}$ represents the estimated number of clusters for factor j in the t_i^{th} MCMC iteration, and $\hat{\mathbf{w}}_o^{(t_1)}, \dots, \hat{\mathbf{w}}_o^{(t_n)}$ denote the corresponding posterior samples of weights parameters for all m locations from $n \in \mathbb{N}$ selected kept post-burn-in MCMC iterations. Under our model in Section 2.2, the matrix $(\hat{\mathbf{w}}_o^{(t_1)}, \hat{\mathbf{w}}_o^{(t_2)}, \dots, \hat{\mathbf{w}}_o^{(t_n)})$ is of dimension $m \times nkL$ instead, and we can opt to apply k-means clustering to the corresponding posterior mean matrix $\hat{\mathbf{w}}_o = [\hat{\mathbf{w}}_o(\mathbf{s}_1), \dots, \hat{\mathbf{w}}_o(\mathbf{s}_m)]_{m \times nkL}^\top$ as well.

6 Simulation Experiments

This section presents a series of simulation experiments that primarily aim to showcase the significant improvements in computational efficiency and scalability by incorporating our proposed slice sampling (Section 3), spatial latent NNGP and sequential updating algorithms (Section 4) and thus verify the theoretical results we obtained in Appendix H. This section also demonstrates our novel frameworks' great comprehensive modeling performances and inferential capabilities. We consider four models with spatial clustering capabilities, which we shall denote as `fullGPFixedL`, `NNGPblockFixedL`, `NNGPsequenFixedL`, and `NNGPsequenVaryLj`, respectively. The first three models are under our framework delineated in Section 2.2 with a common number of spatial mixture components L across all factors, where `fullGPFixedL` adopts the full spatial GP prior, and the latter two models adopt our spatial latent NNGP prior (Section 4) with α_{jl} 's updated in the block-wise (Equation (4.6)) and sequential (Section 4.4) manners. The last model `NNGPsequenVaryLj` is under our framework depicted in Section 3 with a varying number of mixture components L_j ($j = 1, \dots, k$) assumed, the spatial latent NNGP prior assigned, and α_{jl} 's sampled sequentially.

6.1 Computational Efficiency and Goodness-of-Fit for Main Model Fitting

We first corroborate the great posterior sampling acceleration capabilities (Appendix H) and reasonably satisfactory overall performances of our guaranteed non-increasing cluster number (Section 3) and high spatial scalability (Section 4) techniques in terms of fitting our main spatiotemporal Bayesian Gaussian factor analysis models.

We simulated data from a full model with exponential temporal covariance, spatial dependence under a Gaussian process, and the PSBP clustering mechanism. A unanimous cluster

number upper bound of 20 was set, and the actual numbers of clusters for the k factors were randomly sampled between 1 and 20. We set the number of observation types $O = 1$, the number of latent factors $k = 6$, the spatial tuning parameter $\rho = 0.8$, the temporal tuning parameter $\psi = 2.3$, and $\sigma^2(\mathbf{s}_i) = 0.01$ for all $i \in \{1, \dots, m\}$. We specified $T = 30$ equal-distanced time points $t = 1, \dots, 30$ and $m = 30^2 = 900$ spatial locations $\mathbf{s}_i = (i_1, i_2)$ for $i = 1, 2, \dots, 900$ on an equispaced 2-dimensional grid, where $i_1, i_2 \in \{1, 2, \dots, 30\}$ satisfy $30 \cdot (i_1 - 1) + i_2 = i$ for each i . m is deliberately set large to highlight the computation time differences between our models.

When fitting all four models, we specified the temporal correlation structure and spatial neighborhood structure matrices as $[H(\psi)]_{tt'} = \exp\{-\psi|t - t'|\}$ for all $t, t' \in \{1, \dots, T\}$ and $F(\rho) = \exp\{-\rho D\}$, respectively, where $D_{m \times m}$ denotes the Euclidean distance matrix for our m spatial locations. We also assumed no additional covariates $\mathbf{x}_t(\mathbf{s}_{i,o})$'s. For the last three models with spatial latent NNGP priors, we set $h = 15$. The fixed cluster number L is specified to be $\min\{60, m\}$ for the first three models, and a starting value and hence upper bound of $\min\{100, m\}$ is assigned to all L_j 's for the last model `NNGPsequenVaryLj`. We ran each MCMC chain for 10^4 post-burn-in iterations, which were thinned to 5000 samples for analysis. For each of our four models, quite a few choices of burn-in lengths were tried to determine appropriate ones leading to satisfactorily converged MCMC chains within the post-burn-in ranges.

Model	Burn-in and Post-burn-in Lengths	Computation Time
<code>fullGPFixedL</code>	20000 + 10000 = 30000	20.6 days
<code>NNGPblockFixedL</code>	20000 + 10000 = 30000	20.21 days
<code>NNGPsequenFixedL</code>	20000 + 10000 = 30000	22.96 hours
	40000 + 10000 = 50000	2.28 days
<code>NNGPsequenVaryLj</code>	20000 + 10000 = 30000	9.12 hours
	40000 + 10000 = 50000	22.36 hours

Table 1: Model fitting time for our four spatiotemporal Bayesian Gaussian factor models with 10^4 post-burn-in MCMC iterations and various burn-in lengths.

As shown by Table 1, `NNGPblockFixedL` is slightly faster than `fullGPFixedL` in terms of model fitting, which results from replacing $F(\rho)_{m \times m}$ under the full GP prior by a sparse $\tilde{F}(\rho)_{m \times m}$ under our spatial latent NNGP prior (Section 4.3). One of our most eminent achievements here is rapidly increasing the MCMC's computation speed by more than 20 times via sequentially updating the latent α_{jl} 's in `NNGPsequenFixedL`, which justifies our claims on computational complexity improvements made near the end of Section 4.4. Aligning with our discussions in Sections 3 and 4.4, computation time per MCMC iteration can further be significantly reduced by upgrading our modeling framework from the one in Section 2.2 to its counterpart in Section 3. The resultant `NNGPsequenVaryLj` model stays as the conspicuous fastest since it incorporates both non-increasing estimates for the spatial cluster number parameters L_j 's guaranteed by our slice sampling construction (Section 3) and great spatial scalability from our latent NNGP prior (Section 4.3) and corresponding sequential updating approach (Equation (4.9)).

Figure 1 suggests that compared to their `fullGPFixedL` counterpart, the posterior deviances for our latter two models decrease significantly slower as the number of MCMC iterations increases. Hence, it may take more iterations for the MCMC chain corresponding to

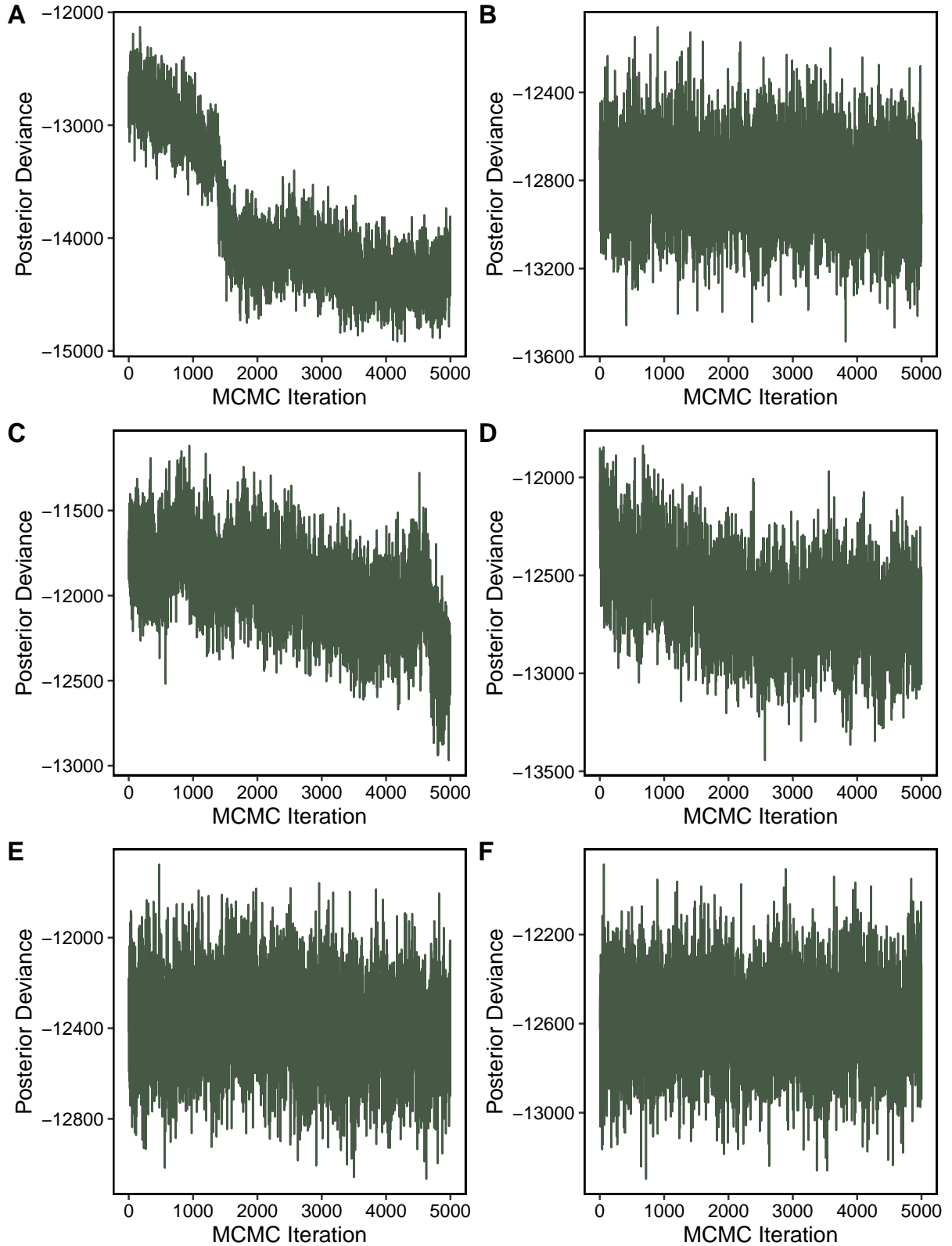


Figure 1: Posterior deviance plots for the six settings under our four models given in Table 1 (A: fullGPfixedL 20000 burn-in; B: NNGPblockFixedL 20000 burn-in; C: NNGPsequenFixedL 20000 burn-in; D: NNGPsequenFixedL 40000 burn-in; E: NNGPsequenVaryLj 20000 burn-in; F: NNGPsequenVaryLj 40000 burn-in). For each of the six trace plots, the horizontal axis denotes the kept $10000 \div 2 = 5000$ post-burn-in MCMC iterations, and the vertical axis presents the corresponding posterior deviance values.

NNGPsequenFixedL or NNGPsequenVaryLj to fully converge. However, the substantial gain in computational efficiency per MCMC iteration outweighs the extra time needed to run moderately longer chains, and thus the overall till-convergence model fitting time can still be considerably reduced by adopting the spatial NNGP prior and sequential updating algorithms in our latter two models NNGPsequenFixedL and NNGPsequenVaryLj.

In terms of posterior deviance alone, fullGPFixedL appears to be the clear best among the four models, followed by NNGPblockFixedL, NNGPsequenVaryLj, and finally NNGPsequenFixedL, after taking convergence speed and extent as well as post-convergence deviance values into consideration (Figure 1). To get a more complete picture of all models' diverse fitting performances, we further consider an array of diagnostics statistics as defined below.

We first devise some diagnostics metrics based on in-sample prediction. Let $N = m \times O \times T$ and denote \mathbf{y}_{obs} as our $N \times 1$ observed outcome vector. For each of the kept $W = 5000$ post-burn-in MCMC iterations, we draw a predicted outcome vector $\hat{\mathbf{y}}_{N \times 1}^{(w)}$, $w \in \{1, \dots, W\}$, based on the w^{th} sampled posterior parameters. Let

$$\begin{aligned} \text{postMeanMSE} &= \frac{1}{mOT} \sum_{t=1}^T \sum_{o=1}^O \sum_{i=1}^m \left(\left[\frac{1}{W} \sum_{w=1}^W \hat{y}^{(w)}(i, o, t) \right] - y_{\text{obs}}(i, o, t) \right)^2, \\ \text{postMSE} &= \frac{1}{mOT} \sum_{t=1}^T \sum_{o=1}^O \sum_{i=1}^m \left\{ \frac{1}{W} \sum_{w=1}^W \left[\hat{y}^{(w)}(i, o, t) - y_{\text{obs}}(i, o, t) \right]^2 \right\}, \text{ and} \\ \text{postVar} &= \frac{1}{mOT} \sum_{t=1}^T \sum_{o=1}^O \sum_{i=1}^m \text{Var} \left(\hat{\mathbf{y}}^{(1:W)}(i, o, t) \right). \end{aligned}$$

Then `postMeanMSE` and `postMSE` adequately assess model accuracy, and `postVar` is an appropriate precision measure. Small values for the three statistics are desired.

We further consider two sets of diagnostics statistics based on the posterior mean estimates and all 5000 kept iterations' posterior parameter estimates, both of which stem from the posterior log-likelihoods and incorporate goodness-of-fit assessments as well as over-complexity penalty terms. The main deviance information criterion DIC (Spiegelhalter et al. 2002) statistic `dic` can be written as the sum of two values, one of which portrays model complexity and is denoted as `pD`. The Watanabe–Akaike information criterion WAIC (Vehtari, Gelman, and Gabry 2017) consists of two over-fit measurements `p_waic_1`, `p_waic_2`, a log predictive density `lppd`, and a main metric `waic = -2lppd + 2p_waic_2`. For all involved metrics except `lppd`, smaller values imply better model fit.

Table 2 presents our obtained values of the nine aforementioned diagnostics metrics that gauge the quality of model fitting, which reassure us that all six model settings do lead to satisfactorily good comprehensive modeling performances. Quite evidently, `fullGPFixedL` appears to be the best, followed by `NNGPblockFixedL`, `NNGPsequenVaryLj`, and finally `NNGPsequenFixedL`.

As demonstrated by the attained simulation results in Tables 1 and 2, our novel proposals of adopting slice sampling, spatial latent NNGP prior and sequential updating methods elaborated in Sections 3 and 4 markedly accelerate the Bayesian posterior sampling compared to full GP-based spatiotemporal Bayesian factor modeling in Berchuck et al. (2022) while maintaining satisfactory model fitting performances, and are thus tremendously helpful in numerous practical application settings.

Model	fullGPfixedL	NNGPblockFixedL	NNGPsequenFixedL		NNGPsequenVaryLj	
Burn-in Length	20000	20000	20000	40000	20000	40000
postMeanMSE	0.01230704	0.01484547	0.01502469	0.01423334	0.01483675	0.01518092
postMSE	0.09525559	0.1004471	0.103372	0.1010104	0.1018498	0.1011682
postVar	0.08297621	0.08561875	0.08836496	0.08679443	0.08703041	0.08600445
pD	-201218.8	-81137.15	-231.4574	-1583.148	-11656.51	-1915.569
dic	-186963.2	-93951.24	-12184.04	-14210.3	-24045.39	-14510.32
p_waic.1	646.7417	700.5938	998.857	800.128	660.0966	686.2738
p_waic.2	12213.33	9794.118	16176.54	13082.57	10034.08	10056.2
lppd	7451.174	6757.339	6475.722	6713.638	6524.489	6640.51
waic	9524.304	6073.557	19401.63	12737.87	7019.178	6831.377

Table 2: Obtained values of our aforementioned nine diagnostics statistics for the six selected settings under our four models (Table 1). Each setting has $10000 \div 2 = 5000$ kept post-burn-in MCMC iterations for analysis. The first column only utilizes posterior samples from the latter 3000 of the 5000 iterations due to convergence concerns (Figure 1), whereas all other columns are based on all 5000 kept iterations’ posterior parameter estimates.

6.2 Efficiency, Accuracy, and Precision for Predictions at New Locations

We next perform two simulation experiments, one with a moderately large T and a relatively small m and the other with a moderately large m and a small T , to validate the significant spatial prediction acceleration (Appendices H.1, H.2 and H.4) attributable to our slice sampling techniques (Section 3) and spatial latent NNGP prior (Section 4) and to showcase our four models’ adequate out-of-sample prediction capabilities at new locations, respectively. Throughout this subsection, we run 20000 burn-in iterations and keep $W = 5000$ out of 10000 post-burn-in iterations’ posterior samples for our MCMC chains.

Equations (5.2) and (G.12) suggest that NNGPsequenVaryLj should be markedly faster than the other three models in spatial prediction, especially when the number of spatial mixture components is moderate to large. The formulae for obtaining a predicted spatial latent parameter $\hat{\alpha}_{jl}(\mathbf{s}_{(m+1):(m+r)})$ for any $(j, l) \in \{1, \dots, k\} \times \{1, \dots, L - 1\}$ presented in the case discussion portion at the end of Appendix G.2.2 indicate that fullGPfixedL should take noticeably longer time to predict outcomes at new spatial locations than NNGPblockFixedL and NNGPsequenFixedL, especially when the number of spatial locations is moderate to large. Since there are no differences between the spatial prediction procedures for NNGPblockFixedL and NNGPsequenFixedL, these two models should be comparably fast. See Table 8 in Appendix H.4.

Our first experiment aims to substantiate these implications and thus corroborate our previous statements (Sections 3 and 4.5) on and theoretical results obtained (Appendix H.4) regarding spatial prediction acceleration. A total of $N_1 = 48$ samples of data were simulated with five selected random number generation seeds under the same data generation mechanism in Section 6.1, except that we specified $k = 3$, $T = 20$, and $m = 6^2 = 36$ here. When fitting the four models, we followed our specifications in Section 6.1 with $h = 15$, except that we set 25 as both the fixed cluster number L for the first three models and the upper bound for all L_j ’s for the last model NNGPsequenVaryLj.

We utilize a leave-one-out cross-validation approach to record sufficient spatial prediction

time instances for analysis. For each of our N_1 simulated data sets and each of the m location points, we first formulate a sub data set excluding only observations from this particular location. Then for each of our four models, we use this sub data set to obtain a model fit object, which is then used to make predictions for the outcome variable at the taken-out location. Figure 2 and Table 3 display the box and violin plots of and some summary statistics for our recorded four sets of $N_1 \cdot m$ spatial prediction time realizations. Reassuringly, `NNGPsequenVaryLj` does turn out to be the conspicuous fastest, and `fullGPfixedL` does appear to be the evident slowest. `NNGPblockFixedL` and `NNGPsequenFixedL` indeed have quite close spatial prediction times.

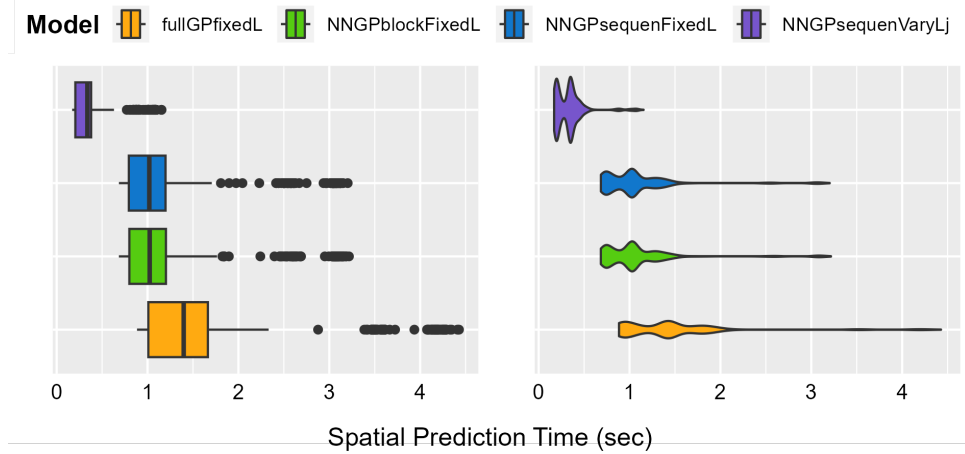


Figure 2: Box and violin plots of the $N_1 \cdot m$ time realizations (in seconds) for making predictions at a taken-out location based on a model fit with all other locations' observed data we obtained for our four models.

Model	Min	1 st Quantile	Median	Mean	3 rd Quantile	Max
<code>fullGPfixedL</code>	0.884	1.008	1.398	1.446	1.664	4.427
<code>NNGPblockFixedL</code>	0.6842	0.7999	1.0237	1.0859	1.2025	3.2165
<code>NNGPsequenFixedL</code>	0.6847	0.7940	1.0195	1.0758	1.1978	3.2028
<code>NNGPsequenVaryLj</code>	0.1700	0.2056	0.3380	0.3358	0.3795	1.1545

Table 3: Summary statistics for the time (in seconds) it needs to make predictions at a taken-out location based on a model fit with all other locations' observed data for our four major models. Each row of the table presents some summary statistics for the $N_1 \cdot m$ time intervals (in seconds) corresponding to one of our four modeling frameworks.

Our second experiment is designed to demonstrate the four models' satisfactory performances in new-location prediction. $N_2 = 10$ data sets were simulated from a full model with exponential temporal covariance, spatial dependence under a Gaussian process, and the PSBP clustering mechanism. We set a unanimous cluster number upper bound of 5 for the k actual numbers of spatial mixture components, the number of observation types $O = 1$, the number of latent factors $k = 3$, the spatial tuning parameter $\rho = 0.8$, the temporal tuning parameter $\psi = 2.3$, and $\sigma^2(\mathbf{s}_i) = 0.01$ for all $i \in \{1, \dots, m\}$. We specified $T = 5$ equal-distanced time points $t = 1, 2, \dots, 5$ and $m = 20^2 + 5^2 = 425$ spatial locations $\mathbf{s}_i = (i_1, i_2)$ for $i = 1, 2, \dots, m$ on a 2-dimensional grid, where $(i_1, i_2) \in \{1, 2, \dots, 20\} \times \{1, 2, \dots, 20\} \cup \{8.5, 9.5, 10.5, 11.5, 12.5\} \times$

$\{8.5, 9.5, 10.5, 11.5, 12.5\}$. Each of our N_2 simulated data sets is divided into a training set and a testing set, where the training set consists of data on $m_0 = 20^2 = 400$ spatial locations $\mathbf{s}_i = (i_1, i_2)$ for $i = 1, 2, \dots, m_0$ with $(i_1, i_2) \in \{1, 2, \dots, 20\} \times \{1, 2, \dots, 20\}$, and the testing set consists of data on the remaining $r = 5^2 = 25$ spatial locations $\mathbf{s}_{i_r} = (i_{r_1}, i_{r_2})$ for $i_r = 1, 2, \dots, r$ with $(i_{r_1}, i_{r_2}) \in \{8.5, 9.5, 10.5, 11.5, 12.5\} \times \{8.5, 9.5, 10.5, 11.5, 12.5\}$. We set 5 as both the fixed cluster number L in the first three models and the upper bound for all L_j 's in the last model `NNGPsequenVaryLj` and $h = 15$ for the last three models with spatial latent NNGP priors.

Fix any arbitrary $n \in \{1, \dots, N_2\}$ and consider the corresponding simulated data set. Let

$$\begin{aligned} \text{postMeanMSE}_n &= \frac{1}{rOT} \sum_{i_r=1}^r \sum_{t=1}^T \sum_{o=1}^O \left(\left[\frac{1}{W} \sum_{w=1}^W \hat{y}^{(w)}(i_r, o, t) \right] - y_{\text{actual}}(i_r, o, t) \right)^2, \\ \text{postMSE}_n &= \frac{1}{rOT} \sum_{i_r=1}^r \sum_{t=1}^T \sum_{o=1}^O \left\{ \frac{1}{W} \sum_{w=1}^W \left[\hat{y}^{(w)}(i_r, o, t) - y_{\text{actual}}(i_r, o, t) \right]^2 \right\}, \text{ and} \\ \text{postVar}_n &= \frac{1}{rOT} \sum_{i_r=1}^r \sum_{t=1}^T \sum_{o=1}^O \text{Var} \left(\hat{\mathbf{y}}^{(1:W)}(i_r, o, t) \right), \end{aligned}$$

where for each (i_r, o, t, w) , $\hat{y}^{(w)}(i_r, o, t)$ represents our out-of-sample predicted outcome for observation type o at location \mathbf{s}_{i_r} and time t based on the w^{th} kept post-burn-in MCMC iteration's posterior parameter estimates from a model fit with observed data from all m_0 training locations, and $y_{\text{actual}}(i_r, o, t)$ is the corresponding actual observed outcome value not utilized when fitting the models. Then $\text{medianPostMeanMSE} = \text{median}(\{\text{postMeanMSE}_n : n \in \{1, \dots, N_2\}\})$ and $\text{medianPostMSE} = \text{median}(\{\text{postMSE}_n : n \in \{1, \dots, N_2\}\})$ can decently assess the accuracy of our new-location predictions, and an appropriate prediction precision measure here would be $\text{medianPostVar} = \text{median}(\{\text{postVar}_n : n \in \{1, \dots, N_2\}\})$. As Table 4 suggests, all our four models deliver satisfactory spatial prediction performances. Reassuringly, `NNGPsequenVaryLj` yields adequate new-location predictions comparable to the other three models, whose performances are quite close to each other in terms of all three metrics.

Model	medianPostMeanMSE	medianPostMSE	medianPostVar
fullGPFixedL	0.3135884	1.721560	1.383646
NNGPblockFixedL	0.3103727	1.721162	1.385365
NNGPsequenFixedL	0.3122864	1.719186	1.385953
NNGPsequenVaryLj	0.3088113	2.280650	1.918565

Table 4: Our obtained values of the aforementioned three metrics for our four models. Smaller values for any of the three statistics imply better new-location prediction capabilities of a particular model.

6.3 Accuracy for Spatial Clustering of Temporal Trends

Finally, we design and implement a simulation experiment to demonstrate our four models' satisfactory performances regarding our prime goal of clustering spatial locations into regions with similar temporal trajectories.

We adopted a data generation mechanism specifically designed to assess clustering accuracy. The number of factors was set to $k = 2$, and the actual numbers of clusters for both factors were also set to 2. We specified $\theta_{11} = \theta_{12} = 5$, $\theta_{21} = 10$, and $\theta_{22} = -10$ for the atoms θ_{jl} 's. For each of our $N = 100$ simulated data sets, $m = 10^2 = 100$ spatial points $\mathbf{s}_i = (i_1, i_2)$ for $i = 1, 2, \dots, 100$ on an equispaced 2-dimensional grid, where $i_1, i_2 \in \{1, 2, \dots, 10\}$ satisfy $10 \cdot (i_1 - 1) + i_2 = i$ for each i , were randomly assigned to one of the two actual spatial groups (one corresponding to $(\theta_{11}, \theta_{21}) = (5, 10)$ and the other corresponding to $(\theta_{12}, \theta_{22}) = (5, -10)$) with equal probabilities. All other settings are almost identical to their counterparts in the previous two subsections. We set $O = 1$, $\psi = 2.3$, $\sigma^2(\mathbf{s}_i) = 0.01$ for all i and specified $T = 30$ time points $t = 1, 2, \dots, 30$. When fitting the models, a burn-in length of 20000 and a post-burn-in length of 10000 (thinned to 5000) were used throughout.

For each of the $N = 100$ simulated data sets and each of our four models, we performed k-means clustering on three posterior weights matrices formulated from 10, 100, and 1000 selected equally dispersed kept post-burn-in MCMC iterations' parameter estimates, as described by the last paragraph in Section 5.2. We then computed the $N \cdot 4 \cdot 3$ accuracy ratios and calculated the Rand index between the actual spatial grouping and each of our obtained $N \cdot 4 \cdot 3$ clustering outcomes to assess spatial clustering performances. Since we specified only 2 actual spatial groups and k-means clusters, there are no label-switching issues. As shown by our constructed box plots and violin plots (Figures 3 and 4), `fullGPfixedL` and `NNGPblockFixedL`, whose performances are quite close, both produce highly accurate spatial clustering results, in that the majority of their corresponding accuracy ratios and Rand indices are very close to 1. `NNGPsequenFixedL` performs conspicuously worse than the aforementioned two models but still leads to satisfactorily accurate clustering outcomes. Although `NNGPsequenVaryLj` is notably behind the other 3 models in terms of spatial clustering accuracy, its performance is still acceptably good.

Last but not least, we present one specific spatial clustering example, where the actual grouping of the $m = 10^2$ spatial points is depicted in Figure 5A. Reassuringly, the clustering outcomes we obtained from three of our four models, `fullGPfixedL`, `NNGPblockFixedL`, and `NNGPsequenFixedL`, all agree exactly with Figure 5A and are thus completely accurate. The fourth model, `NNGPsequenVaryLj`, also produces largely accurate clustering results (Figure 5B).

7 Discussion

This article introduces several strategies to enhance the scalability of Bayesian nonparametric factor analysis applied to spatiotemporal data. We derive a new slice sampling algorithm that accommodates unknown varying numbers of spatial mixture components across all factors. In addition, we integrate within the PSBP prior a nearest-neighbor Gaussian process along with new sequential updating methods for the spatially varying latent variables. The main goal is to significantly reduce the computational complexities and ease the storage requirements associated with two of the most computationally intensive steps in Berchuck et al. (2022)'s original MCMC algorithm, that is, the sampling of factor loadings under a Bayesian nonparametric spatial mixture prior and the sampling of spatially varying latent variables from a Gaussian process prior. Our refined MCMC algorithms lead to considerably accelerated posterior sam-

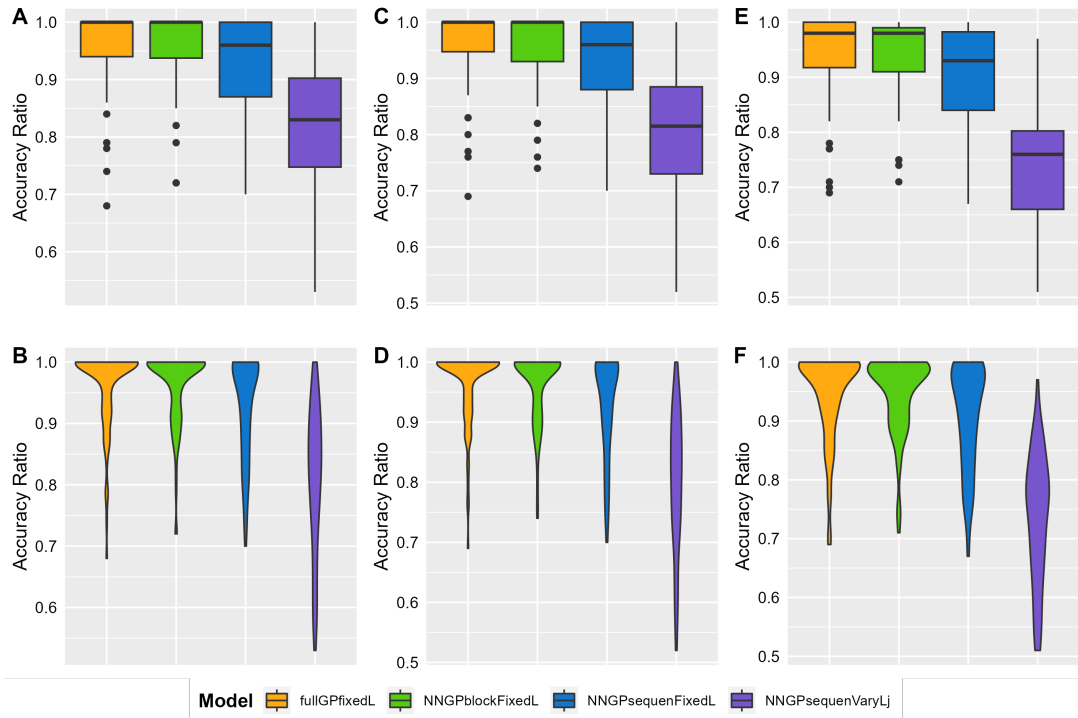


Figure 3: Box and violin plots of the $N = 100$ spatial clustering accuracy ratios calculated from 1000 (A, B), 100 (C, D), and 10 (E, F) selected equally dispersed kept post-burn-in MCMC iterations' posterior weights parameter estimates based on our four models.

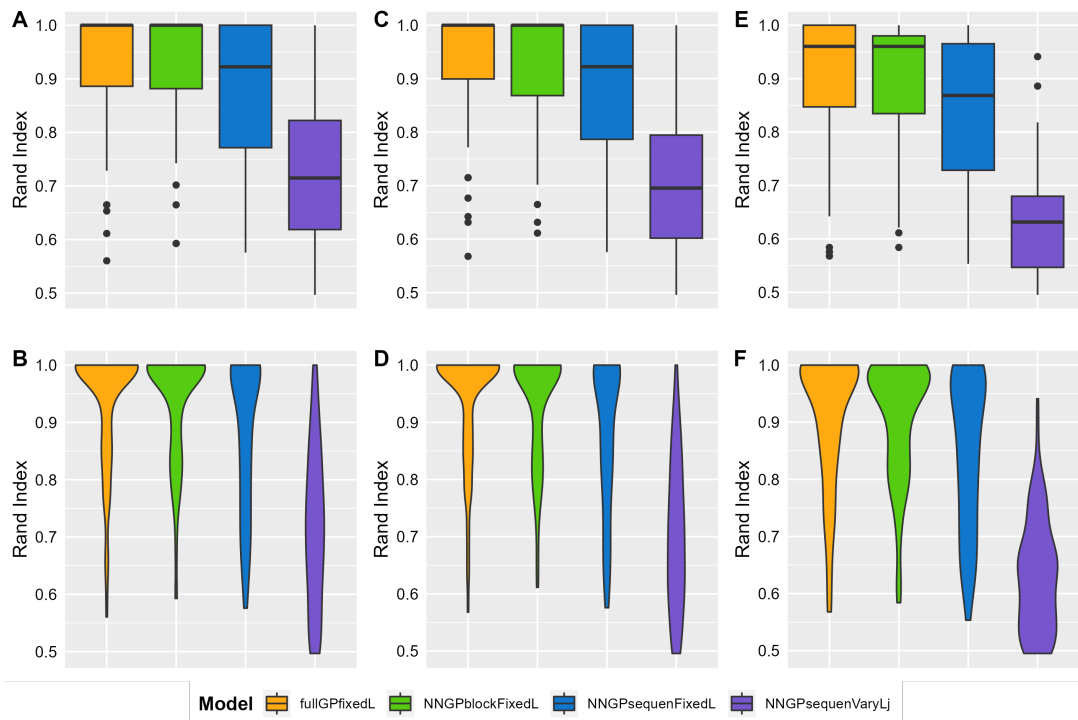


Figure 4: Box and violin plots of the Rand index between the actual spatial clustering and each of our obtained $N = 100$ clustering outcomes calculated from 1000 (A, B), 100 (C, D), and 10 (E, F) selected equally dispersed kept post-burn-in MCMC iterations' posterior weights parameter estimates based on our four models.

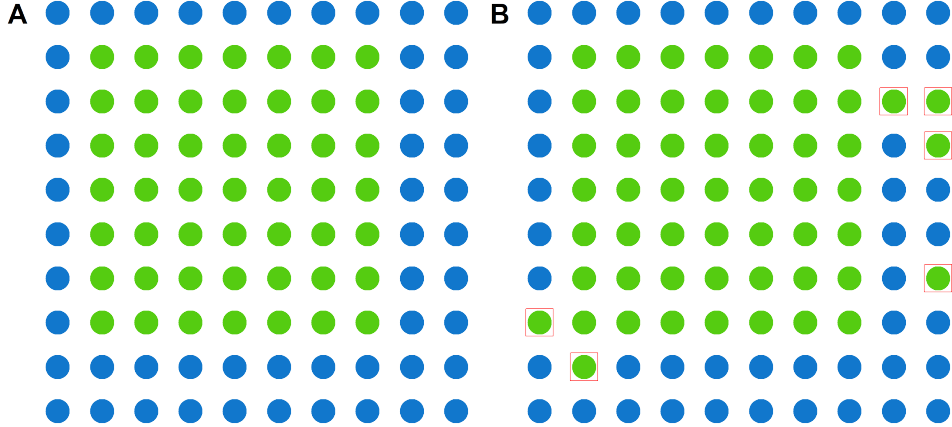


Figure 5: The actual spatial grouping (**A**), which also turns out to be the clustering outcome from our models `fullGPfixedL`, `NNGPblockFixedL`, and `NNGPsequenFixedL`, and the obtained clustering outcome from our model `NNGPsequenVaryLj` (**B**) for our specific example. The two colors represent the two groups for our $m = 10^2 = 100$ spatial locations, and the spatial points with outer red squares (**B**) are the ones clustered wrongly by the model `NNGPsequenVaryLj`. For each of our four models, the attained clustering results are the same for all three choices of numbers of selected kept post-burn-in MCMC iterations (10, 100, and 1000) from which our posterior weights matrices for k-means clustering (Section 5.2) are formulated.

pling and spatial prediction while maintaining comparable comprehensive performances in main model fitting and pivotal inferential procedures including spatial prediction and temporal trends clustering, as substantiated by our simulation experiments.

We discuss several potential extensions for our current work. First, although we have adopted the same PSBP prior as in Berchuck et al. (2022), slice sampling for stick-breaking processes with non-probit links can be similarly derived. Second, we have incorporated the NNGP prior mainly for the computational advantages of sparse GP approximation methods. Since NNGP falls in the broader class of Vecchia approximation (Vecchia 1988, Katzfuss and Guinness 2021), there are possibilities to integrate other versions of Vecchia approximation that better characterize the adjacency of spatial locations while maintaining accurate sparse approximations to the GP precision matrix. Third, our treatment of latent temporal trajectories assumes homoscedastic and stationary processes for $\{\boldsymbol{\eta}_t\}_{t=1}^T$, which is inadequate for certain data sets. To enable temporal structure generalizations, we may explore and integrate into our models pertinent Bayesian GARCH (Jensen and Maheu 2013, Virbickaite, Ausín, and Galeano 2015) ideas. Finally, the Gaussian response model in the main article is inapplicable to an array of common non-normal observed data types. In Appendix I, we have accommodated the binary response model with a logit link by utilizing a Pólya-Gamma data augmentation technique. Further extensions could involve other generalized linear models with non-Gaussian likelihoods such as Poisson regression, which will be particularly useful for modeling spatiotemporal count data. We will explore these directions in future research.

The Appendices are structured as follows. Appendix A provides full Gibbs sampling details for our three spatiotemporal Bayesian Gaussian factor models (Sections 2.1, 2.2 and 3). Appendix B elaborates on temporal-related computational burdens for a large number of time points $T \in \mathbb{N}$, $T > 1$ and our corresponding powerful acceleration solutions when all time points are equally spaced. Appendix C models the latent temporal process $\{\boldsymbol{\eta}_t\}_{t=1}^T$ using a VAR(1) structure for evenly dispersed time points. Appendices D to H complement Sections 2 to 5, respectively. More specifically, Appendix D presents detailed methodology and justification with respect to introducing latent normal variables $z_{jl}(\mathbf{s}_{i,o}) \stackrel{\text{ind}}{\sim} N(\alpha_{jl}(\mathbf{s}_{i,o}), 1)$ to bring about conjugacy for $\boldsymbol{\alpha}_{jl}$'s and thus enabling computationally feasible posterior sampling for our model in Section 2.2; Appendix E offers some pivotal notes regarding our novel approach adapting slice sampling (Walker 2007) for computationally and storage-wise efficient Bayesian spatial clustering not mentioned in Section 3; Appendix F gives some general comments on the Nearest-Neighbor Gaussian Process (NNGP); Appendix G discusses detailed procedures for predictions at future time points and cases pertaining to spatial prediction not covered in Section 5.1; Appendix H summarizes the computational complexity and memory improvements (with respect to MCMC-based posterior sampling and subsequent vital inferential tasks including spatial prediction and clustering) corresponding to each of our three novelties, i.e., slice sampling, spatial NNGP prior, and sequential updates. Finally, Appendix I extends our models to address three non-normal observation data types that still correspond to Gaussian kernels, possibly after some shrewd transformations.

A Gibbs Samplers for Our Spatiotemporal Bayesian Gaussian Factor Models

Throughout this section, `include.time = TRUE` and `include.space = TRUE` refer to the scenarios when temporal correlation and spatial dependence are taken into consideration, respectively, i.e., when the temporal correlation structure matrix $H(\psi)_{T \times T}$ and spatial neighborhood structure matrix $F(\rho)_{m \times m}$ are not fixed as identity matrices. The four specifications of `temporal.structure` - 'ar1', 'exponential', 'sar1', and 'sexponential', denote AR(1), the exponential process, and their seasonal counterparts (Section 2.1), respectively. In almost all circumstances, `spatial.structure = 'continuous'`, i.e., we set $F(\rho) = \exp\{-\rho D\}$, where $D_{m \times m}$ represents the Euclidean distance matrix for our m spatial locations. In the very rare situation when `spatial.structure = 'discrete'`, we consider $F(\rho)^{-1} = D_\omega - \rho W$, which corresponds to a Gaussian Markov random field for discrete spatial data. Finally, `spatApprox` is a logical indicating whether the spatial NNGP prior (Section 4) is adopted in place of the full GP prior. If `spatApprox = TRUE`, then `spatial.structure` must be 'continuous'.

In all three models elaborated in Sections 2.1, 2.2 and 3, the Gibbs sampling steps with respect to $\boldsymbol{\eta}_t$'s, $\Upsilon_{k \times k}$, ψ , $\boldsymbol{\beta}_{p \times 1}$, $\sigma^2(\mathbf{s}_{i,o})$'s are exactly the same and given as below.

1. Sampling from the full conditional distributions of $\boldsymbol{\eta}_t$'s:

Fix any arbitrary $t \in \{1, \dots, T\}$. Denote $\boldsymbol{\eta}_{-t}$ as the vector $(\boldsymbol{\eta}_1^\top, \dots, \boldsymbol{\eta}_{t-1}^\top, \boldsymbol{\eta}_{t+1}^\top, \dots, \boldsymbol{\eta}_T^\top)^\top$, which is of length $k(T-1)$. Let $H_{(1:T)_{-t}, (1:T)_{-t}}$, $H_{(1:T)_{-t}, t}$, $H_{t, (1:T)_{-t}}$, $H_{t, t}$ be the corresponding $(T-1) \times (T-1)$, $(T-1) \times 1$, $1 \times (T-1)$, 1×1 sub-matrices of the temporal correlation

structure matrix $H(\psi)_{T \times T}$. Then by properties of conditional distributions of jointly multivariate normals, $f(\boldsymbol{\eta}_t | \boldsymbol{\eta}_{-t}, \Upsilon, \psi) \sim N_k(\mathbb{E}_{0\boldsymbol{\eta}_t}, \mathbb{C}_{0\boldsymbol{\eta}_t})$, where $\mathbb{E}_{0\boldsymbol{\eta}_t} = (H_t^+ \otimes I_{k \times k}) \boldsymbol{\eta}_{-t}$ and $\mathbb{C}_{0\boldsymbol{\eta}_t} = H_t^* \otimes \Upsilon_{k \times k}$ with $H_t^+ = H_{t,(1:T)-t} H_{(1:T)-t,(1:T)-t}^{-1}$ and $H_t^* = H_{t,t} - H_t^+ H_{(1:T)-t,t} = H_{t,t} - H_{t,(1:T)-t} H_{(1:T)-t,(1:T)-t}^{-1} H_{(1:T)-t,t}$. Hence

$$\begin{aligned}
f(\boldsymbol{\eta}_t | \cdot) &\propto f(\mathbf{y}_t | \Lambda, \boldsymbol{\eta}_t, \boldsymbol{\beta}, \Xi) \times f(\boldsymbol{\eta}_{1:T} | \Upsilon, \psi) \\
&= f(\mathbf{y}_t | \Lambda, \boldsymbol{\eta}_t, \boldsymbol{\beta}, \Xi) \times f(\boldsymbol{\eta}_t | \boldsymbol{\eta}_{-t}, \Upsilon, \psi) \times f(\boldsymbol{\eta}_{-t} | \Upsilon, \psi) \\
&\propto f(\mathbf{y}_t | \Lambda, \boldsymbol{\eta}_t, \boldsymbol{\beta}, \Xi) \times f(\boldsymbol{\eta}_t | \boldsymbol{\eta}_{-t}, \Upsilon, \psi) \\
&\propto \exp \left\{ -\frac{1}{2} (\mathbf{y}_t - \Lambda \boldsymbol{\eta}_t - X_t \boldsymbol{\beta})^\top \Xi^{-1} (\mathbf{y}_t - \Lambda \boldsymbol{\eta}_t - X_t \boldsymbol{\beta}) \right\} \times \\
&\quad \exp \left\{ -\frac{1}{2} (\boldsymbol{\eta}_t - \mathbb{E}_{0\boldsymbol{\eta}_t})^\top \mathbb{C}_{0\boldsymbol{\eta}_t}^{-1} (\boldsymbol{\eta}_t - \mathbb{E}_{0\boldsymbol{\eta}_t}) \right\} \\
&\propto \exp \left\{ -\frac{1}{2} \boldsymbol{\eta}_t^\top \left[\mathbb{C}_{0\boldsymbol{\eta}_t}^{-1} + \Lambda^\top \Xi^{-1} \Lambda \right] \boldsymbol{\eta}_t + \boldsymbol{\eta}_t^\top \left[\mathbb{C}_{0\boldsymbol{\eta}_t}^{-1} \mathbb{E}_{0\boldsymbol{\eta}_t} + \Lambda^\top \Xi^{-1} (\mathbf{y}_t - X_t \boldsymbol{\beta}) \right] \right\} \\
&\sim N_k(\mathbb{C}_{\boldsymbol{\eta}_t} \boldsymbol{\mu}_{\boldsymbol{\eta}_t}, \mathbb{C}_{\boldsymbol{\eta}_t}), \text{ where} \\
\mathbb{C}_{\boldsymbol{\eta}_t} &= \left[\mathbb{C}_{0\boldsymbol{\eta}_t}^{-1} + \Lambda^\top \Xi^{-1} \Lambda \right]^{-1} \text{ and } \boldsymbol{\mu}_{\boldsymbol{\eta}_t} = \mathbb{C}_{0\boldsymbol{\eta}_t}^{-1} \mathbb{E}_{0\boldsymbol{\eta}_t} + \Lambda^\top \Xi^{-1} (\mathbf{y}_t - X_t \boldsymbol{\beta}).
\end{aligned} \tag{A.1}$$

2. Sampling from the full conditional distribution of $\Upsilon_{k \times k}$:

$$\begin{aligned}
f(\Upsilon | \cdot) &\propto f(\boldsymbol{\eta}_{1:T} | \Upsilon, \psi) \times f_0(\Upsilon) \sim \mathcal{IW}(T + \zeta, \Phi H(\psi)^{-1} \Phi^\top + \Omega), \\
\text{where } \Phi_{k \times T} &= (\boldsymbol{\eta}_1, \dots, \boldsymbol{\eta}_T).
\end{aligned} \tag{A.2}$$

When the number of factors $k = 1$, the above Inverse-Wishart distribution simplifies to an Inverse-Gamma distribution $\mathcal{IG}\left(\frac{T+\zeta}{2}, \frac{\Phi H(\psi)^{-1} \Phi^\top + \Omega}{2}\right)$.

3. Sampling ψ via a Metropolis step when `include.time = TRUE`:

$$f(\psi | \cdot) \propto f(\boldsymbol{\eta}_{1:T} | \Upsilon, \psi) \times f_0(\psi) \times \left| \frac{\partial}{\partial \Delta} h^{-1}(\Delta) \right| \text{ with } \boldsymbol{\eta}_{1:T} | \Upsilon, \psi \sim N_{Tk}(\mathbf{0}, H(\psi) \otimes \Upsilon). \tag{A.3}$$

In Equation (A.3), $f_0(\psi)$ refers to the uniform prior $\text{Unif}(a_\psi, b_\psi)$ when `temporal.structure = "exponential"` or `"sexponential"` and the transformed Beta prior with p.d.f $f_0(\psi) \propto (1 + \psi)^{\gamma-1} \times (1 - \psi)^{\beta-1}$ when `temporal.structure = "ar1"` or `"sar1"`. Δ is a new parameter defined to be $h(\psi) = \ln\left(\frac{\psi - a_\psi}{b_\psi - \psi}\right)$. Hence $\psi = h^{-1}(\Delta) = \frac{b_\psi \exp(\Delta) + a_\psi}{1 + \exp(\Delta)}$ and $\left| \frac{\partial}{\partial \Delta} h^{-1}(\Delta) \right| \propto \frac{\exp(\Delta)}{[1 + \exp(\Delta)]^2}$.

At each MCMC iteration $s \in \mathbb{N}$, let the current parameter estimate for ψ be $\psi^{(s)}$. We propose a new parameter value $\psi^* = h^{-1}(\Delta^*)$ with Δ^* sampled from a symmetric kernel $N(\Delta^{(s)}, \delta)$, where $\Delta^{(s)} = h(\psi^{(s)})$ and $\delta > 0$ is a tuning parameter decided after the burn-in MCMC iterations based on the acceptance rate for ψ^* , and set

$$\psi^{(s+1)} = \begin{cases} \psi^*, & \text{w.p. } \alpha(\psi^{(s)}, \psi^*) = \min\left\{\frac{f(\psi^* | \cdot)}{f(\psi^{(s)} | \cdot)}, 1\right\} \\ \psi^{(s)}, & \text{w.p. } 1 - \alpha(\psi^{(s)}, \psi^*) \end{cases}.$$

4. Sampling from the full conditional distribution of $\boldsymbol{\beta}_{p \times 1}$ when there are additional covariates \boldsymbol{x} :

$$\begin{aligned}
f(\boldsymbol{\beta}|\cdot) &\propto \prod_{t=1}^T f(\mathbf{y}_t|\Lambda, \boldsymbol{\eta}_t, \boldsymbol{\beta}, \Xi) \times f_0(\boldsymbol{\beta}) \\
&\propto \exp\left\{-\frac{1}{2}(\boldsymbol{\beta} - \boldsymbol{\mu}_{0\boldsymbol{\beta}})^\top \Sigma_{0\boldsymbol{\beta}}^{-1}(\boldsymbol{\beta} - \boldsymbol{\mu}_{0\boldsymbol{\beta}})\right\} \times \\
&\quad \prod_{t=1}^T \exp\left\{-\frac{1}{2}(\mathbf{y}_t - \Lambda\boldsymbol{\eta}_t - X_t\boldsymbol{\beta})^\top \Xi^{-1}(\mathbf{y}_t - \Lambda\boldsymbol{\eta}_t - X_t\boldsymbol{\beta})\right\} \\
&\propto \exp\left\{-\frac{1}{2}\boldsymbol{\beta}^\top \left[\Sigma_{0\boldsymbol{\beta}}^{-1} + \sum_{t=1}^T X_t^\top \Xi^{-1} X_t\right] \boldsymbol{\beta} + \boldsymbol{\beta}^\top \left[\Sigma_{0\boldsymbol{\beta}}^{-1} \boldsymbol{\mu}_{0\boldsymbol{\beta}} + \sum_{t=1}^T X_t^\top \Xi^{-1}(\mathbf{y}_t - \Lambda\boldsymbol{\eta}_t)\right]\right\} \\
&\sim N_p(V_\boldsymbol{\beta} \boldsymbol{\mu}_\boldsymbol{\beta}, V_\boldsymbol{\beta}), \text{ where} \\
V_\boldsymbol{\beta} &= \left[\Sigma_{0\boldsymbol{\beta}}^{-1} + \sum_{t=1}^T X_t^\top \Xi^{-1} X_t\right]^{-1} \text{ and } \boldsymbol{\mu}_\boldsymbol{\beta} = \Sigma_{0\boldsymbol{\beta}}^{-1} \boldsymbol{\mu}_{0\boldsymbol{\beta}} + \sum_{t=1}^T X_t^\top \Xi^{-1}(\mathbf{y}_t - \Lambda\boldsymbol{\eta}_t).
\end{aligned} \tag{A.4}$$

5. Sampling from the full conditional distributions of $\sigma^2(\mathbf{s}_{i,o})$'s:¹

Fix any arbitrary $(i, o) \in \{1, \dots, m\} \times \{1, \dots, O\}$. Then

$$\begin{aligned}
f(\sigma^2(\mathbf{s}_{i,o})|\cdot) &\propto f_0(\sigma^2(\mathbf{s}_{i,o})) \times \prod_{t=1}^T f(y_t(\mathbf{s}_{i,o})|\Lambda(\mathbf{s}_{i,o}), \boldsymbol{\eta}_t, \boldsymbol{\beta}, \sigma^2(\mathbf{s}_{i,o})) \\
&\propto [\sigma^2(\mathbf{s}_{i,o})]^{-a-1} \exp\left\{-\frac{b}{\sigma^2(\mathbf{s}_{i,o})}\right\} \times \\
&\quad \left[\sigma^2(\mathbf{s}_{i,o})\right]^{-\frac{T}{2}} \exp\left\{-\frac{1}{2\sigma^2(\mathbf{s}_{i,o})} \sum_{t=1}^T [y_t(\mathbf{s}_{i,o}) - \mathbf{x}_t(\mathbf{s}_{i,o})^\top \boldsymbol{\beta} - \boldsymbol{\lambda}(\mathbf{s}_{i,o})^\top \boldsymbol{\eta}_t]^2\right\} \\
&\propto [\sigma^2(\mathbf{s}_{i,o})]^{-a-\frac{T}{2}-1} \exp\left\{-\frac{1}{\sigma^2(\mathbf{s}_{i,o})} \left(b + \frac{1}{2} \sum_{t=1}^T [y_t(\mathbf{s}_{i,o}) - \mathbf{x}_t(\mathbf{s}_{i,o})^\top \boldsymbol{\beta} - \boldsymbol{\lambda}(\mathbf{s}_{i,o})^\top \boldsymbol{\eta}_t]^2\right)\right\} \\
&\sim \mathcal{IG}\left(a + \frac{T}{2}, b + \frac{1}{2} \sum_{t=1}^T [y_t(\mathbf{s}_{i,o}) - \mathbf{x}_t(\mathbf{s}_{i,o})^\top \boldsymbol{\beta} - \boldsymbol{\lambda}(\mathbf{s}_{i,o})^\top \boldsymbol{\eta}_t]^2\right), \text{ where} \\
&\boldsymbol{\lambda}(\mathbf{s}_{i,o})_{1 \times k}^\top \text{ denotes the row in } \Lambda_{mO \times k} \text{ corresponding to location } i \text{ and observation type } o.
\end{aligned} \tag{A.5}$$

A.1 Full Gibbs Sampling Details for Our Baseline Model in Section 2.1

When we do not consider the PSBP clustering mechanism and directly impose spatially correlated Gaussian Processes on the columns $\{\boldsymbol{\lambda}_j\}_{j=1}^k$ of the factor loadings matrix $\Lambda_{mO \times k}$, i.e., assign the prior $\boldsymbol{\lambda}_j \stackrel{\text{iid}}{\sim} N_{Om}(\mathbf{0}, \kappa_{O \times O} \otimes F(\rho)_{m \times m})$, $j \in \{1, \dots, k\}$, the corresponding Gibbs sampler steps are detailed in the following. The parameters $\boldsymbol{\lambda}_j$'s and $\boldsymbol{\sigma}^2$ ¹ are all ordered first spatially and then by observation type, i.e., the first m components of each above $Om \times 1$ vector are from observation type 1, the next m components are from observation type 2, and so on.

1. Sampling from the full conditional distributions of $\boldsymbol{\lambda}_j$'s:

Fix any arbitrary $j \in \{1, \dots, k\}$. Let $\Xi_{Om \times Om} = \text{Diag}(\boldsymbol{\sigma}_1^2, \dots, \boldsymbol{\sigma}_O^2)$, where $\boldsymbol{\sigma}_o^2 = (\sigma^2(\mathbf{s}_{1,o}), \dots, \sigma^2(\mathbf{s}_{m,o}))^\top \forall o \in \{1, \dots, O\}$. Denote Λ_{-j} as $(\boldsymbol{\lambda}_1, \dots, \boldsymbol{\lambda}_{j-1}, \boldsymbol{\lambda}_{j+1}, \dots, \boldsymbol{\lambda}_k)$,

¹ When not all observations are from the distribution family 'binomial' (Appendix I).

the sub-matrix obtained by removing the j^{th} column from $\Lambda_{Om \times k}$. For each t , let $\boldsymbol{\eta}_t^{-j}$ represent the length- $(k-1)$ sub-vector of $\boldsymbol{\eta}_t$ obtained by removing its j^{th} element. Then

$$\begin{aligned}
f(\boldsymbol{\lambda}_j|\cdot) &\propto \prod_{t=1}^T f(\mathbf{y}_t|\Lambda, \boldsymbol{\eta}_t, \boldsymbol{\beta}, \Xi) \times \pi(\boldsymbol{\lambda}_j|\kappa, \rho) \\
&\propto \exp\left\{-\frac{1}{2}\boldsymbol{\lambda}_j^{\text{T}}[\kappa^{-1} \otimes F(\rho)^{-1}]\boldsymbol{\lambda}_j\right\} \times \\
&\quad \prod_{t=1}^T \exp\left\{-\frac{1}{2}\left(\mathbf{y}_t - X_t\boldsymbol{\beta} - \Lambda_{-j}\boldsymbol{\eta}_t^{-j} - \eta_{tj}\boldsymbol{\lambda}_j\right)^{\text{T}}\Xi^{-1}\left(\mathbf{y}_t - X_t\boldsymbol{\beta} - \Lambda_{-j}\boldsymbol{\eta}_t^{-j} - \eta_{tj}\boldsymbol{\lambda}_j\right)\right\} \\
&\propto \exp\left\{-\frac{1}{2}\boldsymbol{\lambda}_j^{\text{T}}\left(\kappa^{-1} \otimes F(\rho)^{-1} + \sum_{t=1}^T \eta_{tj}^2 \Xi^{-1}\right)\boldsymbol{\lambda}_j + \boldsymbol{\lambda}_j^{\text{T}}\Xi^{-1}\left[\sum_{t=1}^T \eta_{tj}\left(\mathbf{y}_t - \Lambda_{-j}\boldsymbol{\eta}_t^{-j} - X_t\boldsymbol{\beta}\right)\right]\right\} \\
&\sim N_{Om}\left(V_{\boldsymbol{\lambda}_j}, \boldsymbol{\mu}_{\boldsymbol{\lambda}_j}, V_{\boldsymbol{\lambda}_j}\right), \text{ where} \\
V_{\boldsymbol{\lambda}_j} &= \left[\kappa^{-1} \otimes F(\rho)^{-1} + \sum_{t=1}^T \eta_{tj}^2 \Xi^{-1}\right]^{-1} \text{ and } \boldsymbol{\mu}_{\boldsymbol{\lambda}_j} = \Xi^{-1}\left[\sum_{t=1}^T \eta_{tj}\left(\mathbf{y}_t - \Lambda_{-j}\boldsymbol{\eta}_t^{-j} - X_t\boldsymbol{\beta}\right)\right].
\end{aligned} \tag{A.6}$$

When the NNGP instead of the full GP prior is adopted for the $\boldsymbol{\lambda}_j$'s, we replace $\pi(\boldsymbol{\lambda}_j|\kappa, \rho)$ and $F(\rho)$ by $\tilde{\pi}(\boldsymbol{\lambda}_j|\kappa, \rho)$ and $\tilde{F}(\rho)$ in the above equations.

2. Sampling from the full conditional distribution of $\kappa_{O \times O}$:

$$\begin{aligned}
f(\kappa|\cdot) &\propto \prod_{j=1}^k \pi(\boldsymbol{\lambda}_j|\kappa, \rho) \times f_0(\kappa) \sim \mathcal{IW}\left(mk + \nu, \sum_{j=1}^k S_{\lambda_j^{\rho}} + \Theta\right), \\
\text{where } S_{\lambda_j^{\rho}} &= A_j^{\text{T}}F(\rho)^{-1}A_j \text{ with } (A_j)_{m \times O} = (\boldsymbol{\lambda}_{j1}, \dots, \boldsymbol{\lambda}_{jO}) \forall j.
\end{aligned} \tag{A.7}$$

In Equation (A.7), we have written the $Om \times 1$ vector $\boldsymbol{\lambda}_j$ as $(\boldsymbol{\lambda}_{j1}^{\text{T}}, \dots, \boldsymbol{\lambda}_{jO}^{\text{T}})^{\text{T}}$ for all $j \in \{1, \dots, k\}$.

When $O = 1$, Equation (A.7) reduces to $\mathcal{IG}\left(\frac{mk+\nu}{2}, \frac{\sum_{j=1}^k S_{\lambda_j^{\rho}} + \Theta}{2}\right)$.

When the NNGP prior rather than the full GP prior is adopted for the $\boldsymbol{\lambda}_j$'s, we replace $\pi(\boldsymbol{\lambda}_j|\kappa, \rho)$ and $F(\rho)$ in Equation (A.7) by $\tilde{\pi}(\boldsymbol{\lambda}_j|\kappa, \rho)$ and $\tilde{F}(\rho)$ respectively.

3. Sampling ρ via a Metropolis step when `include.space = TRUE`:

$$\begin{aligned}
f(\rho|\cdot) &\propto \prod_{j=1}^k \pi(\boldsymbol{\lambda}_j|\kappa, \rho) \times f_0(\rho) \times \left|\frac{\partial}{\partial \Delta} h^{-1}(\Delta)\right| \\
&\quad \text{with } \boldsymbol{\lambda}_j|\kappa, \rho \sim N_{Om}(\mathbf{0}, \kappa \otimes F(\rho)) \quad \forall j.
\end{aligned} \tag{A.8}$$

When the NNGP prior rather than the full GP prior is adopted for the $\boldsymbol{\lambda}_j$'s, we replace $\pi(\boldsymbol{\lambda}_j|\kappa, \rho)$ and $F(\rho)$ in Equation (A.8) by $\tilde{\pi}(\boldsymbol{\lambda}_j|\kappa, \rho)$ and $\tilde{F}(\rho)$ respectively.

In Equation (A.8), $f_0(\rho)$ refers to the uniform prior $\text{Unif}(a_{\rho}, b_{\rho})$, where $a_{\rho} = 0, b_{\rho} = 1$ when `spatial.structure = 'discrete'` and $a_{\rho}, b_{\rho} \in \mathbb{R}^+$ when `spatial.structure = 'continuous'`. Δ is a new parameter defined to be $h(\rho) = \ln\left(\frac{\rho - a_{\rho}}{b_{\rho} - \rho}\right)$. Hence $\rho = h^{-1}(\Delta) = \frac{b_{\rho} \exp(\Delta) + a_{\rho}}{1 + \exp(\Delta)}$ and $\left|\frac{\partial}{\partial \Delta} h^{-1}(\Delta)\right| \propto \frac{\exp(\Delta)}{[1 + \exp(\Delta)]^2}$.

At each MCMC iteration $s \in \mathbb{N}$, let the current parameter estimate for ρ be $\rho^{(s)}$. We propose a new parameter value $\rho^* = h^{-1}(\Delta^*)$ with Δ^* sampled from a symmetric kernel $N(\Delta^{(s)}, \delta)$, where $\Delta^{(s)} = h(\rho^{(s)})$ and $\delta > 0$ is a tuning parameter decided after the burn-in MCMC iterations based on the acceptance rate for ρ^* , and set

$$\rho^{(s+1)} = \begin{cases} \rho^*, & \text{w.p. } \alpha(\rho^{(s)}, \rho^*) = \min\left\{\frac{f(\rho^*|\cdot)}{f(\rho^{(s)}|\cdot)}, 1\right\} \\ \rho^{(s)}, & \text{w.p. } 1 - \alpha(\rho^{(s)}, \rho^*) \end{cases}.$$

4. Same as Step 1 given at the start of Appendix A.
5. Same as Step 2 given at the start of Appendix A.
6. Same as Step 3 given at the start of Appendix A.
7. Same as Step 4 given at the start of Appendix A.
8. Same as Step 5 given at the start of Appendix A.

A.2 Full Gibbs Sampling Details for Our Model in Section 2.2

When we adopt the spatial PSBP clustering mechanism with a pre-determined fixed common $L \in \mathbb{N}, L > 1$ for all factors and assign the prior $\alpha_{jl} \stackrel{\text{iid}}{\sim} N_{mO}(\mathbf{0}, F(\rho)_{m \times m} \otimes \kappa_{O \times O})$, $j \in \{1, \dots, k\}, l \in \{1, \dots, L-1\}$, the corresponding Gibbs sampler steps are detailed in the following. We take note that only z_{jl} 's and α_{jl} 's are ordered first by observation type and then spatially, i.e., the first O components of each above $mO \times 1$ vector are from location point 1, the next O components are from location point 2, and so on. All other concerned parameters, i.e., \mathbf{w}_{jl} 's, ξ_j 's, λ_j 's, and σ^2 ,¹ are ordered first spatially and then by observation type, i.e., the first m components of each above $Om \times 1$ vector are from observation type 1, the next m components are from observation type 2, and so on.

1. Sampling from the marginal conditional distributions of $\xi_j(\mathbf{s}_{i,o})$'s with the introduced latent normal $z_{jl}(\mathbf{s}_{i,o})$'s integrated out:

Fix any arbitrary $j \in \{1, \dots, k\}$.

$$\begin{aligned} & \forall (o, i) \in \{1, \dots, O\} \times \{1, \dots, m\}, \forall l \in \{1, \dots, L\}, \mathbb{P}(\xi_j(\mathbf{s}_{i,o}) = l | \cdot) \\ & \propto \mathbb{P}(\xi_j(\mathbf{s}_{i,o}) = l | \alpha_{jr}(\mathbf{s}_{i,o}), r \leq L-1) \prod_{t=1}^T f\left(y_t(\mathbf{s}_{i,o}) | \beta, \boldsymbol{\eta}_t, \sigma^2(\mathbf{s}_{i,o}), \xi_j(\mathbf{s}_{i,o}) = l, \boldsymbol{\xi}_{-j}(\mathbf{s}_{i,o}), \boldsymbol{\theta}_{\xi(\mathbf{s}_{i,o})}\right) \\ & \propto w_{jl}(\mathbf{s}_{i,o}) \times \exp\left\{-\frac{1}{2}\sigma^{-2}(\mathbf{s}_{i,o}) \sum_{t=1}^T \left[y_t(\mathbf{s}_{i,o}) - \mathbf{x}_t(\mathbf{s}_{i,o})^\top \beta - \sum_{h \neq j} \theta_{h\xi_h(\mathbf{s}_{i,o})} \eta_{th} - \theta_{jl} \eta_{tj}\right]^2\right\}. \end{aligned} \quad (\text{A.9})$$

2. Sampling from the full conditional distributions of θ_{jl} 's for $l \leq L$:

Fix any arbitrary $(j, l) \in \{1, \dots, k\} \times \{1, \dots, L\}$. Then

$$f(\theta_{jl} | \cdot) \propto f_0(\theta_{jl} | \tau_j) \times \prod_{(i,o): \xi_j(\mathbf{s}_{i,o})=l} \prod_{t=1}^T f\left(y_t(\mathbf{s}_{i,o}) | \beta, \boldsymbol{\eta}_t, \sigma^2(\mathbf{s}_{i,o}), \boldsymbol{\xi}(\mathbf{s}_{i,o}), \boldsymbol{\theta}_{\xi(\mathbf{s}_{i,o})}\right). \quad (\text{A.10})$$

If $\nexists (i, o)$ s.t. $\xi_j(\mathbf{s}_{i,o}) = l$, then $f(\theta_{jl}|\cdot) = f_0(\theta_{jl}|\tau_j) \sim N(0, \tau_j^{-1})$.

If $\exists (i, o)$ s.t. $\xi_j(\mathbf{s}_{i,o}) = l$, then

$$f(\theta_{jl}|\cdot) \sim N(V_{\theta_{jl}}\mu_{\theta_{jl}}, V_{\theta_{jl}}), \text{ where } V_{\theta_{jl}} = \left[\tau_j + \sum_{(i,o):\xi_j(\mathbf{s}_{i,o})=l} \sigma^{-2}(\mathbf{s}_{i,o}) \sum_{t=1}^T \eta_{tj}^2 \right]^{-1}$$

$$\text{and } \mu_{\theta_{jl}} = \sum_{(i,o):\xi_j(\mathbf{s}_{i,o})=l} \sigma^{-2}(\mathbf{s}_{i,o}) \sum_{t=1}^T \eta_{tj} \left[y_t(\mathbf{s}_{i,o}) - \mathbf{x}_t(\mathbf{s}_{i,o})^\top \boldsymbol{\beta} - \sum_{h \neq j} \theta_{h\xi_h(\mathbf{s}_{i,o})} \eta_{th} \right].$$

3. Sampling from the full conditional distributions of δ_h 's:

If a multiplicative gamma process shrinkage prior is placed on the atoms so that $\forall (j, l)$, $\theta_{jl} \stackrel{\text{ind}}{\sim} N(0, \tau_j^{-1})$ with $\tau_j = \prod_{h=1}^j \delta_h$, $\delta_1 \sim \text{Gamma}(a_1, 1)$, $\delta_h \sim \text{Gamma}(a_2, 1) \forall h \geq 2$, then for any arbitrary fixed $h \in \{1, \dots, k\}$,

$$f(\delta_h|\cdot) \propto \prod_{j=h}^k \prod_{l=1}^L f(\theta_{jl}|\tau_j) \times f_0(\delta_h) \quad (\text{A.11})$$

$$\sim \text{Gamma} \left(a_h + \frac{(k-h+1)L}{2}, 1 + \frac{\sum_{j=h}^k \left[\prod_{x=1, x \neq h}^j \delta_x \right] \sum_{l=1}^L \theta_{jl}^2}{2} \right).$$

If we consider the non-shrinkage prior $\theta_{jl} \stackrel{\text{ind}}{\sim} N(0, \tau_j^{-1} = \delta_j^{-1}) \forall (j, l)$ with $\delta_j \stackrel{\text{iid}}{\sim} \text{Gamma}(a_1, a_2) \forall j$, then for any arbitrary fixed $j \in \{1, \dots, k\}$,

$$f(\delta_j|\cdot) \propto \prod_{l=1}^L f(\theta_{jl}|\delta_j) \times f_0(\delta_j) \sim \text{Gamma} \left(a_1 + \frac{L}{2}, a_2 + \frac{\sum_{l=1}^L \theta_{jl}^2}{2} \right). \quad (\text{A.12})$$

4. Sampling from the full conditional distributions of $z_{jl}(\mathbf{s}_{i,o})$'s for $l \in \{1, \dots, L-1\}$:

For any arbitrary fixed $(j, i, o, l) \in \{1, \dots, k\} \times \{1, \dots, m\} \times \{1, \dots, O\} \times \{1, \dots, L-1\}$,

$$f(z_{jl}(\mathbf{s}_{i,o})|\cdot) \propto f(\xi_j(\mathbf{s}_{i,o})|z_{jl}(\mathbf{s}_{i,o})) \times f(z_{jl}(\mathbf{s}_{i,o})|\alpha_{jl}(\mathbf{s}_{i,o})) \quad (\text{A.13})$$

$$\sim \mathbb{1}_{\{\xi_j(\mathbf{s}_{i,o}) > l\}} N(\alpha_{jl}(\mathbf{s}_{i,o}), 1)_{\mathbb{R}_-} + \mathbb{1}_{\{\xi_j(\mathbf{s}_{i,o}) = l\}} N(\alpha_{jl}(\mathbf{s}_{i,o}), 1)_{\mathbb{R}_+} + \mathbb{1}_{\{\xi_j(\mathbf{s}_{i,o}) < l\}} N(\alpha_{jl}(\mathbf{s}_{i,o}), 1).$$

5. Sampling from the full conditional distributions of $\boldsymbol{\alpha}_{jl}$'s for $l \in \{1, \dots, L-1\}$:

For any arbitrary fixed $(j, l) \in \{1, \dots, k\} \times \{1, \dots, L-1\}$,

$$f(\boldsymbol{\alpha}_{jl}|\cdot) \propto \prod_{(i,o)} f(z_{jl}(\mathbf{s}_{i,o})|\alpha_{jl}(\mathbf{s}_{i,o})) \times \pi(\boldsymbol{\alpha}_{jl}|\kappa, \rho) = f(\mathbf{z}_{jl}|\boldsymbol{\alpha}_{jl}) \times \pi(\boldsymbol{\alpha}_{jl}|\kappa, \rho)$$

$$\sim N_{mO} \left([I_{mO} + F(\rho)^{-1} \otimes \kappa^{-1}]^{-1} \mathbf{z}_{jl}, [I_{mO} + F(\rho)^{-1} \otimes \kappa^{-1}]^{-1} \right). \quad (\text{A.14})$$

When the NNGP prior rather than the full GP prior is adopted for the $\boldsymbol{\alpha}_{jl}$'s, we replace $\pi(\boldsymbol{\alpha}_{jl}|\kappa, \rho)$ and $F(\rho)$ in Equation (A.14) by $\tilde{\pi}(\boldsymbol{\alpha}_{jl}|\kappa, \rho)$ and $\tilde{F}(\rho)$ respectively.

After obtaining our new parameter estimates for $\alpha_{jl}(\mathbf{s}_{i,o})$'s ($l \in \{1, \dots, L-1\}$), we calculate our new samples for the corresponding weights parameters $w_{jl}(\mathbf{s}_{i,o})$'s ($l \in \{1, \dots, L\}$) via the formula

$$w_{jl}(\mathbf{s}_{i,o}) = \begin{cases} \Phi(\alpha_{jl}(\mathbf{s}_{i,o})) \prod_{r < l} [1 - \Phi(\alpha_{jr}(\mathbf{s}_{i,o}))], & \text{if } l \in \{1, \dots, L-1\} \\ \prod_{r < L} [1 - \Phi(\alpha_{jr}(\mathbf{s}_{i,o}))], & \text{if } l = L \end{cases} \quad (\text{A.15})$$

for any arbitrary $(j, o, i) \in \{1, \dots, k\} \times \{1, \dots, O\} \times \{1, \dots, m\}$ and $l \in \{1, \dots, L\}$.

Sequentially Updating $\alpha_{jl} = (\alpha_{jl}(\mathbf{s}_1))^T, \dots, \alpha_{jl}(\mathbf{s}_m)^T \forall (j, l)$

Under the circumstance when `include.space = TRUE`, `spatial.structure = "continuous"`, and `spatApprox = TRUE`, we can opt to sequentially update the α_{jl} 's instead:

Under our NNGP prior $\tilde{\pi}(\alpha_{jl}|\kappa, \rho) = N_{mO}(\mathbf{0}, \tilde{F}(\rho) \otimes \kappa)$ for all (j, l) , for any arbitrary fixed $(j, l, i) \in \{1, \dots, k\} \times \{1, \dots, L-1\} \times \{1, \dots, m\}$,

$$\begin{aligned} f(\alpha_{jl}(\mathbf{s}_i)|\cdot) &\propto f(\mathbf{z}_{jl}(\mathbf{s}_i)|\alpha_{jl}(\mathbf{s}_i)) \times \tilde{f}(\alpha_{jl}|\cdot) = f(\mathbf{z}_{jl}(\mathbf{s}_i)|\alpha_{jl}(\mathbf{s}_i)) \prod_{r=1}^m f(\alpha_{jl}(\mathbf{s}_r)|\alpha_{jl, N(\mathbf{s}_r)}, \kappa, \rho) \\ &\propto f(\mathbf{z}_{jl}(\mathbf{s}_i)|\alpha_{jl}(\mathbf{s}_i)) \times f(\alpha_{jl}(\mathbf{s}_i)|\alpha_{jl, N(\mathbf{s}_i)}, \kappa, \rho) \prod_{r:\mathbf{s}_i \in N(\mathbf{s}_r)} f(\alpha_{jl}(\mathbf{s}_r)|\alpha_{jl, N(\mathbf{s}_r)}, \kappa, \rho) \\ &\propto \exp\left\{-\frac{1}{2}(\mathbf{z}_{jl}(\mathbf{s}_i) - \alpha_{jl}(\mathbf{s}_i))^T I_O (\mathbf{z}_{jl}(\mathbf{s}_i) - \alpha_{jl}(\mathbf{s}_i))\right\} \times \\ &\quad \exp\left\{-\frac{1}{2}(\alpha_{jl}(\mathbf{s}_i) - B_{\mathbf{s}_i} \alpha_{jl, N(\mathbf{s}_i)})^T F_{\mathbf{s}_i}^{-1} (\alpha_{jl}(\mathbf{s}_i) - B_{\mathbf{s}_i} \alpha_{jl, N(\mathbf{s}_i)})\right\} \times \\ &\quad \exp\left\{-\frac{1}{2} \sum_{r:\mathbf{s}_i \in N(\mathbf{s}_r)} (\alpha_{jl}(\mathbf{s}_r) - B_{\mathbf{s}_r} \alpha_{jl, N(\mathbf{s}_r)})^T F_{\mathbf{s}_r}^{-1} (\alpha_{jl}(\mathbf{s}_r) - B_{\mathbf{s}_r} \alpha_{jl, N(\mathbf{s}_r)})\right\} \end{aligned} \quad (\text{A.16})$$

$$\sim N_O(V_{\mathbf{s}_i} \boldsymbol{\mu}_{jl, \mathbf{s}_i}, V_{\mathbf{s}_i}), \text{ where } V_{\mathbf{s}_i} = \left[I_O + F_{\mathbf{s}_i}^{-1} + \sum_{r:\mathbf{s}_i \in N(\mathbf{s}_r)} B_{\mathbf{s}_r, k_r(\mathbf{s}_i)}^T F_{\mathbf{s}_r}^{-1} B_{\mathbf{s}_r, k_r(\mathbf{s}_i)} \right]^{-1} \text{ and} \quad (\text{A.17})$$

$$\boldsymbol{\mu}_{jl, \mathbf{s}_i} = \mathbf{z}_{jl}(\mathbf{s}_i) + F_{\mathbf{s}_i}^{-1} B_{\mathbf{s}_i} \alpha_{jl, N(\mathbf{s}_i)} + \sum_{r:\mathbf{s}_i \in N(\mathbf{s}_r)} B_{\mathbf{s}_r, k_r(\mathbf{s}_i)}^T F_{\mathbf{s}_r}^{-1} \left\{ \alpha_{jl}(\mathbf{s}_r) - \sum_{\substack{1 \leq k \leq |N(\mathbf{s}_r)| \\ k \neq k_r(\mathbf{s}_i)}} B_{\mathbf{s}_r, k} \alpha_{jl, N(\mathbf{s}_r)[k]} \right\}.$$

For each r such that $\mathbf{s}_i \in N(\mathbf{s}_r)$, $k_r(\mathbf{s}_i)$ in the above refers to the positive integer less than or equal to $|N(\mathbf{s}_r)|$ such that $\mathbf{s}_i = N(\mathbf{s}_r)[k_r(\mathbf{s}_i)]$. We have written the $O \times (|N(\mathbf{s}_r)| \cdot O)$ matrix $B_{\mathbf{s}_r}$ as $(B_{\mathbf{s}_r, 1}, \dots, B_{\mathbf{s}_r, |N(\mathbf{s}_r)|})$, where each sub-matrix is $O \times O$, and written the $(|N(\mathbf{s}_r)| \cdot O) \times 1$ vector $\alpha_{jl, N(\mathbf{s}_r)}$ as $(\alpha_{jl, N(\mathbf{s}_r)[1]}^T, \dots, \alpha_{jl, N(\mathbf{s}_r)[|N(\mathbf{s}_r)|]}^T)^T$ so that $B_{\mathbf{s}_r} \alpha_{jl, N(\mathbf{s}_r)} = \sum_{k=1}^{|N(\mathbf{s}_r)|} B_{\mathbf{s}_r, k} \alpha_{jl, N(\mathbf{s}_r)[k]}$. Note that we only need to consider $r = i+1, \dots, m$ for each $i < m$ in order to find out the set $\{r \in \{1, \dots, m\} : \mathbf{s}_i \in N(\mathbf{s}_r)\}$. Also note that $F_{\mathbf{s}_1} = \kappa_{O \times O}$, $N(\mathbf{s}_1) = \emptyset \Rightarrow$ we can let $F_{\mathbf{s}_1}^{-1} B_{\mathbf{s}_1} \alpha_{jl, N(\mathbf{s}_1)} = \mathbf{0}_{O \times 1}$.

6. Sampling from the full conditional distribution of $\kappa_{O \times O}$:

$$f(\kappa|\cdot) \propto \prod_{j=1}^k \prod_{l=1}^{L-1} \pi(\alpha_{jl}|\kappa, \rho) \times f_0(\kappa) \sim \mathcal{IW}\left(mk(L-1) + \nu, \sum_{j=1}^k \sum_{l=1}^{L-1} S_{\alpha_p^{jl}} + \Theta\right), \quad (\text{A.18})$$

where $S_{\alpha_p^{jl}} = A_{jl} F(\rho)^{-1} A_{jl}^T$ with $(A_{jl})_{O \times m} = (\alpha_{jl}(\mathbf{s}_1), \dots, \alpha_{jl}(\mathbf{s}_m)) \forall (j, l)$.

When $O = 1$, Equation (A.18) reduces to $\mathcal{IG}\left(\frac{mk(L-1) + \nu}{2}, \frac{\sum_{j=1}^k \sum_{l=1}^{L-1} S_{\alpha_p^{jl}} + \Theta}{2}\right)$.

When the NNGP prior rather than the full GP prior is adopted for the α_{jl} 's, we replace $\pi(\alpha_{jl}|\kappa, \rho)$ and $F(\rho)$ in Equation (A.18) by $\tilde{\pi}(\alpha_{jl}|\kappa, \rho)$ and $\tilde{F}(\rho)$ respectively.

7. Sampling ρ via a Metropolis step when `include.space = TRUE`:

$$f(\rho|\cdot) \propto \prod_{j=1}^k \prod_{l=1}^{L-1} \pi(\boldsymbol{\alpha}_{jl}|\kappa, \rho) \times f_0(\rho) \times \left| \frac{\partial}{\partial \Delta} h^{-1}(\Delta) \right| \quad (\text{A.19})$$

with $\boldsymbol{\alpha}_{jl}|\kappa, \rho \sim N_{mO}(\mathbf{0}, F(\rho) \otimes \kappa) \quad \forall (j, l)$.

When the NNGP prior rather than the full GP prior is adopted for the $\boldsymbol{\alpha}_{jl}$'s, we replace $\pi(\boldsymbol{\alpha}_{jl}|\kappa, \rho)$ and $F(\rho)$ in Equation (A.19) by $\tilde{\pi}(\boldsymbol{\alpha}_{jl}|\kappa, \rho)$ and $\tilde{F}(\rho)$ respectively.

In Equation (A.19), $f_0(\rho)$ refers to the uniform prior $\text{Unif}(a_\rho, b_\rho)$, where $a_\rho = 0, b_\rho = 1$ when `spatial.structure = 'discrete'` and $a_\rho, b_\rho \in \mathbb{R}^+$ when `spatial.structure = 'continuous'`. Δ is a new parameter defined to be $h(\rho) = \ln\left(\frac{\rho - a_\rho}{b_\rho - \rho}\right)$. Hence $\rho = h^{-1}(\Delta) = \frac{b_\rho \exp(\Delta) + a_\rho}{1 + \exp(\Delta)}$ and $|\frac{\partial}{\partial \Delta} h^{-1}(\Delta)| \propto \frac{\exp(\Delta)}{[1 + \exp(\Delta)]^2}$.

At each MCMC iteration $s \in \mathbb{N}$, let the current parameter estimate for ρ be $\rho^{(s)}$. We propose a new parameter value $\rho^* = h^{-1}(\Delta^*)$ with Δ^* sampled from a symmetric kernel $N(\Delta^{(s)}, \delta)$, where $\Delta^{(s)} = h(\rho^{(s)})$ and $\delta > 0$ is a tuning parameter decided after the burn-in MCMC iterations based on the acceptance rate for ρ^* , and set

$$\rho^{(s+1)} = \begin{cases} \rho^*, & \text{w.p. } \alpha(\rho^{(s)}, \rho^*) = \min\left\{\frac{f(\rho^*|\cdot)}{f(\rho^{(s)}|\cdot)}, 1\right\} \\ \rho^{(s)}, & \text{w.p. } 1 - \alpha(\rho^{(s)}, \rho^*) \end{cases}.$$

8. Same as Step 1 given at the start of Appendix A.
9. Same as Step 2 given at the start of Appendix A.
10. Same as Step 3 given at the start of Appendix A.
11. Same as Step 4 given at the start of Appendix A.
12. Same as Step 5 given at the start of Appendix A.

A.3 Full Gibbs Sampling Details for Our Model in Section 3

When we adopt the spatial PSBP clustering mechanism and further integrate pertinent ideas of slice sampling (Walker 2007) by introducing new parameters $L_j \in \mathbb{N} \setminus \{0\}$, $j \in \{1, \dots, k\}$ and $u_j(\mathbf{s}_{i,o})$, $(j, i, o) \in \{1, \dots, k\} \times \{1, \dots, m\} \times \{1, \dots, O\}$ so that the spatial prior becomes $\boldsymbol{\alpha}_{jl_j} \stackrel{\text{iid}}{\sim} N_{mO}(\mathbf{0}, F(\rho)_{m \times m} \otimes \kappa_{O \times O})$, $j \in \{1, \dots, k\}$, $l_j \in \{1, \dots, L_j - 1\}$, the corresponding Gibbs sampler steps are detailed in the following. We take note that only $\boldsymbol{\alpha}_{jl_j}$'s are ordered first by observation type and then spatially, i.e., the first O components of each above $mO \times 1$ vector are from location point 1, the next O components are from location point 2, and so on. All other concerned parameters, i.e., \mathbf{u}_j 's, \mathbf{w}_{jl_j} 's, $\boldsymbol{\xi}_j$'s, $\boldsymbol{\lambda}_j$'s, and $\boldsymbol{\sigma}^2$,¹ are ordered first spatially and then by observation type, i.e., the first m components of each above $Om \times 1$ vector are from observation type 1, the next m components are from observation type 2, and so on.

1. Sampling from the full conditional distributions of $u_j(\mathbf{s}_{i,o})$'s:

$$\text{For any arbitrary } (i, o, j), f(u_j(\mathbf{s}_{i,o})|\cdot) \propto \mathbb{1}_{\{u_j(\mathbf{s}_{i,o}) < w_{j\xi_j(\mathbf{s}_{i,o})}(\mathbf{s}_{i,o})\}} \sim \text{Unif}\left(0, w_{j\xi_j(\mathbf{s}_{i,o})}(\mathbf{s}_{i,o})\right).$$

2. Updating the L_j 's and sampling from the full conditional distributions of $\xi_j(\mathbf{s}_{i,o})$'s:

Fix any arbitrary $j \in \{1, \dots, k\}$.

$$\forall (i, o), \text{ let } L_j^{i,o} = \text{the smallest positive integer s.t. } \sum_{l_j=1}^{L_j^{i,o}} w_{jl_j}(\mathbf{s}_{i,o}) > 1 - u_j(\mathbf{s}_{i,o})$$

$$\text{and let } L_j^{\text{new}} = \max \left\{ L_j^{i,o} : i = 1, \dots, m, o = 1, \dots, O \right\}. \quad (\text{A.20})$$

After obtaining $\{L_j^{\text{new}} : j = 1, \dots, k\}$ by Equation (A.20), we immediately update the parameter estimates objects $\boldsymbol{\alpha}_{jl_j}$'s (by only keeping the $mO \times 1$ vectors corresponding to $l_j \in \{1, 2, \dots, L_j^{\text{new}} - 1\}$ and discarding the ones corresponding to $l_j \in \{L_j^{\text{new}}, L_j^{\text{new}} + 1, \dots, L_j^{\text{old}} - 1\}$) and w_{jl_j} 's correspondingly. Note that

- $\forall l_j \in \{L_j^{\text{new}} + 1, L_j^{\text{new}} + 2, \dots, L_j^{\text{old}}\}$, $w_{jl_j}^{\text{old}}(\mathbf{s}_{i,o}) < u_j(\mathbf{s}_{i,o})$. Hence, $\{1, \dots, L_j^{\text{new}}\}$ comprises of all possible choices for $\xi_j(\mathbf{s}_{i,o}) \forall (i, o)$,
- $\forall j \in \{1, \dots, k\}, 1 \leq L_j^{\text{new}} \leq L_j^{\text{old}} < \infty$, and
- $\forall (j, i, o) \in \{1, \dots, k\} \times \{1, \dots, m\} \times \{1, \dots, O\}$, $w_{jl_j}^{\text{old}}(\mathbf{s}_{i,o}) = w_{jl_j}^{\text{new}}(\mathbf{s}_{i,o}) \forall l_j \in \{1, \dots, L_j^{\text{new}} - 1\}$ and $w_{jL_j^{\text{new}}}^{\text{old}}(\mathbf{s}_{i,o}) \leq w_{jL_j^{\text{new}}}^{\text{new}}(\mathbf{s}_{i,o})$. Hence, $\xi_j(\mathbf{s}_{i,o})^{\text{old}}$ is still in the support for $\xi_j(\mathbf{s}_{i,o})^{\text{new}}$.

Hence, we can update our parameter estimates for $\xi_j(\mathbf{s}_{i,o})$'s via the following:

$$\forall l_j \in \{1, \dots, L_j^{\text{new}}\}, \forall (i, o), \mathbb{P}(\xi_j(\mathbf{s}_{i,o}) = l_j | \cdot) \propto \mathbb{1}_{\{w_{jl_j}^{\text{new}}(\mathbf{s}_{i,o}) > u_j(\mathbf{s}_{i,o})\}} \quad (\text{A.21})$$

$$\times \prod_{t=1}^T f\left(y_t(\mathbf{s}_{i,o}) | \boldsymbol{\beta}, \boldsymbol{\eta}_t, \sigma^2(\mathbf{s}_{i,o}), \xi_j(\mathbf{s}_{i,o}) = l_j, \boldsymbol{\xi}_{-j}(\mathbf{s}_{i,o}), \boldsymbol{\theta}_{\xi(\mathbf{s}_{i,o})}\right),$$

where $\forall (i, o, j, l_j)$ s.t. $w_{jl_j}^{\text{new}}(\mathbf{s}_{i,o}) > u_j(\mathbf{s}_{i,o}), \forall t \in \{1, \dots, T\}$,

$$f\left(y_t(\mathbf{s}_{i,o}) | \boldsymbol{\beta}, \boldsymbol{\eta}_t, \sigma^2(\mathbf{s}_{i,o}), \xi_j(\mathbf{s}_{i,o}) = l_j, \boldsymbol{\xi}_{-j}(\mathbf{s}_{i,o}), \boldsymbol{\theta}_{\xi(\mathbf{s}_{i,o})}\right) \quad (\text{A.22})$$

$$= (2\pi)^{-\frac{1}{2}} \sigma^{-1}(\mathbf{s}_{i,o}) \exp \left\{ -\frac{1}{2} \sigma^{-2}(\mathbf{s}_{i,o}) \left[y_t(\mathbf{s}_{i,o}) - \mathbf{x}_t(\mathbf{s}_{i,o})^T \boldsymbol{\beta} - \sum_{h \neq j} \theta_{h\xi_h(\mathbf{s}_{i,o})} \eta_{th} - \theta_{jl_j} \eta_{tj} \right]^2 \right\}.$$

3. Sampling from the full conditional distributions of θ_{jl_j} 's for $l_j \leq L_j$, as we have assumed a finite mixture model with L_j 's as the spatial cluster numbers in this MCMC iteration :

Fix any arbitrary $j \in \{1, \dots, k\}$ and $l_j \in \{1, \dots, L_j\}$. Then

$$f(\theta_{jl_j} | \cdot) \propto f_0(\theta_{jl_j} | \tau_j) \times \prod_{(i,o): \xi_j(\mathbf{s}_{i,o}) = l_j} \prod_{t=1}^T f\left(y_t(\mathbf{s}_{i,o}) | \boldsymbol{\beta}, \boldsymbol{\eta}_t, \sigma^2(\mathbf{s}_{i,o}), \boldsymbol{\xi}(\mathbf{s}_{i,o}), \boldsymbol{\theta}_{\xi(\mathbf{s}_{i,o})}\right). \quad (\text{A.23})$$

If $\nexists (i, o)$ s.t. $\xi_j(\mathbf{s}_{i,o}) = l_j$, then $f(\theta_{jl_j} | \cdot) = f_0(\theta_{jl_j} | \tau_j) \sim N(0, \tau_j^{-1})$.

If $\exists (i, o)$ s.t. $\xi_j(\mathbf{s}_{i,o}) = l_j$, then

$$f(\theta_{jl_j} | \cdot) \sim N\left(V_{\theta_{jl_j}} \mu_{\theta_{jl_j}}, V_{\theta_{jl_j}}\right), \text{ where } V_{\theta_{jl_j}} = \left[\tau_j + \sum_{(i,o): \xi_j(\mathbf{s}_{i,o}) = l_j} \sigma^{-2}(\mathbf{s}_{i,o}) \sum_{t=1}^T \eta_{tj}^2 \right]^{-1}$$

$$\text{and } \mu_{\theta_{jl_j}} = \sum_{(i,o):\xi_j(\mathbf{s}_{i,o})=l_j} \sigma^{-2}(\mathbf{s}_{i,o}) \sum_{t=1}^T \eta_{tj} \left[y_t(\mathbf{s}_{i,o}) - \mathbf{x}_t(\mathbf{s}_{i,o})^\top \boldsymbol{\beta} - \sum_{h \neq j} \theta_{h\xi_h(\mathbf{s}_{i,o})} \eta_{th} \right].$$

4. Sampling from the full conditional distributions of δ_h 's:

If a multiplicative gamma process shrinkage prior is placed on the atoms so that $\forall (j, l_j)$, $\theta_{jl_j} \stackrel{\text{ind}}{\sim} N(0, \tau_j^{-1})$ with $\tau_j = \prod_{h=1}^j \delta_h$, $\delta_1 \sim \text{Gamma}(a_1, 1)$, $\delta_h \sim \text{Gamma}(a_2, 1) \forall h \geq 2$, then for any arbitrary fixed $h \in \{1, \dots, k\}$,

$$\begin{aligned} f(\delta_h | \cdot) &\propto \prod_{j=h}^k \prod_{l_j=1}^{L_j} f(\theta_{jl_j} | \tau_j) \times f_0(\delta_h) \\ &\sim \text{Gamma} \left(a_h + \frac{\sum_{j=h}^k L_j}{2}, 1 + \frac{\sum_{j=h}^k \left[\prod_{x=1, x \neq h}^j \delta_x \right] \sum_{l_j=1}^{L_j} \theta_{jl_j}^2}{2} \right). \end{aligned} \quad (\text{A.24})$$

If we consider the non-shrinkage prior $\theta_{jl_j} \stackrel{\text{ind}}{\sim} N(0, \tau_j^{-1} = \delta_j^{-1}) \forall (j, l_j)$ with $\delta_j \stackrel{\text{iid}}{\sim} \text{Gamma}(a_1, a_2) \forall j$, then for any arbitrary fixed $j \in \{1, \dots, k\}$,

$$f(\delta_j | \cdot) \propto \prod_{l_j=1}^{L_j} f(\theta_{jl_j} | \delta_j) \times f_0(\delta_j) \sim \text{Gamma} \left(a_1 + \frac{L_j}{2}, a_2 + \frac{\sum_{l_j=1}^{L_j} \theta_{jl_j}^2}{2} \right). \quad (\text{A.25})$$

5. Sampling from the full conditional distributions of $\boldsymbol{\alpha}_{jl_j}$'s ($l_j \in \{1, \dots, L_j - 1\}$ for each j) and calculating new weights $w_{jl_j}(\mathbf{s}_{i,o})$'s ($l_j \in \{1, \dots, L_j\}$ for each j) when $L_j > 1$:

If $L_j = 1$, then we do not need to sample any $\boldsymbol{\alpha}_{jl_j}$'s for this j . The corresponding $w_{j1}(\mathbf{s}_{i,o})$'s have already been set to 1 in the previous Gibbs sampler step for $\xi_j(\mathbf{s}_{i,o})$'s in this same MCMC iteration.

For any arbitrary fixed (j, l_j) where $j \in \{1, \dots, k\}$ and $l_j \in \{1, \dots, L_j - 1\}$,

$$\begin{aligned} f(\boldsymbol{\alpha}_{jl_j} | \cdot) &\propto \pi(\boldsymbol{\alpha}_{jl_j} | \kappa, \rho) \times \prod_{i=1}^m \prod_{o=1}^O \mathbb{1}_{\{l_j > \xi_j(\mathbf{s}_{i,o}) \text{ or } u_j(\mathbf{s}_{i,o}) < w_{j\xi_j(\mathbf{s}_{i,o})}(\mathbf{s}_{i,o})\}} \\ &\sim N_{mO}(\mathbf{0}, F(\rho) \otimes \kappa) \times \prod_{i=1}^m \prod_{o=1}^O \mathbb{1}_{\{l_j > \xi_j(\mathbf{s}_{i,o}) \text{ or } u_j(\mathbf{s}_{i,o}) < w_{j\xi_j(\mathbf{s}_{i,o})}(\mathbf{s}_{i,o})\}} \\ &\sim N_{mO}(\mathbf{0}, F(\rho) \otimes \kappa) \times \prod_{i=1}^m \prod_{o=1}^O \begin{cases} 1, & \text{if } l_j > \xi_j(\mathbf{s}_{i,o}) \\ \mathbb{1}_{\{\alpha_{jl_j}^{\text{new}}(\mathbf{s}_{i,o}) > \text{lowerBound}_{(j,l_j,i,o)}\}}, & \text{if } l_j = \xi_j(\mathbf{s}_{i,o}), \\ \mathbb{1}_{\{\alpha_{jl_j}^{\text{new}}(\mathbf{s}_{i,o}) < \text{upperBound}_{(j,l_j,i,o)}\}}, & \text{if } l_j < \xi_j(\mathbf{s}_{i,o}) \end{cases} \end{aligned} \quad (\text{A.26})$$

where $\forall (j, l_j, i, o)$,

$$\text{lowerBound}_{(j,l_j,i,o)} = \Phi^{-1} \left(\frac{u_j(\mathbf{s}_{i,o}) \cdot \Phi(\alpha_{jl_j}^{\text{old}}(\mathbf{s}_{i,o}))}{w_{j\xi_j(\mathbf{s}_{i,o})}(\mathbf{s}_{i,o})} \right) \text{ and} \quad (\text{A.28})$$

$$\text{upperBound}_{(j,l_j,i,o)} = \Phi^{-1} \left(1 - \frac{u_j(\mathbf{s}_{i,o}) \cdot [1 - \Phi(\alpha_{jl_j}^{\text{old}}(\mathbf{s}_{i,o}))]}{w_{j\xi_j(\mathbf{s}_{i,o})}(\mathbf{s}_{i,o})} \right). \quad (\text{A.29})$$

When the NNGP instead of the full GP prior is adopted for the α_{jl_j} 's, we replace $\pi(\alpha_{jl_j}|\kappa, \rho)$ and $F(\rho)$ by $\tilde{\pi}(\alpha_{jl_j}|\kappa, \rho)$ and $\tilde{F}(\rho)$ in the above equations.

After obtaining our new parameter estimates for $\alpha_{jl_j}(\mathbf{s}_{i,o})$'s ($l_j \in \{1, \dots, L_j - 1\}$), we calculate our new samples for the corresponding weights parameters $w_{jl_j}(\mathbf{s}_{i,o})$'s ($l_j \in \{1, \dots, L_j\}$) via

$$w_{jl_j}(\mathbf{s}_{i,o}) = \begin{cases} \Phi(\alpha_{jl_j}(\mathbf{s}_{i,o})) \prod_{r_j < l_j} [1 - \Phi(\alpha_{jr_j}(\mathbf{s}_{i,o}))], & \text{if } l_j \in \{1, \dots, L_j - 1\} \\ \prod_{r_j < L_j} [1 - \Phi(\alpha_{jr_j}(\mathbf{s}_{i,o}))], & \text{if } l_j = L_j \end{cases} \quad (\text{A.30})$$

for any arbitrary $(j, o, i) \in \{1, \dots, k\} \times \{1, \dots, O\} \times \{1, \dots, m\}$ and $l_j \in \{1, \dots, L_j\}$.

The truncated multivariate normal posterior distributions of α_{jl_j} 's (Equation (A.27)) can be directly sampled by multivariate rejection sampling via for instance the `rtmvnorm` function in the R package `tmvtnorm`. One noteworthy problem with multivariate rejection sampling, in this case, is that it typically gets very inefficient when m is large due to an excessively small acceptance rate associated with sampling from a high-dimensional truncated mO -variate normal distribution. This issue can be successfully addressed by integrating spatial scalability via assuming an NNGP prior and sequentially sampling α_{jl_j} 's instead.

$$\text{Sequentially Updating } \alpha_{jl_j} = (\alpha_{jl_j}(\mathbf{s}_1)^T, \dots, \alpha_{jl_j}(\mathbf{s}_m)^T)^T \quad \forall (j, l_j)$$

Under the circumstance when `include.space = TRUE`, `spatial.structure = "continuous"`, and `spatApprox = TRUE`, we can opt to sequentially update the α_{jl_j} 's instead:

Under our NNGP prior $\tilde{\pi}(\alpha_{jl_j}|\kappa, \rho) = N_{mO}(\mathbf{0}, \tilde{F}(\rho) \otimes \kappa)$ for all (j, l_j) , for any arbitrary fixed (j, l_j, i) where $j \in \{1, \dots, k\}$, $l_j \in \{1, \dots, L_j - 1\}$, and $i \in \{1, \dots, m\}$,

$$f(\alpha_{jl_j}(\mathbf{s}_i)|\cdot) \propto \tilde{f}(\alpha_{jl_j}|\cdot) \times \prod_{o=1}^O \mathbb{1}_{\{l_j > \xi_j(\mathbf{s}_{i,o}) \text{ or } u_j(\mathbf{s}_{i,o}) < w_j \xi_j(\mathbf{s}_{i,o})(\mathbf{s}_{i,o})\}} \quad (\text{A.31})$$

$$\begin{aligned} &= \prod_{r=1}^m f(\alpha_{jl_j}(\mathbf{s}_r)|\alpha_{jl_j, N(\mathbf{s}_r)}, \kappa, \rho) \times \prod_{o=1}^O \mathbb{1}_{\{l_j > \xi_j(\mathbf{s}_{i,o}) \text{ or } u_j(\mathbf{s}_{i,o}) < w_j \xi_j(\mathbf{s}_{i,o})(\mathbf{s}_{i,o})\}} \\ &\propto \prod_{r: r=i \text{ or } \mathbf{s}_i \in N(\mathbf{s}_r)} f(\alpha_{jl_j}(\mathbf{s}_r)|\alpha_{jl_j, N(\mathbf{s}_r)}, \kappa, \rho) \times \prod_{o=1}^O \mathbb{1}_{\{l_j > \xi_j(\mathbf{s}_{i,o}) \text{ or } u_j(\mathbf{s}_{i,o}) < w_j \xi_j(\mathbf{s}_{i,o})(\mathbf{s}_{i,o})\}} \\ &\propto \prod_{o=1}^O \mathbb{1}_{\{l_j > \xi_j(\mathbf{s}_{i,o}) \text{ or } u_j(\mathbf{s}_{i,o}) < w_j \xi_j(\mathbf{s}_{i,o})(\mathbf{s}_{i,o})\}} \times \end{aligned} \quad (\text{A.32})$$

$$\begin{aligned} &\exp \left\{ -\frac{1}{2} \left(\alpha_{jl_j}(\mathbf{s}_i) - B_{\mathbf{s}_i} \alpha_{jl_j, N(\mathbf{s}_i)} \right)^T F_{\mathbf{s}_i}^{-1} \left(\alpha_{jl_j}(\mathbf{s}_i) - B_{\mathbf{s}_i} \alpha_{jl_j, N(\mathbf{s}_i)} \right) \right\} \times \\ &\exp \left\{ -\frac{1}{2} \sum_{r: \mathbf{s}_i \in N(\mathbf{s}_r)} \left(\alpha_{jl_j}(\mathbf{s}_r) - B_{\mathbf{s}_r} \alpha_{jl_j, N(\mathbf{s}_r)} \right)^T F_{\mathbf{s}_r}^{-1} \left(\alpha_{jl_j}(\mathbf{s}_r) - B_{\mathbf{s}_r} \alpha_{jl_j, N(\mathbf{s}_r)} \right) \right\}. \end{aligned}$$

$$\sim N_O(V_{\mathbf{s}_i} \boldsymbol{\mu}_{jl_j, \mathbf{s}_i}, V_{\mathbf{s}_i}) \times \prod_{o=1}^O \mathbb{1}_{\{l_j > \xi_j(\mathbf{s}_{i,o}) \text{ or } u_j(\mathbf{s}_{i,o}) < w_j \xi_j(\mathbf{s}_{i,o})(\mathbf{s}_{i,o})\}}, \quad (\text{A.33})$$

$$\text{where } V_{\mathbf{s}_i} = \left[F_{\mathbf{s}_i}^{-1} + \sum_{r: \mathbf{s}_i \in N(\mathbf{s}_r)} B_{\mathbf{s}_r, k_r(\mathbf{s}_i)}^T F_{\mathbf{s}_r}^{-1} B_{\mathbf{s}_r, k_r(\mathbf{s}_i)} \right]^{-1} \text{ and}$$

$$\boldsymbol{\mu}_{jl_j, \mathbf{s}_i} = F_{\mathbf{s}_i}^{-1} B_{\mathbf{s}_i} \boldsymbol{\alpha}_{jl_j, N(\mathbf{s}_i)} + \sum_{r: \mathbf{s}_i \in N(\mathbf{s}_r)} B_{\mathbf{s}_r, k_r(\mathbf{s}_i)}^T F_{\mathbf{s}_r}^{-1} \left\{ \boldsymbol{\alpha}_{jl_j}(\mathbf{s}_r) - \sum_{\substack{1 \leq k_j \leq |N(\mathbf{s}_r)| \\ k_j \neq k_r(\mathbf{s}_i)}} B_{\mathbf{s}_r, k_j} \boldsymbol{\alpha}_{jl_j, N(\mathbf{s}_r)[k_j]} \right\}.$$

For each r such that $\mathbf{s}_i \in N(\mathbf{s}_r)$, $k_r(\mathbf{s}_i)$ in the above refers to the positive integer less than or equal to $|N(\mathbf{s}_r)|$ such that $\mathbf{s}_i = N(\mathbf{s}_r)[k_r(\mathbf{s}_i)]$. We have written the $O \times (|N(\mathbf{s}_r)| \cdot O)$ matrix $B_{\mathbf{s}_r}$ as $(B_{\mathbf{s}_r, 1}, \dots, B_{\mathbf{s}_r, |N(\mathbf{s}_r)|})$, where each sub-matrix is $O \times O$, and written the $(|N(\mathbf{s}_r)| \cdot O) \times 1$ vector $\boldsymbol{\alpha}_{jl_j, N(\mathbf{s}_r)}$ as $(\boldsymbol{\alpha}_{jl_j, N(\mathbf{s}_r)[1]}^T, \dots, \boldsymbol{\alpha}_{jl_j, N(\mathbf{s}_r)[|N(\mathbf{s}_r)|]}^T)^T$ so that $B_{\mathbf{s}_r} \boldsymbol{\alpha}_{jl_j, N(\mathbf{s}_r)} = \sum_{k_j=1}^{|N(\mathbf{s}_r)|} B_{\mathbf{s}_r, k_j} \boldsymbol{\alpha}_{jl_j, N(\mathbf{s}_r)[k_j]}$. Note that we only need to consider $r = i + 1, \dots, m$ for each $i < m$ in order to find out the set $\{r \in \{1, \dots, m\} : \mathbf{s}_i \in N(\mathbf{s}_r)\}$. Also note that $F_{\mathbf{s}_1} = \kappa_{O \times O}$, $N(\mathbf{s}_1) = \emptyset \Rightarrow$ we can let $F_{\mathbf{s}_1}^{-1} B_{\mathbf{s}_1} \boldsymbol{\alpha}_{jl_j, N(\mathbf{s}_1)} = \mathbf{0}_{O \times 1}$.

6. Sampling from the full conditional distribution of $\kappa_{O \times O}$:

$$f(\kappa|\cdot) \propto \prod_{j=1}^k \prod_{l_j=1}^{L_j-1} \pi(\boldsymbol{\alpha}_{jl_j}|\kappa, \rho) \times f_0(\kappa) \sim \mathcal{IW} \left(m \sum_{j=1}^k (L_j - 1) + \nu, \sum_{j=1}^k \sum_{l_j=1}^{L_j-1} S_{\alpha_\rho}^{jl_j} + \Theta \right), \quad (\text{A.34})$$

where $S_{\alpha_\rho}^{jl_j} = A_{jl_j} F(\rho)^{-1} A_{jl_j}^T$ with $(A_{jl_j})_{O \times m} = (\boldsymbol{\alpha}_{jl_j}(\mathbf{s}_1), \dots, \boldsymbol{\alpha}_{jl_j}(\mathbf{s}_m)) \forall (j, l_j)$.

When $O = 1$, Equation (A.34) reduces to $\mathcal{IG} \left(\frac{m \sum_{j=1}^k (L_j - 1) + \nu}{2}, \frac{\sum_{j=1}^k \sum_{l_j=1}^{L_j-1} S_{\alpha_\rho}^{jl_j} + \Theta}{2} \right)$.

When the NNGP prior rather than the full GP prior is adopted for the $\boldsymbol{\alpha}_{jl_j}$'s, we replace $\pi(\boldsymbol{\alpha}_{jl_j}|\kappa, \rho)$ and $F(\rho)$ in Equation (A.34) by $\tilde{\pi}(\boldsymbol{\alpha}_{jl_j}|\kappa, \rho)$ and $\tilde{F}(\rho)$ respectively.

7. Sampling ρ via a Metropolis step when `include.space = TRUE`:

$$f(\rho|\cdot) \propto \prod_{j=1}^k \prod_{l_j=1}^{L_j-1} \pi(\boldsymbol{\alpha}_{jl_j}|\kappa, \rho) \times f_0(\rho) \times \left| \frac{\partial}{\partial \Delta} h^{-1}(\Delta) \right| \quad (\text{A.35})$$

with $\boldsymbol{\alpha}_{jl_j}|\kappa, \rho \sim N_{mO}(\mathbf{0}, F(\rho) \otimes \kappa) \quad \forall (j, l_j)$.

When the NNGP prior rather than the full GP prior is adopted for the $\boldsymbol{\alpha}_{jl_j}$'s, we replace $\pi(\boldsymbol{\alpha}_{jl_j}|\kappa, \rho)$ and $F(\rho)$ in Equation (A.35) by $\tilde{\pi}(\boldsymbol{\alpha}_{jl_j}|\kappa, \rho)$ and $\tilde{F}(\rho)$ respectively.

In Equation (A.35), $f_0(\rho)$ refers to the uniform prior $\text{Unif}(a_\rho, b_\rho)$, where $a_\rho = 0, b_\rho = 1$ when `spatial.structure = 'discrete'` and $a_\rho, b_\rho \in \mathbb{R}^+$ when `spatial.structure = 'continuous'`. Δ is a new parameter defined to be $h(\rho) = \ln\left(\frac{\rho - a_\rho}{b_\rho - \rho}\right)$. Hence $\rho = h^{-1}(\Delta) = \frac{b_\rho \exp(\Delta) + a_\rho}{1 + \exp(\Delta)}$ and $\left| \frac{\partial}{\partial \Delta} h^{-1}(\Delta) \right| \propto \frac{\exp(\Delta)}{[1 + \exp(\Delta)]^2}$.

At each MCMC iteration $s \in \mathbb{N}$, let the current parameter estimate for ρ be $\rho^{(s)}$. We propose a new parameter value $\rho^* = h^{-1}(\Delta^*)$ with Δ^* sampled from a symmetric kernel $N(\Delta^{(s)}, \delta)$, where $\Delta^{(s)} = h(\rho^{(s)})$ and $\delta > 0$ is a tuning parameter decided after the burn-in MCMC iterations based on the acceptance rate for ρ^* , and set

$$\rho^{(s+1)} = \begin{cases} \rho^*, & \text{w.p. } \alpha(\rho^{(s)}, \rho^*) = \min\left\{\frac{f(\rho^*|\cdot)}{f(\rho^{(s)}|\cdot)}, 1\right\} \\ \rho^{(s)}, & \text{w.p. } 1 - \alpha(\rho^{(s)}, \rho^*) \end{cases}.$$

8. Same as Step 1 given at the start of Appendix A.
9. Same as Step 2 given at the start of Appendix A.
10. Same as Step 3 given at the start of Appendix A.
11. Same as Step 4 given at the start of Appendix A.
12. Same as Step 5 given at the start of Appendix A.

B Temporal Portion Sampling Acceleration for Evenly Dispersed Time Points

Throughout this section, we sometimes write $H(\psi)$ as H to simplify notations.

B.1 Temporal Part Computational Burdens When T is Large

Our Gibbs sampling steps with respect to temporal-related parameters $\boldsymbol{\eta}_t$'s, $\Upsilon_{k \times k}$, and ψ given at the start of Appendix A can get very slow when T is large due to the primary reasons listed below, especially the last one. In each MCMC iteration in any of our three Gibbs samplers (Appendix A),

- The full conditional distribution of $\Upsilon_{k \times k}$ (Equation (A.2)) concerns $H(\psi)^{-1}$, whose computation requires $O(T^3)$ flops via standard methods;
 - To sample ψ via a Metropolis step,
 - We need to calculate $\ln [f(\psi|\cdot)]$ for both the current parameter estimate and the newly proposed value of ψ . As the full conditional density of ψ is given by Equation (A.3), we have to evaluate $H(\psi)^{-1}$ and $\ln [\det (H(\psi))]$,² which both require $O(T^3)$ flops under standard methods.
- Let $\text{Rooti}(H) = [\text{Chol}(H)]^{-1}$ be the upper triangular matrix with positive diagonal entries such that $H(\psi)^{-1} = \text{Rooti}(H) [\text{Rooti}(H)]^T$. Then $\det (H(\psi))$ can also be conveniently calculated as the inverse of the square of the product of all diagonal entries in $\text{Rooti}(H)$. Adopting $\text{Rooti}(H)$ instead of $H(\psi)^{-1}$ and $\det (H(\psi))$ for this step is usually faster, but $\text{Rooti}(H)$ also has a computational complexity of $O(T^3)$ for a general $H(\psi)_{T \times T}$ without any special structures.
- The temporal correlation structure matrix $H(\psi)_{T \times T}$ must be positive definite (PD). However, not all ψ 's lead to PD $H(\psi)_{T \times T}$'s given a general set of time points. Hence, we may need to sample multiple values for ψ until we get one resulting in a PD $H(\psi)_{T \times T}$ in each MCMC iteration, which might be computationally demanding.

- When sampling $\boldsymbol{\eta}_t$'s from their full conditional distributions (Equation (A.1)), we would need to loop over $t \in \{1, 2, \dots, T\}$ and calculate $H_t^+ = H_{t, (1:T)-t} H_{(1:T)-t, (1:T)-t}^{-1}$, $H_t^* =$

²Note that these two quantities suffice for the ψ part since $[H(\psi) \otimes \Upsilon]^{-1} = H(\psi)^{-1} \otimes \Upsilon^{-1}$ and $\ln [\det (H(\psi) \otimes \Upsilon)] = k \cdot \ln [\det (H(\psi))] + T \cdot \ln [\det (\Upsilon)]$.

$H_{t,t} - H_t^+ H_{(1:T)_{-t},t} = H_{t,t} - H_{t,(1:T)_{-t}} H_{(1:T)_{-t},(1:T)_{-t}}^{-1} H_{(1:T)_{-t},t}$ for each t . This can be computationally intimidating when T is large given that we need to invert T many $(T-1) \times (T-1)$ principal sub-matrices of $H(\psi)_{T \times T}$, which results in an overall computational complexity of $O(T^4)$. Also, we would have to compute and store the entire $H(\psi)_{T \times T}$ matrix to extract out its aforementioned sub-matrices.

The above points do not exist as problems when temporal independence is assumed, i.e., when the temporal correlation structure matrix $H(\psi)_{T \times T}$ is fixed as the $T \times T$ identity matrix. In that case,

- When sampling $\Upsilon_{k \times k}$ from its full conditional distribution, we can directly take $H(\psi)_{T \times T}^{-1}$ as $I_{T \times T}$ throughout;
- We no longer need to sample ψ anymore in any MCMC iteration;
- The step sampling η_t 's can be greatly simplified and accelerated:

$$\begin{aligned} H &= H(\psi) = I_{T \times T} \\ \Rightarrow H_t^+ &= (0, 0, \dots, 0)_{1 \times (T-1)} I_{(T-1) \times (T-1)} = (0, 0, \dots, 0)_{1 \times (T-1)} \text{ and} \\ H_t^* &= 1 - (0, 0, \dots, 0)_{1 \times (T-1)} (0, 0, \dots, 0)_{(T-1) \times 1}^T = 1 - 0 = 1 \quad \forall t \in \{1, 2, \dots, T\}. \end{aligned}$$

Hence $\mathbb{C}_{0\eta_t} = \Upsilon_{k \times k}$ and $\mathbb{E}_{0\eta_t} = (0, 0, \dots, 0)_{k \times 1}^T \forall t$

$$\Rightarrow \mathbb{C}_{\eta_t} = (\Lambda^T \Xi^{-1} \Lambda + \Upsilon^{-1})^{-1} \text{ and } \mu_{\eta_t} = \Lambda^T \Xi^{-1} (\mathbf{y}_t - X_t \boldsymbol{\beta}) \forall t \text{ in Equation (A.1).}$$

Under most circumstances, however, temporal correlation should indeed be taken into consideration. Fortunately, under a widely encountered special application scenario when all our time points are equally spaced, substantial computational acceleration is indeed achievable by exploiting the corresponding temporal correlation matrix's special structure.

B.2 Some Set-Up and Notations

Throughout the rest of this section, we assume the scenario when temporal correlation is included and all time points are equispaced with the adjacent distances normalized to 1. Four temporal structures – `ar1`, `exponential`, `sar1`, `sexponential`, which denote AR(1), the exponential process, and their seasonal counterparts (Section 2.1), respectively, are considered.

$$\text{Let } \rho = \begin{cases} \psi \in (0, 1), & \text{if temporal.structure} = \text{'ar1'} \text{ or 'sar1'} \\ e^{-\psi} \in (0, 1), & \text{if temporal.structure} = \text{'exponential'} \text{ or 'sexponential'} \end{cases}.$$

Then for $T \geq 3$, the $T \times T$ temporal correlation structure matrix, which is ensured positive definite (Appendix B.3), is

$$H = H(\psi) = \begin{pmatrix} 1 & \rho & \rho^2 & \dots & \rho^{T-1} \\ \rho & 1 & \rho & \dots & \rho^{T-2} \\ \rho^2 & \rho & 1 & \dots & \rho^{T-3} \\ \vdots & \vdots & \vdots & \ddots & \vdots \\ \rho^{T-1} & \rho^{T-2} & \rho^{T-3} & \dots & 1 \end{pmatrix}$$

if `temporal.structure` = "ar1" or "exponential", and $H = H(\psi, d) =$

$$\begin{aligned}
&= \begin{pmatrix} 1 & -\rho & 0 & 0 & \dots & 0 \\ 0 & 1 & -\rho & 0 & \dots & 0 \\ 0 & 0 & 1 & -\rho & \dots & 0 \\ \vdots & \vdots & \vdots & \ddots & \ddots & \vdots \\ 0 & 0 & 0 & \dots & 1 & -\rho \\ 0 & 0 & 0 & \dots & 0 & 1 \end{pmatrix} \begin{pmatrix} 1 & 0 & 0 & \dots & 0 \\ 0 & \frac{1}{\sqrt{1-\rho^2}} & 0 & \dots & 0 \\ 0 & 0 & \frac{1}{\sqrt{1-\rho^2}} & \dots & 0 \\ \vdots & \vdots & \vdots & \ddots & \vdots \\ 0 & 0 & 0 & \dots & \frac{1}{\sqrt{1-\rho^2}} \end{pmatrix} \\
&= \begin{pmatrix} 1 & -\frac{\rho}{\sqrt{1-\rho^2}} & 0 & 0 & \dots & 0 \\ 0 & \frac{1}{\sqrt{1-\rho^2}} & -\frac{\rho}{\sqrt{1-\rho^2}} & 0 & \dots & 0 \\ 0 & 0 & \frac{1}{\sqrt{1-\rho^2}} & -\frac{\rho}{\sqrt{1-\rho^2}} & \dots & 0 \\ \vdots & \vdots & \vdots & \ddots & \ddots & \vdots \\ 0 & 0 & 0 & \dots & \frac{1}{\sqrt{1-\rho^2}} & -\frac{\rho}{\sqrt{1-\rho^2}} \\ 0 & 0 & 0 & \dots & 0 & \frac{1}{\sqrt{1-\rho^2}} \end{pmatrix}_{T \times T}, \text{ and} \\
H^{-1} &= (L^{-1})^T D^{-1} L^{-1} = \text{Rooti}(H) [\text{Rooti}(H)]^T
\end{aligned}$$

$$= \frac{1}{1-\rho^2} \begin{pmatrix} 1 & -\rho & & & & & \\ -\rho & 1+\rho^2 & -\rho & & & & \\ & -\rho & 1+\rho^2 & \ddots & & & \\ & & -\rho & \ddots & -\rho & & \\ & & & \ddots & 1+\rho^2 & -\rho & \\ & & & & -\rho & 1+\rho^2 & -\rho \\ & & & & & -\rho & 1 \end{pmatrix}_{T \times T}.$$

B.3.2 When temporal.structure = 'sar1' or 'sexponential'

Let $L_{T \times T} =$

B.4.2 When temporal.structure = ‘sar1’ or ‘sexponential’

We have

$$H_t^+ = \begin{cases} \left(0, \dots, 0, \frac{t+d-1}{\rho}, 0, \dots, 0 \right), & \text{if } t \in \{1, 2, \dots, d\} \\ \left(0, \dots, 0, \frac{\rho}{1+\rho^2}, 0, \dots, 0, \frac{t+d-1}{1+\rho^2}, 0, \dots, 0 \right), & \text{if } t \in \{d+1, d+2, \dots, T-d\} \\ \left(0, \dots, 0, \frac{t-d}{\rho}, 0, \dots, 0 \right), & \text{if } t \in \{T-d+1, \dots, T-1, T\} \end{cases} \quad (\text{B.1})$$

\Rightarrow

$$H_t^* = \begin{cases} 1 - \rho^2, & \text{if } t \in \{1, 2, \dots, d, T-d+1, \dots, T-1, T\} \\ 1 - 2 \cdot \rho \cdot \frac{\rho}{1+\rho^2} = \frac{1-\rho^2}{1+\rho^2}, & \text{if } t \in \{d+1, d+2, \dots, T-d\} \end{cases} \quad (\text{B.2})$$

since the t^{th} position in the t^{th} column of $H_{T \times T}$ is 1 and thus

- The $(t+d-1)^{\text{th}}$ position in the $(T-1) \times 1$ vector $H_{(1:T)_{-t,t}}$ is ρ for $t \in \{1, 2, \dots, d\}$;
- The $(t-d)^{\text{th}}$ and $(t+d-1)^{\text{th}}$ positions in the $(T-1) \times 1$ vector $H_{(1:T)_{-t,t}}$ are both ρ for $t \in \{d+1, d+2, \dots, T-d\}$;
- The $(t-d)^{\text{th}}$ position in the $(T-1) \times 1$ vector $H_{(1:T)_{-t,t}}$ is ρ for $t \in \{T-d+1, \dots, T-1, T\}$.

We leave the proof of Equation (B.1) to Appendix B.5.

B.4.3 Attained Acceleration Outcomes Pertaining to Sampling η_t 's

As shown by Appendices B.4.1 and B.4.2, we have simple sparse closed-form representations for the T vectors $H_t^+ = H_{t,-t} H_{-t,-t}^{-1}$ of length $T-1$ and repetitive closed-form solutions for the T scalars $H_t^* = H_{t,t} - H_t^+ H_{-t,t} = H_{t,t} - H_{t,-t} H_{-t,-t}^{-1} H_{-t,t}$, $t \in \{1, \dots, T\}$. Hence, in each MCMC iteration,

1. We take $d=1$ when there is no temporal seasonality. Then

$$H_t^* = \begin{cases} 1 - \rho^2 & \forall t \in \{1, 2, \dots, d, T-d+1, \dots, T-1, T\} \\ \frac{1-\rho^2}{1+\rho^2} & \forall t \in \{d+1, d+2, \dots, T-d\} \end{cases} \quad \text{and thus} \\ \mathbb{C}_{0\eta_t} = H_t^* \otimes \Upsilon_{k \times k} = \begin{cases} (1 - \rho^2) \cdot \Upsilon & \forall t \in \{1, 2, \dots, d, T-d+1, \dots, T-1, T\} \\ \frac{1-\rho^2}{1+\rho^2} \cdot \Upsilon & \forall t \in \{d+1, d+2, \dots, T-d\} \end{cases}.$$

Hence, the values of these quantities can be directly specified rather than calculated. Furthermore, we can opt to first specify $H_t^* = \frac{1-\rho^2}{1+\rho^2}$ and $\mathbb{C}_{0\eta_t} = \frac{1-\rho^2}{1+\rho^2} \cdot \Upsilon \forall t \in \{1, \dots, T\}$ outside of the loop over t and then only modify these two values inside the loop over t for $t \in \{1, 2, \dots, d, T-d+1, \dots, T-1, T\}$.

2. For each $t \in \{1, \dots, T\}$ inside the loop over t , we can specify H_t^+ by modifying one or two entries on the zero vector of length $T-1$ instead of calculating H_t^+ from $H_{(1:T)_{-t}, (1:T)_{-t}}^{-1}$.
3. We no longer need to compute and store $H(\psi)_{T \times T}$ itself, since $H(\psi)$ is only used when sampling η_t 's in the entire Gibbs sampler, where we extract out its sub-matrices $H_{-t,-t}$'s, $H_{t,-t}$'s $H_{-t,t}$'s, $H_{t,t}$'s to calculate H_t^+ 's and H_t^* 's.

and

$$* = \begin{cases} \frac{1^2}{1-\rho^4} + \frac{(-\rho)^2}{1-\rho^2} = \frac{\rho^4 + \rho^2 + 1}{1-\rho^4}, & \text{if } t + d - 1 < T - d \iff t \in \{d + 1, d + 2, \dots, T - 2d\} \\ \frac{1^2}{1-\rho^4} = \frac{1}{1-\rho^4}, & \text{if } t + d - 1 \geq T - d \iff t \in \{T - 2d + 1, T - 2d + 2, \dots, T - d\} \end{cases}. \quad (\text{B.4})$$

$$\begin{aligned} \text{Hence, } H_t^+ &= [H_{t,(1:T)-t}]_{1 \times (T-1)} H_{(1:T)-t,(1:T)-t}^{-1} \\ &= \left(\dots, \overset{t-2d}{\rho^2}, \dots, 0, \overset{t-d}{\rho^1}, 0, \dots, 0, \overset{t+d-1}{\rho^1}, 0, \dots, \overset{t+2d-1}{\rho^2}, \dots \right) H_{(1:T)-t,(1:T)-t}^{-1} \\ &= \left(0, \dots, 0, \overset{t-d}{\frac{\rho}{1+\rho^2}}, 0, \dots, 0, \overset{t+d-1}{\frac{\rho}{1+\rho^2}}, 0, \dots, 0 \right) \forall t \in \{d + 1, d + 2, \dots, T - d\}. \end{aligned}$$

□

Notes: $\forall t \in \{d + 1, d + 2, \dots, T - d\}$,

- The $(t - d)^{\text{th}}$ entry in the length- $(T - 1)$ vector H_t^+ is (by Equation (B.3))

$$\begin{aligned} &\rho \times \left(+ - \frac{\rho^2}{1 - \rho^4} \right) + \mathbb{1}_{\{t > 2d\}} \times \rho^2 \times \left(- \frac{\rho}{1 - \rho^2} \right) \\ &= \begin{cases} \rho \times \left(\frac{\rho^4 + \rho^2 + 1}{1 - \rho^4} - \frac{\rho^2}{1 - \rho^4} \right) + \rho^2 \times \left(- \frac{\rho}{1 - \rho^2} \right) = \rho \times \left(\frac{\rho^4 + 1}{1 - \rho^4} - \frac{\rho^2}{1 - \rho^2} \right) = \rho \times \frac{\rho^4 + 1 - \rho^2(1 + \rho^2)}{1 - \rho^4} \\ = \rho \times \frac{1 - \rho^2}{1 - \rho^4} = \frac{\rho}{1 + \rho^2}, & \text{if } t > 2d \iff t \in \{2d + 1, \dots, T - d\} \\ \rho \times \left(\frac{1}{1 - \rho^4} - \frac{\rho^2}{1 - \rho^4} \right) = \rho \times \frac{1}{1 + \rho^2} = \frac{\rho}{1 + \rho^2}, & \text{if } t \leq 2d \iff t \in \{d + 1, \dots, 2d\} \end{cases} \\ &= \frac{\rho}{1 + \rho^2} \forall t \in \{d + 1, d + 2, \dots, T - d\}. \end{aligned}$$

- Similarly, $(t + d - 1)^{\text{th}}$ entry in the length- $(T - 1)$ vector H_t^+ is (by Equation (B.4))

$$\begin{aligned} &\rho \times \left(* - \frac{\rho^2}{1 - \rho^4} \right) + \mathbb{1}_{\{t \leq T - 2d\}} \times \rho^2 \times \left(- \frac{\rho}{1 - \rho^2} \right) \\ &= \begin{cases} \rho \times \left(\frac{\rho^4 + \rho^2 + 1}{1 - \rho^4} - \frac{\rho^2}{1 - \rho^4} \right) + \rho^2 \times \left(- \frac{\rho}{1 - \rho^2} \right) = \rho \times \left(\frac{\rho^4 + 1}{1 - \rho^4} - \frac{\rho^2}{1 - \rho^2} \right) = \rho \times \frac{\rho^4 + 1 - \rho^2(1 + \rho^2)}{1 - \rho^4} \\ = \rho \times \frac{1 - \rho^2}{1 - \rho^4} = \frac{\rho}{1 + \rho^2}, & \text{if } t \leq T - 2d \iff t \in \{d + 1, \dots, T - 2d\} \\ \rho \times \left(\frac{1}{1 - \rho^4} - \frac{\rho^2}{1 - \rho^4} \right) = \rho \times \frac{1}{1 + \rho^2} = \frac{\rho}{1 + \rho^2}, & \text{if } t > T - 2d \iff t \in \{T - 2d + 1, \dots, T - d\} \end{cases} \\ &= \frac{\rho}{1 + \rho^2} \forall t \in \{d + 1, d + 2, \dots, T - d\}. \end{aligned}$$

- The $\{(t - d), (t - d)\}^{\text{th}}$ entry in $H_{-t,-t} [H_{-t,-t}]^{-1} = 1$ because

– if $t > 2d$, then this entry equals

$$\begin{aligned} &(\rho, 1, \rho^2) \left(- \frac{\rho}{1 - \rho^2}, \frac{1}{1 - \rho^2} + \frac{\rho^4}{1 - \rho^4}, - \frac{\rho^2}{1 - \rho^4} \right)^{\text{T}} \\ &= \frac{1}{1 - \rho^2} [\rho \cdot (-\rho) + 1 \cdot 1] + \frac{1}{1 - \rho^4} [1 \cdot \rho^4 + \rho^2 \cdot (-\rho^2)] = 1 + 0 = 1; \end{aligned}$$

– if $t \leq 2d$, then this entry equals

$$(1, \rho^2) \left(\frac{1}{1 - \rho^4}, - \frac{\rho^2}{1 - \rho^4} \right)^{\text{T}} = 1.$$

- Similarly, the $\{(t+d-1), (t+d-1)\}^{\text{th}}$ entry in $H_{-t,-t} [H_{-t,-t}]^{-1} = 1$ because
 - if $t \leq T - 2d$, then this entry equals

$$\begin{aligned} & (\rho^2, 1, \rho) \left(-\frac{\rho^2}{1-\rho^4}, \frac{1}{1-\rho^4} + \frac{\rho^2}{1-\rho^2}, -\frac{\rho}{1-\rho^2} \right)^{\text{T}} \\ &= \frac{1}{1-\rho^4} [\rho^2 \cdot (-\rho^2) + 1 \cdot 1] + \frac{1}{1-\rho^2} [1 \cdot \rho^2 - \rho \cdot \rho] = 1 + 0 = 1; \end{aligned}$$

- if $t > T - 2d$, then this entry equals

$$(\rho^2, 1) \left(-\frac{\rho^2}{1-\rho^4}, \frac{1}{1-\rho^4} \right)^{\text{T}} = 1.$$

C A VAR(1) Process for the Latent Temporal Factors $\boldsymbol{\eta}_{1:T}$

Throughout this section, we assume evenly dispersed time points corresponding to our observed data. To model the zero-mean $k \times 1$ latent temporal factors $\boldsymbol{\eta}_t$, $t \in \{1, 2, \dots, T\}$, we consider a VAR(1) model in reduced form

$$\boldsymbol{\eta}_t = A\boldsymbol{\eta}_{t-1} + \boldsymbol{\epsilon}_t, \quad \boldsymbol{\epsilon}_t \sim N_k(\mathbf{0}, \Upsilon), \quad t = 1, 2, \dots, T, \quad (\text{C.1})$$

where $\Upsilon_{k \times k}$ is positive definite, $A_{k \times k}$ is invertible, and $\boldsymbol{\eta}_0$ is assumed to be $\mathbf{0}_{k \times 1}$. Equation (C.1) simplifies to an AR(1) model if we take $A_{k \times k} = \psi I_{k \times k}$ for some $\psi \in (0, 1)$. We assign priors $f_0(A)$ and $\Upsilon \sim \mathcal{IW}_k(\zeta, \Omega)$ (the Inverse Wishart distribution with degrees of freedom $\zeta > k - 1$ and $k \times k$ positive definite scale matrix Ω) to parameters A and Υ respectively. By modifying the original Gibbs sampling steps for temporal-related parameters, we can form integrated spatiotemporal Bayesian Gaussian factor models that permit convenient adequate predictions at any arbitrary future time points.

C.1 New Gibbs Sampling Steps for Temporal-Related Parameters

The temporal-related parameters in our new holistic modeling frameworks are now $\{\boldsymbol{\eta}_{1:T}, \Upsilon, A\}$ instead of $\{\boldsymbol{\eta}_{1:T}, \Upsilon, \psi\}$. We detail the corresponding new Gibbs sampler steps in what ensues.

Sampling From the Full Conditional Distributions of the $k \times 1$ Vectors $\boldsymbol{\eta}_t$'s

Fix any arbitrary $t \in \{1, \dots, T-1\}$. Then

$$\begin{aligned} f(\boldsymbol{\eta}_t | \cdot) &\propto f(\mathbf{y}_t | \boldsymbol{\beta}, \Lambda, \boldsymbol{\eta}_t, \Xi) \times f(\boldsymbol{\eta}_{1:T} | A, \Upsilon) \propto f(\mathbf{y}_t | \boldsymbol{\beta}, \Lambda, \boldsymbol{\eta}_t, \Xi) \times f(\boldsymbol{\eta}_t | \boldsymbol{\eta}_{t-1}, A, \Upsilon) \times f(\boldsymbol{\eta}_{t+1} | \boldsymbol{\eta}_t, A, \Upsilon) \\ &\propto \exp \left\{ -\frac{1}{2} (\mathbf{y}_t - X_t \boldsymbol{\beta} - \Lambda \boldsymbol{\eta}_t)^{\text{T}} \Xi^{-1} (\mathbf{y}_t - X_t \boldsymbol{\beta} - \Lambda \boldsymbol{\eta}_t) \right\} \times \\ &\quad \exp \left\{ -\frac{1}{2} (\boldsymbol{\eta}_t - A \boldsymbol{\eta}_{t-1})^{\text{T}} \Upsilon^{-1} (\boldsymbol{\eta}_t - A \boldsymbol{\eta}_{t-1}) \right\} \times \exp \left\{ -\frac{1}{2} (\boldsymbol{\eta}_{t+1} - A \boldsymbol{\eta}_t)^{\text{T}} \Upsilon^{-1} (\boldsymbol{\eta}_{t+1} - A \boldsymbol{\eta}_t) \right\} \\ &\propto \exp \left\{ -\frac{1}{2} [\boldsymbol{\eta}_t^{\text{T}} V_{\boldsymbol{\eta}_t}^{-1} \boldsymbol{\eta}_t - 2 \cdot \boldsymbol{\eta}_t^{\text{T}} (\Lambda^{\text{T}} \Xi^{-1} (\mathbf{y}_t - X_t \boldsymbol{\beta}) + \Upsilon^{-1} A \boldsymbol{\eta}_{t-1} + A^{\text{T}} \Upsilon^{-1} \boldsymbol{\eta}_{t+1})] \right\} \\ &\Rightarrow \boldsymbol{\eta}_t | \cdot \sim N_k(V_{\boldsymbol{\eta}_t} [\Lambda^{\text{T}} \Xi^{-1} (\mathbf{y}_t - X_t \boldsymbol{\beta}) + \Upsilon^{-1} A \boldsymbol{\eta}_{t-1} + A^{\text{T}} \Upsilon^{-1} \boldsymbol{\eta}_{t+1}], V_{\boldsymbol{\eta}_t}), \\ &\quad \text{where } V_{\boldsymbol{\eta}_t} = [\Lambda^{\text{T}} \Xi^{-1} \Lambda + \Upsilon^{-1} + A^{\text{T}} \Upsilon^{-1} A]^{-1}. \end{aligned} \quad (\text{C.2})$$

For $t = T$,

$$\begin{aligned}
f(\boldsymbol{\eta}_T|\cdot) &\propto f(\mathbf{y}_T|\boldsymbol{\beta}, \Lambda, \boldsymbol{\eta}_T, \Xi) \times f(\boldsymbol{\eta}_{1:T}|A, \Upsilon) \propto f(\mathbf{y}_T|\boldsymbol{\beta}, \Lambda, \boldsymbol{\eta}_T, \Xi) \times f(\boldsymbol{\eta}_T|\boldsymbol{\eta}_{T-1}, A, \Upsilon) \\
&\propto \exp\left\{-\frac{1}{2}(\mathbf{y}_T - X_T\boldsymbol{\beta} - \Lambda\boldsymbol{\eta}_T)^\top \Xi^{-1}(\mathbf{y}_T - X_T\boldsymbol{\beta} - \Lambda\boldsymbol{\eta}_T)\right\} \times \\
&\quad \exp\left\{-\frac{1}{2}(\boldsymbol{\eta}_T - A\boldsymbol{\eta}_{T-1})^\top \Upsilon^{-1}(\boldsymbol{\eta}_T - A\boldsymbol{\eta}_{T-1})\right\} \\
&\propto \exp\left\{-\frac{1}{2}[\boldsymbol{\eta}_T^\top (\Lambda^\top \Xi^{-1} \Lambda + \Upsilon^{-1}) \boldsymbol{\eta}_T - 2 \cdot \boldsymbol{\eta}_T^\top (\Lambda^\top \Xi^{-1}(\mathbf{y}_T - X_T\boldsymbol{\beta}) + \Upsilon^{-1} A\boldsymbol{\eta}_{T-1})]\right\} \\
&\Rightarrow \boldsymbol{\eta}_T | \cdot \sim N_k\left([\Lambda^\top \Xi^{-1} \Lambda + \Upsilon^{-1}]^{-1} [\Lambda^\top \Xi^{-1}(\mathbf{y}_T - X_T\boldsymbol{\beta}) + \Upsilon^{-1} A\boldsymbol{\eta}_{T-1}], [\Lambda^\top \Xi^{-1} \Lambda + \Upsilon^{-1}]^{-1}\right).
\end{aligned} \tag{C.3}$$

Sampling From the Full Conditional Distribution of the Positive Definite Matrix

$$\Upsilon_{k \times k}$$

$$\begin{aligned}
f(\Upsilon|\cdot) &\propto f(\boldsymbol{\eta}_{1:T}|A, \Upsilon, \boldsymbol{\eta}_0 = \mathbf{0}_{k \times 1}) \times f_0(\Upsilon), \text{ where } f_0 = \mathcal{IW}_k(\zeta, \Omega) \\
&\propto |\Upsilon|^{-\frac{T}{2}} \prod_{t=1}^T \exp\left\{-\frac{1}{2}(\boldsymbol{\eta}_t - A\boldsymbol{\eta}_{t-1})^\top \Upsilon^{-1}(\boldsymbol{\eta}_t - A\boldsymbol{\eta}_{t-1})\right\} \times |\Upsilon|^{-\frac{\zeta+k+1}{2}} \exp\left\{-\frac{1}{2}\text{tr}(\Omega\Upsilon^{-1})\right\} \\
&= |\Upsilon|^{-\frac{T+\zeta+k+1}{2}} \exp\left\{-\frac{1}{2}\sum_{t=1}^T \text{tr}((\boldsymbol{\eta}_t - A\boldsymbol{\eta}_{t-1})^\top \Upsilon^{-1}(\boldsymbol{\eta}_t - A\boldsymbol{\eta}_{t-1}))\right\} \cdot \exp\left\{-\frac{1}{2}\text{tr}(\Omega\Upsilon^{-1})\right\} \\
&= |\Upsilon|^{-\frac{T+\zeta+k+1}{2}} \exp\left\{-\frac{1}{2}\left[\sum_{t=1}^T \text{tr}((\boldsymbol{\eta}_t - A\boldsymbol{\eta}_{t-1})(\boldsymbol{\eta}_t - A\boldsymbol{\eta}_{t-1})^\top \Upsilon^{-1}) + \text{tr}(\Omega\Upsilon^{-1})\right]\right\} \\
&= |\Upsilon|^{-\frac{T+\zeta+k+1}{2}} \exp\left\{-\frac{1}{2}\text{tr}\left(\left[\sum_{t=1}^T (\boldsymbol{\eta}_t - A\boldsymbol{\eta}_{t-1})(\boldsymbol{\eta}_t - A\boldsymbol{\eta}_{t-1})^\top + \Omega\right] \Upsilon^{-1}\right)\right\} \\
&\Rightarrow \Upsilon | \cdot \sim \mathcal{IW}_k\left(T + \zeta, \sum_{t=1}^T (\boldsymbol{\eta}_t - A\boldsymbol{\eta}_{t-1})(\boldsymbol{\eta}_t - A\boldsymbol{\eta}_{t-1})^\top + \Omega\right).
\end{aligned} \tag{C.4}$$

Sampling From the Full Conditional Distribution of the Invertible Matrix $A_{k \times k}$

Write $A = (\mathbf{a}_1, \mathbf{a}_2, \dots, \mathbf{a}_k)$, where \mathbf{a}_j denotes the j^{th} column of A for $j = 1, 2, \dots, k$, and let $f_0(A) = \mathcal{MN}_{k,k}(M, \Upsilon, V)$, where $\Upsilon_{k \times k}$ and $V_{k \times k}$ are both positive definite scale matrices and $M_{k \times k}$ is a location matrix. Since $A \sim \mathcal{MN}_{k,k}(M, \Upsilon, V) \iff \text{vec}(A) \sim N_{k^2}(\text{vec}(M), V \otimes \Upsilon)$,

$$\begin{aligned}
f(A|\cdot) &\propto f(\boldsymbol{\eta}_{1:T}|A, \Upsilon, \boldsymbol{\eta}_0 = \mathbf{0}_{k \times 1}) \times f_0(A) \\
&\propto \prod_{t=1}^T \exp\left\{-\frac{1}{2}(\boldsymbol{\eta}_t - A\boldsymbol{\eta}_{t-1})^\top \Upsilon^{-1}(\boldsymbol{\eta}_t - A\boldsymbol{\eta}_{t-1})\right\} \times f_0(A) \\
&\propto \exp\left\{-\frac{1}{2}[\text{vec}(A) - \text{vec}(M)]^\top (V^{-1} \otimes \Upsilon^{-1}) [\text{vec}(A) - \text{vec}(M)]\right\} \times \\
&\quad \prod_{t=1}^T \exp\left\{-\frac{1}{2}(\eta_{t-1,1}\mathbf{a}_1 + \dots + \eta_{t-1,k}\mathbf{a}_k - \boldsymbol{\eta}_t)^\top \Upsilon^{-1}(\eta_{t-1,1}\mathbf{a}_1 + \dots + \eta_{t-1,k}\mathbf{a}_k - \boldsymbol{\eta}_t)\right\} \\
&= \exp\left\{-\frac{1}{2}[\text{vec}(A) - \text{vec}(M)]^\top (V^{-1} \otimes \Upsilon^{-1}) [\text{vec}(A) - \text{vec}(M)]\right\} \times \\
&\quad \prod_{t=1}^T \exp\left[-\frac{1}{2}\text{vec}(A)^\top \{[\boldsymbol{\eta}_{t-1}\boldsymbol{\eta}_{t-1}^\top] \otimes \Upsilon^{-1}\} \text{vec}(A) + \text{vec}(A)^\top (\boldsymbol{\eta}_{t-1} \otimes \Upsilon^{-1}) \boldsymbol{\eta}_t\right]
\end{aligned}$$

$$\begin{aligned}
& \propto \exp \left\{ -\frac{1}{2} \text{vec}(A)^T [V_A^{-1} \otimes \Upsilon^{-1}] \text{vec}(A) + \text{vec}(A)^T \left[(V^{-1} \otimes \Upsilon^{-1}) \text{vec}(M) + \sum_{t=1}^T (\boldsymbol{\eta}_{t-1} \otimes \Upsilon^{-1}) \boldsymbol{\eta}_t \right] \right\} \\
& \quad \text{with } V_A = \left(\sum_{t=1}^T [\boldsymbol{\eta}_{t-1} \boldsymbol{\eta}_{t-1}^T] + V^{-1} \right)^{-1} \\
& \Rightarrow \text{vec}(A) \mid \cdot \sim N_{k^2} \left([V_A V^{-1} \otimes I_{k \times k}] \text{vec}(M) + \sum_{t=1}^T [V_A \boldsymbol{\eta}_{t-1} \otimes I_{k \times k}] \boldsymbol{\eta}_t, V_A \otimes \Upsilon \right) \\
& \iff A \mid \cdot \sim \mathcal{MN}_{k,k} (M_A, \Upsilon, V_A), \tag{C.5}
\end{aligned}$$

where M_A is $k \times k$ with vectorized form $[V_A V^{-1} \otimes I_{k \times k}] \text{vec}(M) + \sum_{t=1}^T [V_A \boldsymbol{\eta}_{t-1} \otimes I_{k \times k}] \boldsymbol{\eta}_t$.

C.2 Predictions at Desired Future Time Points

Suppose we have $q \geq 1$, $q \in \mathbb{N}$ new time points $T+1, \dots, T+q$. Then for predicting $\hat{\mathbf{y}}_{(T+1):(T+q)}$ given $\mathbf{y}_{1:T}$ and covariates matrix $[X_{(T+1):(T+q)}]_{q \times p}$ (if $p \geq 1$) under our integrated frameworks, we can write the posterior predictive distribution (PPD) as

$$f(\mathbf{y}_{(T+1):(T+q)} \mid \mathbf{y}_{1:T}, X_{(T+1):(T+q)}) = \int_{\Theta} f(\mathbf{y}_{(T+1):(T+q)} \mid \Theta, \mathbf{y}_{1:T}, X_{(T+1):(T+q)}) \pi(\Theta \mid \mathbf{y}_{1:T}) d\Theta,$$

$$\text{where } \Theta = \begin{cases} (\Lambda, \boldsymbol{\beta}, \boldsymbol{\sigma}^2, \boldsymbol{\eta}_{(T+1):(T+q)}, \boldsymbol{\eta}, \Upsilon, A), & \text{if clustering} = \text{FALSE} \\ (\boldsymbol{\theta}, \boldsymbol{\xi}, \boldsymbol{\beta}, \boldsymbol{\sigma}^2, \boldsymbol{\eta}_{(T+1):(T+q)}, \boldsymbol{\eta}, \Upsilon, A), & \text{if clustering} = \text{TRUE} \end{cases}, \text{ and } \boldsymbol{\eta} \text{ denotes } \boldsymbol{\eta}_{1:T}, \tag{C.6}$$

where **clustering** = FALSE refers to the scenario when no spatial clustering mechanism is integrated, and **clustering** = TRUE refers to the case when a spatial PSBP clustering mechanism is incorporated. We can then partition the integral in Equation (C.6) into

$$\begin{aligned}
& \int_{\Theta} \underbrace{f(\mathbf{y}_{(T+1):(T+q)} \mid \Lambda, \boldsymbol{\eta}_{(T+1):(T+q)}, \boldsymbol{\beta}, \boldsymbol{\sigma}^2, X_{(T+1):(T+q)})}_{T_1} \underbrace{f(\boldsymbol{\eta}_{(T+1):(T+q)} \mid \boldsymbol{\eta}, \Upsilon, A)}_{T_2} \\
& \quad \times \underbrace{\pi(\Lambda, \boldsymbol{\beta}, \boldsymbol{\sigma}^2, \boldsymbol{\eta}, \Upsilon, A \mid \mathbf{y}_{1:T})}_{T_3} d\Theta \text{ if clustering} = \text{FALSE, and} \tag{C.7}
\end{aligned}$$

$$\begin{aligned}
& \int_{\Theta} \underbrace{f(\mathbf{y}_{(T+1):(T+q)} \mid \boldsymbol{\theta}, \boldsymbol{\xi}, \boldsymbol{\eta}_{(T+1):(T+q)}, \boldsymbol{\beta}, \boldsymbol{\sigma}^2, X_{(T+1):(T+q)})}_{T_1} \underbrace{f(\boldsymbol{\eta}_{(T+1):(T+q)} \mid \boldsymbol{\eta}, \Upsilon, A)}_{T_2} \\
& \quad \times \underbrace{\pi(\boldsymbol{\theta}, \boldsymbol{\xi}, \boldsymbol{\beta}, \boldsymbol{\sigma}^2, \boldsymbol{\eta}, \Upsilon, A \mid \mathbf{y}_{1:T})}_{T_3} d\Theta \text{ if clustering} = \text{TRUE.} \tag{C.8}
\end{aligned}$$

In Equations (C.7) and (C.8), T_1 is the observed likelihood and T_3 is the parameters' posterior distribution obtained from the original model fit's MCMC sampler. For T_2 ,

$$\begin{aligned}
f(\boldsymbol{\eta}_{(T+1):(T+q)} \mid \boldsymbol{\eta}_{1:T}, \Upsilon, A) &= \prod_{r=1}^q f(\boldsymbol{\eta}_{T+r} \mid \boldsymbol{\eta}_{(T+1):(T+r-1)}, \boldsymbol{\eta}_{1:T}, \Upsilon, A) \tag{C.9} \\
&= \prod_{r=1}^q N_k(\boldsymbol{\eta}_{T+r} \mid A \boldsymbol{\eta}_{T+r-1}, \Upsilon),
\end{aligned}$$

where for each r , $N_k(\boldsymbol{\eta}_{T+r} | A\boldsymbol{\eta}_{T+r-1}, \Upsilon)$ denotes the density of a k -variate normal distribution with mean $A\boldsymbol{\eta}_{T+r-1}$ and covariance matrix Υ evaluated at $\boldsymbol{\eta}_{T+r}$. Hence, we can obtain a predicted $\hat{\boldsymbol{\eta}}_{(T+1):(T+q)} | \boldsymbol{\eta}_{1:T}, A, \Upsilon$ by first sampling $\hat{\boldsymbol{\eta}}_{T+1}$ from $N_k(A\boldsymbol{\eta}_T, \Upsilon)$ and then sampling $\hat{\boldsymbol{\eta}}_{T+r}$ from $N_k(A\hat{\boldsymbol{\eta}}_{T+r-1}, \Upsilon)$ one by one for $r = 2, 3, \dots, q$.

D Facilitating Efficient Computation for Spatial PSBP

One major computational issue pertaining to our model in Section 2.2 lies in sampling $\boldsymbol{\alpha}_{jl}$'s from their full conditionals $f(\boldsymbol{\alpha}_{jl} | \cdot)$'s. We notice that $\{\boldsymbol{\alpha}_{jl} : j = 1, \dots, k, l = 1, \dots, L-1\}$ affects the fitted response $\hat{\boldsymbol{y}}$ via $\{\boldsymbol{w}_{jl} : j = 1, \dots, k, l = 1, \dots, L\}$, the set of probability parameters for the multinomial distributions of $\xi_j(\boldsymbol{s}_{i,o})$'s, and that

$$\begin{aligned} \forall (i, o, l) \in \{1, \dots, m\} \times \{1, \dots, O\} \times \{1, \dots, L\}, & \quad (\text{D.1}) \\ \mathbb{P}(\xi_j(\boldsymbol{s}_{i,o}) = l | \boldsymbol{\alpha}_{jr}(\boldsymbol{s}_{i,o}), 1 \leq r \leq L-1) &= \mathbb{P}(\xi_j(\boldsymbol{s}_{i,o}) = l | \boldsymbol{\alpha}_{jr}(\boldsymbol{s}_{i,o}), 1 \leq r \leq \min\{l, L-1\}) \\ = w_{jl}(\boldsymbol{s}_{i,o}) &= \begin{cases} \Phi(\boldsymbol{\alpha}_{jl}(\boldsymbol{s}_{i,o})) \prod_{r < l} [1 - \Phi(\boldsymbol{\alpha}_{jr}(\boldsymbol{s}_{i,o}))], & \text{if } l \in \{1, \dots, L-1\} \\ \prod_{r < L} [1 - \Phi(\boldsymbol{\alpha}_{jr}(\boldsymbol{s}_{i,o}))], & \text{if } l = L \end{cases}. \end{aligned}$$

Hence for any arbitrary $(j, l) \in \{1, \dots, k\} \times \{1, \dots, L-1\}$, $f(\boldsymbol{\alpha}_{jl} | \cdot) \propto f(\boldsymbol{\xi}_j | \boldsymbol{\alpha}_{jr}, 1 \leq r \leq L-1) \times f_0(\boldsymbol{\alpha}_{jl} | \boldsymbol{\kappa}, \rho)$, which is burdensome to sample from due to loss of conjugacy.

This issue can be tackled by adopting ideas put forward by Rodríguez and Dunson (2011). In this context, we introduce a set of latent variables $z_{jl}(\boldsymbol{s}_{i,o}) \stackrel{\text{ind}}{\sim} N(\boldsymbol{\alpha}_{jl}(\boldsymbol{s}_{i,o}), 1)$ and define $\xi_j(\boldsymbol{s}_{i,o})$'s values deterministically based on $z_{jl}(\boldsymbol{s}_{i,o})$'s as follows:

$$\begin{aligned} \forall (j, i, o) \in \{1, \dots, k\} \times \{1, \dots, m\} \times \{1, \dots, O\}, & \quad (\text{D.2}) \\ \forall l \in \{1, \dots, L\}, \xi_j(\boldsymbol{s}_{i,o}) = l &\iff \begin{cases} z_{jl}(\boldsymbol{s}_{i,o}) > 0 \text{ and } z_{jr}(\boldsymbol{s}_{i,o}) < 0 \forall r < l, & \text{if } l < L \\ z_{jr}(\boldsymbol{s}_{i,o}) < 0 \forall r < L, & \text{if } l = L \end{cases}. \end{aligned}$$

Fix any arbitrary (j, i, o) . With this set of introduced latent variables $\{z_{jl}(\boldsymbol{s}_{i,o}) : 1 \leq l \leq L-1\}$ and value of the clustering label parameter $\xi_j(\boldsymbol{s}_{i,o})$ defined according to Equation (D.2), for any arbitrary $l \in \{1, \dots, L\}$,

$$\begin{aligned} \mathbb{P}(\xi_j(\boldsymbol{s}_{i,o}) = l | z_{jr}(\boldsymbol{s}_{i,o}), \boldsymbol{\alpha}_{jr}(\boldsymbol{s}_{i,o}), 1 \leq r \leq L-1) &= \mathbb{P}(\xi_j(\boldsymbol{s}_{i,o}) = l | z_{jr}(\boldsymbol{s}_{i,o}), 1 \leq r \leq L-1), \\ \text{and the expression } \int \dots \int \mathbb{P}(\xi_j(\boldsymbol{s}_{i,o}) = l | z_{jr}(\boldsymbol{s}_{i,o}), \boldsymbol{\alpha}_{jr}(\boldsymbol{s}_{i,o}), 1 \leq r \leq L-1) &\times \\ \mathbb{P}(z_{jr}(\boldsymbol{s}_{i,o}), 1 \leq r \leq L-1 | \boldsymbol{\alpha}_{jr}(\boldsymbol{s}_{i,o}), 1 \leq r \leq L-1) dz_{j1}(\boldsymbol{s}_{i,o}) \dots dz_{j(L-1)}(\boldsymbol{s}_{i,o}) & \\ = \begin{cases} \mathbb{P}(z_{jl}(\boldsymbol{s}_{i,o}) > 0 \text{ and } z_{jr}(\boldsymbol{s}_{i,o}) < 0 \forall r < l | \boldsymbol{\alpha}_{jr}(\boldsymbol{s}_{i,o}), 1 \leq r \leq L-1), & \text{if } l < L \\ \mathbb{P}(z_{jr}(\boldsymbol{s}_{i,o}) < 0 \forall r < L | \boldsymbol{\alpha}_{jr}(\boldsymbol{s}_{i,o}), 1 \leq r \leq L-1), & \text{if } l = L \end{cases} & \\ = \begin{cases} \mathbb{P}(z_{jl}(\boldsymbol{s}_{i,o}) > 0 | \boldsymbol{\alpha}_{jl}(\boldsymbol{s}_{i,o})) \prod_{r=1}^{l-1} \mathbb{P}(z_{jr}(\boldsymbol{s}_{i,o}) < 0 | \boldsymbol{\alpha}_{jr}(\boldsymbol{s}_{i,o})), & \text{if } l < L \\ \prod_{r=1}^{L-1} \mathbb{P}(z_{jr}(\boldsymbol{s}_{i,o}) < 0 | \boldsymbol{\alpha}_{jr}(\boldsymbol{s}_{i,o})), & \text{if } l = L \end{cases} & \\ = \begin{cases} \Phi(\boldsymbol{\alpha}_{jl}(\boldsymbol{s}_{i,o})) \prod_{r < l} [1 - \Phi(\boldsymbol{\alpha}_{jr}(\boldsymbol{s}_{i,o}))], & \text{if } l \in \{1, \dots, L-1\} \\ \prod_{r < L} [1 - \Phi(\boldsymbol{\alpha}_{jr}(\boldsymbol{s}_{i,o}))], & \text{if } l = L \end{cases} \end{aligned}$$

does turn out to be the same as $w_{jl}(\mathbf{s}_{i,o}) = \mathbb{P}(\xi_j(\mathbf{s}_{i,o}) = l | \alpha_{jr}(\mathbf{s}_{i,o}), 1 \leq r \leq L-1)$, where $\xi_j(\mathbf{s}_{i,o})$'s value is obtained probabilistically conditioning on $\alpha_{jr}(\mathbf{s}_{i,o}), 1 \leq r \leq L-1$, as in our original model without the introduced latent normal variables $z_{jr}(\mathbf{s}_{i,o})$'s.

Hence, we can opt to sample $\xi_j(\mathbf{s}_{i,o})$'s from their marginal distributions with the latent variables $z_{jl}(\mathbf{s}_{i,o})$'s integrated out as above. The corresponding Gibbs sampler step for $\xi_j(\mathbf{s}_{i,o})$'s is thus unaffected by the introduction of $z_{jl}(\mathbf{s}_{i,o})$'s:

$$\begin{aligned} & \text{Fix any arbitrary } j \in \{1, \dots, k\}. \quad \forall (o, i) \in \{1, \dots, O\} \times \{1, \dots, m\}, \\ & \forall l \in \{1, \dots, L\}, \mathbb{P}(\xi_j(\mathbf{s}_{i,o}) = l | \cdot) \end{aligned} \quad (\text{D.3})$$

$$\begin{aligned} & \propto \mathbb{P}(\xi_j(\mathbf{s}_{i,o}) = l | \alpha_{jr}(\mathbf{s}_{i,o}), r \leq L-1) \prod_{t=1}^T f\left(y_t(\mathbf{s}_{i,o}) | \beta, \boldsymbol{\eta}_t, \sigma^2(\mathbf{s}_{i,o}), \xi_j(\mathbf{s}_{i,o}) = l, \boldsymbol{\xi}_{-j}(\mathbf{s}_{i,o}), \boldsymbol{\theta}_{\xi(\mathbf{s}_{i,o})}\right) \\ & \propto w_{jl}(\mathbf{s}_{i,o}) \times \exp \left\{ -\frac{1}{2} \sigma^{-2}(\mathbf{s}_{i,o}) \sum_{t=1}^T \left[y_t(\mathbf{s}_{i,o}) - \mathbf{x}_t(\mathbf{s}_{i,o})^\top \beta - \sum_{h \neq j} \theta_{h \xi_h(\mathbf{s}_{i,o})} \eta_{th} - \theta_{jl} \eta_{tj} \right]^2 \right\}. \end{aligned}$$

It is also straightforward to sample from the full conditional distributions of $z_{jl}(\mathbf{s}_{i,o})$'s for $l \in \{1, \dots, L-1\}$:

$$\begin{aligned} & \text{For any arbitrary fixed } (j, i, o, l) \in \{1, \dots, k\} \times \{1, \dots, m\} \times \{1, \dots, O\} \times \{1, \dots, L-1\}, \\ & f(z_{jl}(\mathbf{s}_{i,o}) | \cdot) \propto f(\xi_j(\mathbf{s}_{i,o}) | z_{jl}(\mathbf{s}_{i,o})) \times f(z_{jl}(\mathbf{s}_{i,o}) | \alpha_{jl}(\mathbf{s}_{i,o})) \quad (\text{D.4}) \\ & \sim \mathbb{1}_{\{\xi_j(\mathbf{s}_{i,o}) > l\}} N(\alpha_{jl}(\mathbf{s}_{i,o}), 1)_{\mathbb{R}_-} + \mathbb{1}_{\{\xi_j(\mathbf{s}_{i,o}) = l\}} N(\alpha_{jl}(\mathbf{s}_{i,o}), 1)_{\mathbb{R}_+} + \mathbb{1}_{\{\xi_j(\mathbf{s}_{i,o}) < l\}} N(\alpha_{jl}(\mathbf{s}_{i,o}), 1). \end{aligned}$$

The essence of this latent variables introduction approach lies in bringing about conjugacy for α_{jl} 's. With our introduced $z_{jl}(\mathbf{s}_{i,o})$'s and $\xi_j(\mathbf{s}_{i,o})$'s defined deterministically by Equation (D.2), for any arbitrary fixed $(j, l) \in \{1, \dots, k\} \times \{1, \dots, L-1\}$,

$$f(\alpha_{jl} | \cdot) \propto f(\boldsymbol{\xi}_j, \mathbf{z}_{jr}, 1 \leq r \leq L-1 | \alpha_{jr}, 1 \leq r \leq L-1) \times f_0(\alpha_{jl} | \kappa, \rho),$$

where $f(\boldsymbol{\xi}_j, \mathbf{z}_{jr}, 1 \leq r \leq L-1 | \alpha_{jr}, 1 \leq r \leq L-1)$

$$\begin{aligned} & = f(\boldsymbol{\xi}_j | \mathbf{z}_{jr}, \alpha_{jr}, 1 \leq r \leq L-1) \times f(\mathbf{z}_{jr}, 1 \leq r \leq L-1 | \alpha_{jr}, 1 \leq r \leq L-1) \\ & = f(\boldsymbol{\xi}_j | \mathbf{z}_{jr}, 1 \leq r \leq L-1) \times \prod_{(i,o,r) \in \{1, \dots, m\} \times \{1, \dots, O\} \times \{1, \dots, L-1\}} f(z_{jr}(\mathbf{s}_{i,o}) | \alpha_{jr}(\mathbf{s}_{i,o})) \\ & = f(\boldsymbol{\xi}_j | \mathbf{z}_{jr}, 1 \leq r \leq L-1) \times \prod_{1 \leq r \leq L-1} f(\mathbf{z}_{jr} | \alpha_{jr}). \end{aligned}$$

$$\begin{aligned} & \text{Hence, } f(\alpha_{jl} | \cdot) \propto \prod_{1 \leq r \leq L-1} f(\mathbf{z}_{jr} | \alpha_{jr}) \times f_0(\alpha_{jl} | \kappa, \rho) \propto f(\mathbf{z}_{jl} | \alpha_{jl}) \times f_0(\alpha_{jl} | \kappa, \rho) \\ & \propto \exp \left\{ (\mathbf{z}_{jl} - \alpha_{jl})^\top I_{mO} (\mathbf{z}_{jl} - \alpha_{jl}) + \boldsymbol{\alpha}_{jl}^\top [F(\rho)^{-1} \otimes \kappa^{-1}] \boldsymbol{\alpha}_{jl} \right\} \\ & \propto \exp \left\{ \boldsymbol{\alpha}_{jl}^\top [I_{mO} + F(\rho)^{-1} \otimes \kappa^{-1}] \boldsymbol{\alpha}_{jl} - 2 \cdot \mathbf{z}_{jl}^\top \boldsymbol{\alpha}_{jl} \right\} \\ & \sim N_{mO} \left([I_{mO} + F(\rho)^{-1} \otimes \kappa^{-1}]^{-1} \mathbf{z}_{jl}, [I_{mO} + F(\rho)^{-1} \otimes \kappa^{-1}]^{-1} \right). \quad (\text{D.5}) \end{aligned}$$

Under our model in Section 2.2, \mathbf{z}_{jl} 's and α_{jl} 's are ordered first by observation type and then spatially, whereas \mathbf{w}_{jl} 's, $\boldsymbol{\xi}_j$'s, $\boldsymbol{\lambda}_j$'s and $\boldsymbol{\sigma}^2$ are ordered first spatially and then by observation type. We also take note that Berchuck et al. (2022)'s finite-mixture-version implementation of Equation (2.3) with a common fixed number of spatial mixture components $L \in \mathbb{N}, L > 1$ for all factors contains some mistakes, in that they omitted the term $\mathbb{1}_{\{\xi_j(\mathbf{s}_{i,o}) < l\}} N(\alpha_{jl}(\mathbf{s}_{i,o}), 1)$ in Equation (D.4) for posterior sampling of $z_{jl}(\mathbf{s}_{i,o})$'s, calculated the last mixture weights $w_{jL}(\mathbf{s}_{i,o}) = \prod_{r=1}^{L-1} [1 - \Phi(\alpha_{jr}(\mathbf{s}_{i,o}))] \forall (j, i, o)$ wrongly, and included redundant posterior updating steps for $\alpha_{jL}(\mathbf{s}_{i,o})$'s and $z_{jL}(\mathbf{s}_{i,o})$'s.

E Some Notes on Slice Sampling Adapted in Our Context

Fix any arbitrary $j \in \{1, \dots, k\}$. Under a baseline infinite mixture model, problems pertaining to the normalizing constants emerge when sampling $\xi_j(\mathbf{s}_{i,o})$'s, as the support $\forall \xi_j(\mathbf{s}_{i,o})$ is the countably infinite set \mathbb{Z}^+ . This issue can be tackled by introducing latent variables $u_j(\mathbf{s}_{i,o})$'s with uniform full conditional distributions and thus making the possible values each $\xi_j(\mathbf{s}_{i,o})$ can take finite. However, when deciding the new maximum cluster number estimate L_j in the Gibbs sampling step for $\xi_j(\mathbf{s}_{i,o})$'s, we may well need more $w_{jl_j}(\mathbf{s}_{i,o})$'s for each (i, o) to ensure the criterion in Equation (3.7) due to the slight differences calculating $w_{jl_j}(\mathbf{s}_{i,o})$'s between a finite and an infinite mixture model. We can thus end up with an L_j larger than its counterpart in the previous MCMC iteration. Since L_j 's are not ensured non-increasing through the MCMC iterations under an infinite mixture model, we likely need to sample much more α_{jl_j} 's and θ_{jl_j} 's, especially when the cluster number upper bound mO is large. Computational and storage burdens can thus ensue.

Our approach elaborated in Section 3 successfully bypasses the above concerns. We shall note that Berchuck et al. (2022)'s implementation attempt regarding infinite mixture model via slice sampling in their supplementary material and R package `spBFA` actually does not follow Walker (2007) and is erroneous. One major accomplishment brought about by the introduced latent variables $u_j(\mathbf{s}_{i,o})$'s (Section 3) is that we no longer need to enable feasible posterior sampling of $\alpha_{jl_j}(\mathbf{s}_{i,o})$'s by introducing latent normal parameters $z_{jl_j}(\mathbf{s}_{i,o})$'s (Appendix D). Hence Berchuck et al. (2022)'s Gibbs sampler step for $z_{jl_j}(\mathbf{s}_{i,o})$'s is redundant when slice sampling is adopted. Their procedure updating L_j^* 's is also incorrect and placed wrongly.

F Some Further Comments Regarding the Latent NNGP

The NNGP is a highly scalable alternative to the full parent GP while producing comparably good inferences (Sections 4 and 6), and has numerous advantages over other approaches for modeling large geostatistical data sets.

In terms of scalability, NNGP typically reduces computational complexity from cubic to linear in m in our context setting $\mathcal{S} = \mathcal{T} = \{\mathbf{s}_1, \dots, \mathbf{s}_m\}$ (Sections 4.3 and 4.4) and significantly outperforms alternative methods like low rank approximation. Low rank models typically require approximately $O(mr^2)$ flops, where $r \in \mathbb{N}, r \ll m$ is the number of knots that by empirical experiments must be quite large to approximate the GP well when m is large, thereby making mr^2 computationally prohibitive. NNGP, on the other hand, needs $O(|\mathcal{S} \cup \mathcal{T}| \cdot h^3)$ flops with $|\mathcal{T}| = m$, where $\mathcal{S} = \mathcal{T}$ and a quite small h , e.g., between 10 to 15, have been shown to perform well. NNGP's capabilities in significantly easing storage (Sections 4.2 and 4.3) may also make it the only feasible candidate under some requirements, e.g., delivering process-based inferences, for certain super large geostatistical data sets (Section 5.2 in Datta et al. 2016).

From the inferential perspective, the NNGP incorporates parameter estimation, outcome prediction, and latent process interpolation into a single fully process-based framework (Section 4.5), which had not been explored by any other methods in the literature. A legitimate GP with sparse precision matrices on the entire geographical domain \mathcal{D} , which we shall denote as NNGP($\mathbf{0}, \tilde{C}(\cdot, \cdot | \boldsymbol{\theta})$) derived from the parent Gaussian process GP($\mathbf{0}, C(\cdot, \cdot | \boldsymbol{\theta})$), the latent

NNGP needs not be conceived as an approximation to its parent GP when modeling the latent or observed spatial surface and permits fast and adequate predictions of the latent and outcome variables at arbitrary new locations (our simulation experiments in Section 6.2), a main issue covariance tapering methods are unable to handle. Various simulation experiments (Datta et al. 2016) suggest that NNGP produces estimation & kriging closely resembling those from the parent GP models for diverse covariance functions $C(\cdot, \cdot | \boldsymbol{\theta})$.

Under our spatiotemporal Bayesian Gaussian factor analysis modeling framework, other NNGP methods like Response NNGP and Conjugate NNGP (Finley et al. 2019) are not applicable. A few points to note in our adaptations of the NNGP compared to the framework presented in Datta et al. (2016) not mentioned earlier are as follows:

- The parametric covariance function $C(\cdot, \cdot | \boldsymbol{\theta})$ is over $\mathcal{D} \times \mathcal{D}$, not just over $\mathcal{S} \times \mathcal{S}$. $\forall \mathbf{s}, \mathbf{t} \in \mathcal{D}$, $C(\mathbf{s}, \mathbf{t} | \boldsymbol{\theta})_{q \times q} = \text{Cov}\{\mathbf{w}(\mathbf{s}), \mathbf{w}(\mathbf{t})\}$. q corresponds to O in our model.
- $C_{\mathcal{S}}(\boldsymbol{\theta})$, the covariance function over the reference set \mathcal{S} , corresponds to $F(\rho)_{m \times m} \otimes \kappa_{O \times O}$ in our model.
- We have let $\mathcal{S} = \mathcal{T}$. Thus, $\mathcal{S}^* = \mathcal{T} \cap \mathcal{S} = \mathcal{T}$ and $\mathcal{U} = \mathcal{T} \setminus \mathcal{S}^* = \emptyset$. Hence the likelihood in Equation (10) in Datta et al. (2016) is simplified to only the first portion there, as $k = n = r = m$ in their notations.
- Some software features to further accelerate computation are presented in Section 2.5 of Finley, Datta, and Banerjee (2022).

G More on Predictions at Future Time Points or New Spatial Locations

This section complements Section 5.1 in the main text.

G.1 Predicting $\hat{\mathbf{y}}_{(T+1):(T+q)}$ Given $\mathbf{y}_{1:T}$ and $[X_{(T+1):(T+q)}]_{qO \times p}$ (if $p \geq 1$)

Suppose we have $q \geq 1, q \in \mathbb{N}$ new time points $T + 1, \dots, T + q$ with corresponding time $\nu_{T+1}, \dots, \nu_{T+q}$ (distances standardized to 1 if `include.time = equalTimeDist = TRUE`). Then under all three of our modeling frameworks (Sections 2.1, 2.2 and 3), for Bayesian predictions at $\nu_{(T+1):(T+q)}$ given their corresponding covariates matrix $[X_{(T+1):(T+q)}]_{qO \times p}$, if any, we can write the PPD as

$$f(\mathbf{y}_{(T+1):(T+q)} | \mathbf{y}_{1:T}, X_{(T+1):(T+q)}) = \int_{\Theta} f(\mathbf{y}_{(T+1):(T+q)} | \Theta, \mathbf{y}_{1:T}, X_{(T+1):(T+q)}) \pi(\Theta | \mathbf{y}_{1:T}) d\Theta,$$

$$\text{where } \Theta = \begin{cases} (\Lambda, \boldsymbol{\beta}, \boldsymbol{\sigma}^2, \boldsymbol{\eta}_{(T+1):(T+q)}, \boldsymbol{\eta}, \Upsilon, \psi), & \text{if } \text{clustering} = \text{FALSE} \\ (\boldsymbol{\theta}, \boldsymbol{\xi}, \boldsymbol{\beta}, \boldsymbol{\sigma}^2, \boldsymbol{\eta}_{(T+1):(T+q)}, \boldsymbol{\eta}, \Upsilon, \psi), & \text{if } \text{clustering} = \text{TRUE} \end{cases}, \text{ and } \boldsymbol{\eta} \text{ denotes } \boldsymbol{\eta}_{1:T}, \quad (\text{G.1})$$

where `clustering = FALSE` refers to the scenario when no spatial clustering mechanism is integrated, i.e., when our model in Section 2.1 is adopted, and `clustering = TRUE` refers to the case when a spatial PSBP clustering mechanism is incorporated, i.e., when our model in

Section 2.2 or 3 is adopted. We can then partition the integral in Equation (G.1) into

$$\int_{\Theta} \underbrace{f(\mathbf{y}_{(T+1):(T+q)} | \Lambda, \boldsymbol{\eta}_{(T+1):(T+q)}, \boldsymbol{\beta}, \boldsymbol{\sigma}^2, X_{(T+1):(T+q)})}_{T_1} \underbrace{f(\boldsymbol{\eta}_{(T+1):(T+q)} | \boldsymbol{\eta}, \Upsilon, \psi)}_{T_2} \times \underbrace{\pi(\Lambda, \boldsymbol{\beta}, \boldsymbol{\sigma}^2, \boldsymbol{\eta}, \Upsilon, \psi | \mathbf{y}_{1:T})}_{T_3} d\Theta \text{ if } \text{clustering} = \text{FALSE}, \text{ and} \quad (\text{G.2})$$

$$\int_{\Theta} \underbrace{f(\mathbf{y}_{(T+1):(T+q)} | \boldsymbol{\theta}, \boldsymbol{\xi}, \boldsymbol{\eta}_{(T+1):(T+q)}, \boldsymbol{\beta}, \boldsymbol{\sigma}^2, X_{(T+1):(T+q)})}_{T_1} \underbrace{f(\boldsymbol{\eta}_{(T+1):(T+q)} | \boldsymbol{\eta}, \Upsilon, \psi)}_{T_2} \times \underbrace{\pi(\boldsymbol{\theta}, \boldsymbol{\xi}, \boldsymbol{\beta}, \boldsymbol{\sigma}^2, \boldsymbol{\eta}, \Upsilon, \psi | \mathbf{y}_{1:T})}_{T_3} d\Theta \text{ if } \text{clustering} = \text{TRUE}. \quad (\text{G.3})$$

In Equations (G.2) and (G.3), T_1 is the likelihood, T_3 is the parameters' posterior distribution obtained from the original model fit's MCMC sampler, and T_2 can be calculated by properties of conditional distributions of jointly multivariate normals as follows. Depending on whether a temporal structure is included and whether the distances between adjacent time points are equal, we can get a predicted value $\hat{\boldsymbol{\eta}}_{(T+1):(T+q)}$ conditioning on $\boldsymbol{\eta}_{1:T}, \Upsilon, \psi$:

- When `include.time = FALSE`, i.e., when temporal independence is assumed and the temporal correlation structure matrix $H(\psi)$ is set to the identity matrix

$$f(\boldsymbol{\eta}_{(T+1):(T+q)} | \boldsymbol{\eta}_{1:T}, \Upsilon, \psi) = \pi(\boldsymbol{\eta}_{(T+1):(T+q)} | \Upsilon, \psi) \sim N_{qk}(\mathbf{0}, I_{q \times q} \otimes \Upsilon). \quad (\text{G.4})$$

- When `include.time = TRUE`, i.e., when temporal correlation is taken into consideration

By properties of conditional distributions of jointly multivariate normals,

$$\boldsymbol{\eta}_{(T+1):(T+q)} | \boldsymbol{\eta}_{1:T}, \Upsilon, \psi \sim N_{qk} \left(\left[H_{(T+1):(T+q)}^+ \otimes I_{k \times k} \right] \boldsymbol{\eta}_{1:T}, \left[H_{(T+1):(T+q)}^* \otimes \Upsilon \right] \right), \quad (\text{G.5})$$

where $H_{(T+1):(T+q)}^+ = H_{(T+1):(T+q), (1:T)} H_{(1:T), (1:T)}^{-1}$ and

$$\begin{aligned} H_{(T+1):(T+q)}^* &= H_{(T+1):(T+q), (T+1):(T+q)} - H_{(T+1):(T+q)}^+ H_{(1:T), (T+1):(T+q)} \\ &= H_{(T+1):(T+q), (T+1):(T+q)} - H_{(T+1):(T+q), (1:T)} H_{(1:T), (1:T)}^{-1} H_{(1:T), (T+1):(T+q)} \end{aligned}$$

with $H_{(1:T), (1:T)}, H_{(T+1):(T+q), (1:T)}, H_{(1:T), (T+1):(T+q)}, H_{(T+1):(T+q), (T+1):(T+q)}$ being the corresponding $T \times T, q \times T, T \times q, q \times q$ sub-matrices of the $(T+q) \times (T+q)$ temporal correlation structure matrix $H(\psi)_{1:(T+q)}$ for all $(T+q)$ time points.

- When `equalTimeDist = FALSE`, i.e., when the distances between adjacent time points are unequal, we may only get $H_{(1:T), (1:T)}^{-1}$ by straightforwardly inverting $H_{(1:T), (1:T)}$.
- When `equalTimeDist = TRUE`, i.e., when the time $v_1, \dots, v_T, v_{T+1}, \dots, v_{T+q}$ are equispaced with distances normalized to 1, we can bypass this matrix inversion by directly specifying $H_{(1:T), (1:T)}^{-1}$ according to our formula presented in Appendix B.

G.2 Predicting $\hat{\mathbf{y}}(\mathbf{s}_{(m+1):(m+r)})$ Given $\mathbf{y}(\mathbf{s}_{1:m})$ and $X(\mathbf{s}_{(m+1):(m+r)})_{rTO \times p}$ (if $p \geq 1$) Under Our Models in Section 2

G.2.1 Under Our Baseline Modeling Framework in Section 2.1

When spatially correlated Gaussian Processes are directly imposed on the columns $\{\boldsymbol{\lambda}_j\}_{j=1}^k$ of the factor loadings matrix $\Lambda_{mO \times k}$, for Bayesian predictions at $r \in \mathbb{N}, r \geq 1$ new locations

$\mathbf{s}_{(m+1):(m+r)}$ given their corresponding covariates matrix $X(\mathbf{s}_{(m+1):(m+r)})_{rTO \times p}$, if any, the PPD becomes

$$\begin{aligned} & f(\mathbf{y}(\mathbf{s}_{(m+1):(m+r)}) | \mathbf{y}(\mathbf{s}_{1:m}), X(\mathbf{s}_{(m+1):(m+r)})) \quad (\text{G.6}) \\ &= \int_{\Theta} f(\mathbf{y}(\mathbf{s}_{(m+1):(m+r)}) | \Theta, \mathbf{y}(\mathbf{s}_{1:m}), X(\mathbf{s}_{(m+1):(m+r)})) \pi(\Theta | \mathbf{y}(\mathbf{s}_{1:m})) d\Theta, \text{ where} \\ & \Theta = (\boldsymbol{\eta}, \boldsymbol{\beta}, \boldsymbol{\sigma}^2(\mathbf{s}_{(m+1):(m+r)}), \Lambda(\mathbf{s}_{(m+1):(m+r)}), \Lambda, \kappa, \rho). \end{aligned}$$

In the above, $\Lambda_{mO \times k} = (\boldsymbol{\lambda}_1, \dots, \boldsymbol{\lambda}_k)$ denotes $\Lambda(\mathbf{s}_{1:m})$, with each $mO \times 1$ vector $\boldsymbol{\lambda}_j = \boldsymbol{\lambda}_j(\mathbf{s}_{1:m})$, $j \in \{1, \dots, k\}$ ordered first by observation type and then spatially (different from the ordering of our original factor loadings matrix), i.e., the first O entries correspond to the first location point, the next O entries correspond to the second location point and so on. $\Lambda(\mathbf{s}_{(m+1):(m+r)})_{rO \times k} = (\boldsymbol{\lambda}_1(\mathbf{s}_{(m+1):(m+r)}), \dots, \boldsymbol{\lambda}_k(\mathbf{s}_{(m+1):(m+r)}))$, where for each $j \in \{1, \dots, k\}$, the $rO \times 1$ vector $\boldsymbol{\lambda}_j(\mathbf{s}_{(m+1):(m+r)})$ is ordered first by observation type and then spatially. The integral in Equation (G.6) can then be partitioned into

$$\begin{aligned} & \int_{\Theta} \underbrace{f(\mathbf{y}(\mathbf{s}_{(m+1):(m+r)}) | \Lambda(\mathbf{s}_{(m+1):(m+r)}), \boldsymbol{\eta}, \boldsymbol{\beta}, \boldsymbol{\sigma}^2(\mathbf{s}_{(m+1):(m+r)}), X(\mathbf{s}_{(m+1):(m+r)}))}_{T_1} \\ & \quad \times \underbrace{f(\Lambda(\mathbf{s}_{(m+1):(m+r)}) | \Lambda, \kappa, \rho)}_{T_2} \underbrace{\pi(\boldsymbol{\eta}, \boldsymbol{\beta}, \Lambda, \kappa, \rho | \mathbf{y}(\mathbf{s}_{1:m}))}_{T_3} \underbrace{\pi(\boldsymbol{\sigma}^2(\mathbf{s}_{(m+1):(m+r)}))}_{T_4} d\Theta \quad (\text{G.7}) \end{aligned}$$

since the posterior density $\pi(\boldsymbol{\sigma}^2(\mathbf{s}_{(m+1):(m+r)}) | \mathbf{y}(\mathbf{s}_{1:m}))$ equals the prior $\pi(\boldsymbol{\sigma}^2(\mathbf{s}_{(m+1):(m+r)}))$.

In Equation (G.7), T_1 is the likelihood, T_3 is the parameters' posterior distribution obtained from the original model fit's MCMC sampler, T_4 denotes the prior density for $\boldsymbol{\sigma}^2(\mathbf{s}_{(m+1):(m+r)}) = (\sigma^2(\mathbf{s}_{m+1,1}), \dots, \sigma^2(\mathbf{s}_{m+1,O}), \dots, \sigma^2(\mathbf{s}_{m+r,1}), \dots, \sigma^2(\mathbf{s}_{m+r,O}))$ with $\sigma^2(\mathbf{s}_{m+i_r,o}) \stackrel{\text{iid}}{\sim} \mathcal{IG}(a, b)$, $i_r \in \{1, \dots, r\}$, $o \in \{1, \dots, O\}$, and T_2 can be written as

$$f(\Lambda(\mathbf{s}_{(m+1):(m+r)}) | \Lambda(\mathbf{s}_{1:m}), \kappa, \rho) = \prod_{j=1}^k f(\boldsymbol{\lambda}_j(\mathbf{s}_{(m+1):(m+r)}) | \boldsymbol{\lambda}_j(\mathbf{s}_{1:m}), \kappa, \rho).$$

Hence, we can get a predicted value $\hat{\Lambda}(\mathbf{s}_{(m+1):(m+r)})$ conditioning on $\Lambda(\mathbf{s}_{1:m}), \kappa, \rho$ depending on the following 3 scenarios regarding the spatially extended GP prior on $\boldsymbol{\lambda}_j(\mathbf{s}_{1:(m+r)})$'s (ordered first by observation type and then spatially here):

- When `include.space = FALSE`, i.e., when spatial independence is assumed and the corresponding spatially extended full GP prior $\boldsymbol{\lambda}_j(\mathbf{s}_{1:(m+r)}) \stackrel{\text{iid}}{\sim} N_{(m+r)O}(\mathbf{0}, I_{(m+r) \times (m+r)} \otimes \kappa_{O \times O})$, $j \in \{1, \dots, k\}$ is imposed

$$\begin{aligned} & \text{For any arbitrary } j \in \{1, \dots, k\}, \quad f(\boldsymbol{\lambda}_j(\mathbf{s}_{(m+1):(m+r)}) | \boldsymbol{\lambda}_j(\mathbf{s}_{1:m}), \kappa, \rho) \\ & \quad = \pi(\boldsymbol{\lambda}_j(\mathbf{s}_{(m+1):(m+r)}) | \kappa, \rho) \sim N_{rO}(\mathbf{0}, I_{r \times r} \otimes \kappa). \quad (\text{G.8}) \end{aligned}$$

- When `include.space = TRUE` and `spatApprox = FALSE`, i.e., when spatial dependence is taken into consideration and the spatially extended full GP prior $\boldsymbol{\lambda}_j(\mathbf{s}_{1:(m+r)}) | \kappa, \rho \stackrel{\text{iid}}{\sim} N_{(m+r)O}(\mathbf{0}, F(\rho)_{(m+r) \times (m+r)} \otimes \kappa_{O \times O})$, $j \in \{1, \dots, k\}$ is placed

By properties of conditional distributions of jointly multivariate normals, \forall arbitrary j ,

$$\boldsymbol{\lambda}_j(\mathbf{s}_{(m+1):(m+r)}) | \boldsymbol{\lambda}_j(\mathbf{s}_{1:m}), \boldsymbol{\kappa}, \boldsymbol{\rho} \sim N_{rO} \left(B_{\mathbf{s}_{(m+1):(m+r)}} \boldsymbol{\lambda}_j(\mathbf{s}_{1:m}), F_{\mathbf{s}_{(m+1):(m+r)}} \right), \quad (\text{G.9})$$

where the $rO \times mO$ matrix $B_{\mathbf{s}_{(m+1):(m+r)}} = \left\{ F(\boldsymbol{\rho})_{\mathbf{s}_{(m+1):(m+r)}, \mathbf{s}_{1:m}} [F(\boldsymbol{\rho})_{\mathbf{s}_{1:m}}]^{-1} \right\} \otimes I_{O \times O}$

and the $rO \times rO$ matrix $F_{\mathbf{s}_{(m+1):(m+r)}}$

$$= \left\{ F(\boldsymbol{\rho})_{\mathbf{s}_{(m+1):(m+r)}} - F(\boldsymbol{\rho})_{\mathbf{s}_{(m+1):(m+r)}, \mathbf{s}_{1:m}} [F(\boldsymbol{\rho})_{\mathbf{s}_{1:m}}]^{-1} F(\boldsymbol{\rho})_{\mathbf{s}_{1:m}, \mathbf{s}_{(m+1):(m+r)}} \right\} \otimes \boldsymbol{\kappa}_{O \times O}$$

with $F(\boldsymbol{\rho})_{\mathbf{s}_{1:m}}, F(\boldsymbol{\rho})_{\mathbf{s}_{(m+1):(m+r)}, \mathbf{s}_{1:m}}, F(\boldsymbol{\rho})_{\mathbf{s}_{1:m}, \mathbf{s}_{(m+1):(m+r)}}, F(\boldsymbol{\rho})_{\mathbf{s}_{(m+1):(m+r)}}$ being the corresponding $m \times m, r \times m, m \times r, r \times r$ sub-matrices of the $(m+r) \times (m+r)$ matrix $F(\boldsymbol{\rho})_{\mathbf{s}_{1:(m+r)}}$.

- When `include.space = spatApprox = TRUE`, i.e., when spatial dependence is taken into consideration and the spatially extended NNGP prior $\tilde{\pi}(\boldsymbol{\lambda}_j(\mathbf{s}_{1:(m+r)}) | \boldsymbol{\kappa}, \boldsymbol{\rho}) \forall j$ is placed

Under the spatially extended NNGP prior (Section 4.5) applied to $\boldsymbol{\lambda}_j$'s instead of $\boldsymbol{\alpha}_{jl_j}$'s and by properties of conditional distributions of jointly multivariate normals,

$$\text{for any arbitrary fixed } j \in \{1, \dots, k\}, \quad \tilde{f}(\boldsymbol{\lambda}_j(\mathbf{s}_{(m+1):(m+r)}) | \boldsymbol{\lambda}_j(\mathbf{s}_{1:m}), \boldsymbol{\kappa}, \boldsymbol{\rho}) \quad (\text{G.10})$$

$$= \prod_{i_r=1}^r \tilde{f}(\boldsymbol{\lambda}_j(\mathbf{s}_{(m+i_r)}) | \boldsymbol{\lambda}_j(\mathbf{s}_{1:m}), \boldsymbol{\kappa}, \boldsymbol{\rho}) = \prod_{i_r=1}^r f(\boldsymbol{\lambda}_j(\mathbf{s}_{(m+i_r)}) | \boldsymbol{\lambda}_{j, N(\mathbf{s}_{(m+i_r)})}, \boldsymbol{\kappa}, \boldsymbol{\rho}),$$

where for each $i_r \in \{1, \dots, r\}$,

$$\boldsymbol{\lambda}_j(\mathbf{s}_{(m+i_r)}) | \boldsymbol{\lambda}_{j, N(\mathbf{s}_{(m+i_r)})}, \boldsymbol{\kappa}, \boldsymbol{\rho} \sim N_O \left(B_{\mathbf{s}_{(m+i_r)}} \boldsymbol{\lambda}_{j, N(\mathbf{s}_{(m+i_r)})}, F_{\mathbf{s}_{(m+i_r)}} \right) \text{ with}$$

the $O \times hO$ matrix $B_{\mathbf{s}_{(m+i_r)}} = \left\{ F(\boldsymbol{\rho})_{\mathbf{s}_{(m+i_r)}, N(\mathbf{s}_{(m+i_r)})} [F(\boldsymbol{\rho})_{N(\mathbf{s}_{(m+i_r)})}]^{-1} \right\} \otimes I_{O \times O}$

and the $O \times O$ matrix $F_{\mathbf{s}_{(m+i_r)}}$

$$= \left\{ F(\boldsymbol{\rho})_{\mathbf{s}_{(m+i_r)}} - F(\boldsymbol{\rho})_{\mathbf{s}_{(m+i_r)}, N(\mathbf{s}_{(m+i_r)})} [F(\boldsymbol{\rho})_{N(\mathbf{s}_{(m+i_r)})}]^{-1} F(\boldsymbol{\rho})_{N(\mathbf{s}_{(m+i_r)}), \mathbf{s}_{(m+i_r)}} \right\} \otimes \boldsymbol{\kappa}_{O \times O}.$$

with $F(\boldsymbol{\rho})_{\mathbf{s}_{(m+i_r)}} = 1, F(\boldsymbol{\rho})_{\mathbf{s}_{(m+i_r)}, N(\mathbf{s}_{(m+i_r)})}, F(\boldsymbol{\rho})_{N(\mathbf{s}_{(m+i_r)}), \mathbf{s}_{(m+i_r)}}, F(\boldsymbol{\rho})_{N(\mathbf{s}_{(m+i_r)})}$ being the corresponding $1 \times 1, 1 \times h, h \times 1, h \times h$ sub-matrices of $[F(\boldsymbol{\rho})_{\mathbf{s}_{1:(m+r)}}]_{(m+r) \times (m+r)}$.

G.2.2 Under Our Modeling Framework in Section 2.2

When the prior $\boldsymbol{\alpha}_{jl} \stackrel{\text{iid}}{\sim} N_{mO}(\mathbf{0}, F(\boldsymbol{\rho})_{m \times m} \otimes \boldsymbol{\kappa}_{O \times O})$ for all $(j, l) \in \{1, \dots, k\} \times \{1, \dots, L-1\}$ is assigned, for Bayesian predictions at $r \in \mathbb{N}, r \geq 1$ new locations $\mathbf{s}_{(m+1):(m+r)}$ given their corresponding covariates matrix $X(\mathbf{s}_{(m+1):(m+r)})_{rTO \times p}$, if any, we can write the PPD as

$$\begin{aligned} & f(\mathbf{y}(\mathbf{s}_{(m+1):(m+r)}) | \mathbf{y}(\mathbf{s}_{1:m}), X(\mathbf{s}_{(m+1):(m+r)})) \\ &= \int_{\Theta} f(\mathbf{y}(\mathbf{s}_{(m+1):(m+r)}) | \Theta, \mathbf{y}(\mathbf{s}_{1:m}), X(\mathbf{s}_{(m+1):(m+r)})) \pi(\Theta | \mathbf{y}(\mathbf{s}_{1:m})) d\Theta, \end{aligned}$$

where $\Theta = (\boldsymbol{\eta}, \boldsymbol{\beta}, \boldsymbol{\sigma}^2(\mathbf{s}_{(m+1):(m+r)}), \boldsymbol{\theta}, \boldsymbol{\xi}(\mathbf{s}_{(m+1):(m+r)}), \boldsymbol{\alpha}(\mathbf{s}_{(m+1):(m+r)}), \boldsymbol{\alpha}, \boldsymbol{\kappa}, \boldsymbol{\rho})$ and $\boldsymbol{\alpha}$ denotes $\boldsymbol{\alpha}(\mathbf{s}_{1:m})$, and then partition the integral into

$$\int_{\Theta} \underbrace{f(\mathbf{y}(\mathbf{s}_{(m+1):(m+r)}) | \boldsymbol{\theta}, \boldsymbol{\xi}(\mathbf{s}_{(m+1):(m+r)}), \boldsymbol{\eta}, \boldsymbol{\beta}, \boldsymbol{\sigma}^2(\mathbf{s}_{(m+1):(m+r)}), X(\mathbf{s}_{(m+1):(m+r)}))}_{T_1}$$

$$\begin{aligned}
& \times \underbrace{f(\boldsymbol{\xi}(\mathbf{s}_{(m+1):(m+r)})|\boldsymbol{\alpha}(\mathbf{s}_{(m+1):(m+r)}))}_{T_2} \underbrace{f(\boldsymbol{\alpha}(\mathbf{s}_{(m+1):(m+r)})|\boldsymbol{\alpha}, \boldsymbol{\kappa}, \rho)}_{T_3} \\
& \times \underbrace{\pi(\boldsymbol{\eta}, \boldsymbol{\beta}, \boldsymbol{\theta}, \boldsymbol{\alpha}, \boldsymbol{\kappa}, \rho|\mathbf{y}(\mathbf{s}_{1:m}))}_{T_4} \underbrace{\pi(\boldsymbol{\sigma}^2(\mathbf{s}_{(m+1):(m+r)}))}_{T_5} d\Theta
\end{aligned} \tag{G.11}$$

since the posterior density $\pi(\boldsymbol{\sigma}^2(\mathbf{s}_{(m+1):(m+r)})|\mathbf{y}(\mathbf{s}_{1:m}))$ equals the prior $\pi(\boldsymbol{\sigma}^2(\mathbf{s}_{(m+1):(m+r)}))$.

In Equation (G.11), T_1 is the likelihood, T_4 is the parameters' posterior distribution obtained from the original model fit's MCMC sampler, T_5 denotes the prior density for $\boldsymbol{\sigma}^2(\mathbf{s}_{(m+1):(m+r)}) = (\sigma^2(\mathbf{s}_{m+1,1}), \dots, \sigma^2(\mathbf{s}_{m+1,O}), \dots, \sigma^2(\mathbf{s}_{m+r,1}), \dots, \sigma^2(\mathbf{s}_{m+r,O}))$ with $\sigma^2(\mathbf{s}_{m+i_r,o}) \stackrel{\text{iid}}{\sim} \mathcal{IG}(a, b)$, $i_r \in \{1, \dots, r\}$, $o \in \{1, \dots, O\}$, T_2 is the density of the multinomial distribution described in Section 2.2, and T_3 can be written as

$$f(\boldsymbol{\alpha}(\mathbf{s}_{(m+1):(m+r)})|\boldsymbol{\alpha}(\mathbf{s}_{1:m}), \boldsymbol{\kappa}, \rho) = \prod_{j=1}^k \prod_{l=1}^{L-1} f(\boldsymbol{\alpha}_{jl}(\mathbf{s}_{(m+1):(m+r)})|\boldsymbol{\alpha}_{jl}(\mathbf{s}_{1:m}), \boldsymbol{\kappa}, \rho). \tag{G.12}$$

Hence, we can directly get a predicted value $\hat{\boldsymbol{\alpha}}(\mathbf{s}_{(m+1):(m+r)})$ conditioning on $\boldsymbol{\alpha}(\mathbf{s}_{1:m}), \boldsymbol{\kappa}, \rho$ depending on the following 3 scenarios regarding the spatially extended GP prior on $\boldsymbol{\alpha}_{jl}(\mathbf{s}_{1:(m+r)})$'s:

- When `include.space = FALSE`, i.e., when spatial independence is assumed and the spatial neighborhood structure matrix $F(\rho)$ is set to the identity matrix

$$\begin{aligned}
& \forall (j, l) \in \{1, \dots, k\} \times \{1, \dots, L-1\}, \\
& f(\boldsymbol{\alpha}_{jl}(\mathbf{s}_{(m+1):(m+r)})|\boldsymbol{\alpha}_{jl}(\mathbf{s}_{1:m}), \boldsymbol{\kappa}, \rho) = \pi(\boldsymbol{\alpha}_{jl}(\mathbf{s}_{(m+1):(m+r)})|\boldsymbol{\kappa}, \rho) \sim N_{rO}(\mathbf{0}, I_{r \times r} \otimes \boldsymbol{\kappa}).
\end{aligned} \tag{G.13}$$

- When `include.space = TRUE` and `spatApprox = FALSE`, i.e., when spatial dependence is taken into consideration and the spatially extended full GP prior $\pi(\boldsymbol{\alpha}_{jl}(\mathbf{s}_{1:(m+r)})|\boldsymbol{\kappa}, \rho) = N_{(m+r)O}(\mathbf{0}, F(\rho)_{(m+r) \times (m+r)} \otimes \boldsymbol{\kappa}_{O \times O}) \forall (j, l) \in \{1, \dots, k\} \times \{1, \dots, L-1\}$ is placed

By properties of conditional distributions of jointly multivariate normals, \forall arbitrary (j, l) ,

$$\boldsymbol{\alpha}_{jl}(\mathbf{s}_{(m+1):(m+r)})|\boldsymbol{\alpha}_{jl}(\mathbf{s}_{1:m}), \boldsymbol{\kappa}, \rho \sim N_{rO}\left(B_{\mathbf{s}_{(m+1):(m+r)}} \boldsymbol{\alpha}_{jl}(\mathbf{s}_{1:m}), F_{\mathbf{s}_{(m+1):(m+r)}}\right), \tag{G.14}$$

where the $rO \times mO$ matrix $B_{\mathbf{s}_{(m+1):(m+r)}} = \left\{F(\rho)_{\mathbf{s}_{(m+1):(m+r)}, \mathbf{s}_{1:m}} [F(\rho)_{\mathbf{s}_{1:m}}]^{-1}\right\} \otimes I_{O \times O}$

and the $rO \times rO$ matrix $F_{\mathbf{s}_{(m+1):(m+r)}}$

$$= \left\{F(\rho)_{\mathbf{s}_{(m+1):(m+r)}} - F(\rho)_{\mathbf{s}_{(m+1):(m+r)}, \mathbf{s}_{1:m}} [F(\rho)_{\mathbf{s}_{1:m}}]^{-1} F(\rho)_{\mathbf{s}_{1:m}, \mathbf{s}_{(m+1):(m+r)}}\right\} \otimes \boldsymbol{\kappa}_{O \times O}$$

with $F(\rho)_{\mathbf{s}_{1:m}}, F(\rho)_{\mathbf{s}_{(m+1):(m+r)}, \mathbf{s}_{1:m}}, F(\rho)_{\mathbf{s}_{1:m}, \mathbf{s}_{(m+1):(m+r)}}, F(\rho)_{\mathbf{s}_{(m+1):(m+r)}}$ being the corresponding $m \times m, r \times m, m \times r, r \times r$ sub-matrices of the $(m+r) \times (m+r)$ matrix $F(\rho)_{\mathbf{s}_{1:(m+r)}}$.

- When `include.space = spatApprox = TRUE`, i.e., when spatial dependence is taken into consideration and the spatially extended NNGP prior $\tilde{\pi}(\boldsymbol{\alpha}_{jl}(\mathbf{s}_{1:(m+r)})|\boldsymbol{\kappa}, \rho) \forall (j, l)$ is placed

Under the spatially extended NNGP prior as elaborated in Section 4.5 and by properties of conditional distributions of jointly multivariate normals, for any arbitrary fixed (j, l) ,

$$\tilde{f}(\boldsymbol{\alpha}_{jl}(\mathbf{s}_{(m+1):(m+r)})|\boldsymbol{\alpha}_{jl}(\mathbf{s}_{1:m}), \boldsymbol{\kappa}, \rho) \tag{G.15}$$

$$\begin{aligned}
&= \prod_{i_r=1}^r \tilde{f}(\boldsymbol{\alpha}_{jl}(\mathbf{s}_{(m+i_r)}) | \boldsymbol{\alpha}_{jl}(\mathbf{s}_{1:m}), \boldsymbol{\kappa}, \boldsymbol{\rho}) = \prod_{i_r=1}^r f(\boldsymbol{\alpha}_{jl}(\mathbf{s}_{(m+i_r)}) | \boldsymbol{\alpha}_{jl, N(\mathbf{s}_{(m+i_r)})}, \boldsymbol{\kappa}, \boldsymbol{\rho}), \\
&\text{where for each } i_r \in \{1, \dots, r\}, \\
&\boldsymbol{\alpha}_{jl}(\mathbf{s}_{(m+i_r)}) | \boldsymbol{\alpha}_{jl, N(\mathbf{s}_{(m+i_r)})}, \boldsymbol{\kappa}, \boldsymbol{\rho} \sim N_O \left(B_{\mathbf{s}_{(m+i_r)}} \boldsymbol{\alpha}_{jl, N(\mathbf{s}_{(m+i_r)})}, F_{\mathbf{s}_{(m+i_r)}} \right) \text{ with} \\
&\text{the } O \times hO \text{ matrix } B_{\mathbf{s}_{(m+i_r)}} = \left\{ F(\boldsymbol{\rho})_{\mathbf{s}_{(m+i_r)}, N(\mathbf{s}_{(m+i_r)})} \left[F(\boldsymbol{\rho})_{N(\mathbf{s}_{(m+i_r)})} \right]^{-1} \right\} \otimes I_{O \times O} \\
&\text{and the } O \times O \text{ matrix } F_{\mathbf{s}_{(m+i_r)}} \\
&= \left\{ F(\boldsymbol{\rho})_{\mathbf{s}_{(m+i_r)}} - F(\boldsymbol{\rho})_{\mathbf{s}_{(m+i_r)}, N(\mathbf{s}_{(m+i_r)})} \left[F(\boldsymbol{\rho})_{N(\mathbf{s}_{(m+i_r)})} \right]^{-1} F(\boldsymbol{\rho})_{N(\mathbf{s}_{(m+i_r)}), \mathbf{s}_{(m+i_r)}} \right\} \otimes \kappa_{O \times O}. \\
&F(\boldsymbol{\rho})_{\mathbf{s}_{(m+i_r)}} = 1, F(\boldsymbol{\rho})_{\mathbf{s}_{(m+i_r)}, N(\mathbf{s}_{(m+i_r)})}, F(\boldsymbol{\rho})_{N(\mathbf{s}_{(m+i_r)}), \mathbf{s}_{(m+i_r)}}, F(\boldsymbol{\rho})_{N(\mathbf{s}_{(m+i_r)})} \text{ denote the} \\
&\text{corresponding } 1 \times 1, 1 \times h, h \times 1, h \times h \text{ sub-matrices of } \left[F(\boldsymbol{\rho})_{\mathbf{s}_{1:(m+r)}} \right]_{(m+r) \times (m+r)}.
\end{aligned}$$

H Scalability Improvements Corresponding to Our 3 Novelties – A Summary of Computational Complexity and Memory

Our three novelties for enhancing scalability are **slice sampling**, **spatial NNGP prior**, and **sequential updating algorithms**. We first list some important points to note.

- $O \in \mathbb{N}$ is assumed very small; $h, k, p \ll m$; $1 \leq L$ or L_j 's $\leq m$.
- Slice sampling is useful when L has to be at least moderately large. Moreover, it resolves intimidating storage concerns regarding θ_{jl} 's, $\boldsymbol{\alpha}_{jl}$'s, and \boldsymbol{w}_{jl} 's and thus enables practicable implementation of spatial prediction and clustering when both m and L are large.
- Spatial NNGP prior and sequential updates are helpful for a large m . Sequential updating algorithms can only be adopted when our spatial NNGP prior is specified. Hence, when slice sampling is not adopted, we have 3 models, which we denote as **fullGPFixedL**, **NNGPblockFixedL**, and **NNGPsequenFixedL**.
- When slice sampling is adopted and m is at least moderately large, we may only also specify our spatial NNGP prior with sequential updates for a computationally feasible model, which we shall denote as **NNGPsequenVaryLj**, as multivariate rejection sampling from high-dimensional truncated mO -variate normal distributions of the $\boldsymbol{\alpha}_{jl_j}$'s (Equation (3.10)) is unbearably slow.

Hence, we only implement the four models **fullGPFixedL**, **NNGPblockFixedL**, **NNGPsequenFixedL**, and **NNGPsequenVaryLj** for our simulation experiments. To verify what we have obtained theoretically regarding scalability, we may compare

- **fullGPFixedL** and **NNGPblockFixedL** for effects caused by spatial NNGP prior (without slice sampling, i.e., under our model in Section 2);
- **NNGPblockFixedL** and **NNGPsequenFixedL** for effects caused by sequential updates (without slice sampling, i.e., under our model in Section 2);
- **NNGPsequenFixedL** and **NNGPsequenVaryLj** for effects caused by slice sampling (with our spatial NNGP prior and sequential updating algorithms adopted).

We now elaborate on **theoretical** scalability improvements attributable to each of our three novelties. Computational complexity reduction for certain involved major steps in posterior

sampling and spatial prediction, as well as storage requirements alleviation for some concerned key quantities in main model fitting and spatial prediction & clustering, are considered measures of scalability improvements. **All computational complexity orders in the subsections below are for only one typical MCMC iteration.**

H.1 Flexibility, Computation, and Storage Improvements Brought About by Our **Slice Sampling Approach** in Section 3 with Spatial NNGP & Sequential Updates

We assume that $O(T) \leq O(m)$. Recall that $1 \leq L$ or L_j 's $\leq m$ and that we have assumed $O, h, k, p \ll m$. It is likely restrictive to pre-specify a fixed common $L \in \mathbb{N}$, $L > 1$, as the numbers of spatial mixtures are unknown and may well differ across the k latent factors. Moreover, an at least moderately large L would typically be required to guarantee satisfactory model fitting, resulting in computational burdens and storage issues. Our slice sampling approach (Section 3) not only brings about desired modeling flexibility and adequacy but also decently addresses the involved scalability issues (Table 5) by ensuring non-increasing posterior samples for L_j 's through the MCMC iterations.

Let $N \in \mathbb{N}$ be the number of kept post-burn-in MCMC iterations. We denote the corresponding estimated number(s) of spatial mixture components as $L^{(t_i)}$ or $L_j^{(t_i)}$'s, $i \in \{1, \dots, N\}$, $j \in \{1, \dots, k\}$. In Table 5, overall storage orders correspond to all kept MCMC iterations, whereas overall computational complexity orders are only for one typical MCMC iteration.

With our slicing sampling approach (Section 3) adopted on top of our spatial NNGP prior (Section 4) coupled with sequential updates (Section 4.4), rejection sampling from low-dimensional truncated O -variate normal distributions would have adequate acceptance rates and thus small required numbers $n_{jl_j i}^*$'s of draws from $N_O(V_{s_i}, \boldsymbol{\mu}_{jl_j, s_i}, V_{s_i})$'s (Equation (4.9) in Section 4.4) per sample of $\boldsymbol{\alpha}_{jl_j}(s_i)$'s. If $O\left(\max_{(j, l_j, i)} n_{jl_j i}^*\right) \leq O(m)$, then

$$O\left(\sum_{j=1}^k \left[(L_j - 1) \cdot O^2 m^2 + \sum_{l_j=1}^{L_j-1} \sum_{i=1}^m n_{jl_j i}^* \cdot O^2 \right]\right) = O\left(\sum_{j=1}^k (L_j - 1) \cdot O^2 m^2\right).$$

Domain of Scalability Improvements		Computational Acceleration		Storage Alleviation	
		Posterior Sampling	Spatial Prediction at $r \in \mathbb{N}$ ($r < m$)	new locations	Spatial Clustering
Key Parameters / Quantities Involved		$u_j(s_{i,o})$'s / $z_{jl}(s_{i,o})$'s, $\xi_j(s_{i,o})$'s, α_{jl_j} 's, θ_{jl_j} 's, $\delta_{1:k}$, κ , ρ	$\alpha_{jl_j}(s_{(m+1):(m+r)})$'s	α_{jl_j} 's and θ_{jl_j} 's	w_{jl_j} 's
Overall Standard Computational Complexity or Storage Order	Before	$O(k(L-1)O^2 m^2)$	$O(r[h^3 + O^3 + k(L-1)hO^2])$	$O(mOk \sum_{i=1}^N L^{(t_i)})$	
	After	$O\left(\sum_{j=1}^k (L_j - 1) \cdot O^2 m^2 + \sum_{l_j=1}^{L_j-1} \sum_{i=1}^m n_{jl_j i}^* \cdot O^2\right)$	$O\left(r[h^3 + O^3 + \sum_{j=1}^k (L_j - 1) \cdot hO^2]\right)$	$O\left(mO \sum_{i=1}^N \sum_{j=1}^k L_j^{(t_i)}\right)$	
References		Section(s)	Section 5.1 and Appendix G.2		Section 5.2
		Equations	Equations (5.5) and (G.15)		

Table 5: A theoretical summary table of posterior sampling & spatial prediction computation acceleration and spatial prediction & clustering storage alleviation brought about by our slice sampling approach in Section 3 with our spatial NNGP prior and sequential updates (Section 4). Our simulation experiments comparing the models `NNGPsequenFixedL` and `NNGPsequenVaryLj` should lead to results corresponding well to the table in terms of main model fitting time for the involved parameters and spatial prediction time for $\boldsymbol{\alpha}_{jl_j}(s_{(m+1):(m+r)})$'s.

H.2 Posterior Sampling Computational Acceleration & Storage Alleviation and Faster Spatial Prediction Brought About by Our **Spatial NNGP Prior** in Section 4

Suppose we have a large m . Recall that $1 \leq L$ or L_j 's $\leq m$ and that we have assumed $O, h, k \ll m$. We also assume $r < m$ for spatial prediction at $r \in \mathbb{N}$ new locations $\mathbf{s}_{(m+1):(m+r)}$. Note that $[F(\rho) \otimes \kappa]^{-1} = F(\rho)^{-1} \otimes \kappa^{-1}$ and that $\det(F(\rho) \otimes \kappa) = \det(F(\rho))^O \cdot \det(\kappa)^m$.

Domain of Scalability Improvements		Posterior Sampling		Spatial Prediction
		Acceleration	Storage Alleviation	Acceleration
Parameters Involved		κ and ρ	κ and ρ (and α_{jl_j} 's)	$\alpha_{jl_j}(\mathbf{s}_{(m+1):(m+r)})$'s for all (j, l_j)
Key Quantities Concerned		$F(\rho)^{-1}$ and $\det(F(\rho))$	$F(\rho)$ and $F(\rho)^{-1}$	$f(\alpha_{jl_j}(\mathbf{s}_{(m+1):(m+r)}) \alpha_{jl_j}(\mathbf{s}_{1:m}), \kappa, \rho)$'s
Standard Computational Complexity or Storage Order for the Key Quantities	Before	$O(m^3)$	$O(m^2)$	$O(m^3) + O((rO)^3) = O(m^3)$ for each (j, l_j)
	After	$O(m)$	$O(m)$	$O(rh^3) + O(rO^3) \leq O(m)$ for each (j, l_j)
Overall Standard Order of Computational Complexity Without Slice Sampling	Before	$O(m^3)$		$O(m^3)$
	After	$O(k(L-1)O^2m^2) = O(m^2)$ if $L \ll m$		$O(r[h^3 + O^3 + k(L-1)hO^2])$
Overall Standard Order of Computational Complexity With Slice Sampling	Before	$O(m^3)$		$O(m^3)$
	After	$O(\sum_{j=1}^k (L_j - 1) \cdot O^2m^2) = O(m^2)$ if $\max_{j \in \{1, \dots, k\}} L_j \ll m$		$O(r[h^3 + O^3 + \sum_{j=1}^k (L_j - 1) \cdot hO^2])$
References	Section(s)	Section 4.3	Sections 4.2 and 4.3	Section 5.1 and Appendix G.2.2
	Equations	Equations (A.18), (A.19), (A.34) and (A.35)		Equations (5.4), (5.5), (G.14) and (G.15)

Table 6: A theoretical summary table of posterior sampling computation acceleration & storage alleviation and spatial prediction acceleration brought about by our spatial NNGP prior in Section 4 with or without adopting slice sampling (Section 3). Our simulation experiments comparing the models `fullGPfixedL` and `NNGPblockFixedL` should lead to results corresponding well to the table in terms of main model fitting time for κ and ρ and spatial prediction time for $\alpha_{jl_j}(\mathbf{s}_{(m+1):(m+r)})$'s.

Detailed Derivations Regarding the Overall Computational Complexity Orders

1. Computational Complexity for the Posterior Sampling Steps of ρ and $\kappa_{O \times O}$

(a) The Full Spatial GP Prior Adopted (Before)

Without Slice Sampling (available for simulation comparisons)

$$[O(m^3) + O(k(L-1)(Om)^2)] + O(k(L-1) \cdot Om^2) = O(m^3) \quad (\text{H.1})$$

With Slice Sampling

$$\left[O(m^3) + O\left(\sum_{j=1}^k (L_j - 1) \cdot (Om)^2\right) \right] + O\left(\sum_{j=1}^k (L_j - 1) \cdot Om^2\right) = O(m^3) \quad (\text{H.2})$$

(b) Our Spatial NNGP Prior in Section 4 Adopted (After)

Without Slice Sampling (available for simulation comparisons)

$$[O(m) + O(k(L-1)(Om)^2)] + O(k(L-1) \cdot Om^2) = O(k(L-1)O^2m^2) = O(m^2) \text{ if } L \ll m \quad (\text{H.3})$$

With Slice Sampling

$$\left[O(m) + O\left(\sum_{j=1}^k (L_j - 1) \cdot (Om)^2\right) \right] + O\left(\sum_{j=1}^k (L_j - 1) \cdot Om^2\right)$$

$$= O \left(\sum_{j=1}^k (L_j - 1) \cdot O^2 m^2 \right) = O(m^2) \text{ if } \max_{j \in \{1, \dots, k\}} L_j \ll m \quad (\text{H.4})$$

2. Computational Complexity for the Spatial Prediction Step Obtaining

$\hat{\alpha}_{jl_j}(\mathbf{s}_{(m+1):(m+r)})$ for all (j, l_j)

(a) The Full Spatial GP Prior Adopted (Before)

Without Slice Sampling (available for simulation comparisons)

$$O(m^3) + O((rO)^3) + O(k(L-1) \cdot rO \cdot mO) + O(k(L-1) \cdot (rO)^2) = O(m^3) \quad (\text{H.5})$$

With Slice Sampling

$$O(m^3) + O((rO)^3) + O \left(\sum_{j=1}^k (L_j - 1) \cdot rO \cdot mO \right) + O \left(\sum_{j=1}^k (L_j - 1) \cdot (rO)^2 \right) = O(m^3) \quad (\text{H.6})$$

(b) Our Spatial NNGP Prior in Section 4 Adopted (After)

Without Slice Sampling (available for simulation comparisons)

$$O(rh^3) + O(rO^3) + O(k(L-1) \cdot r \cdot O \cdot hO) + O(k(L-1) \cdot r \cdot O^2) = O(r[h^3 + O^3 + k(L-1)hO^2]) \quad (\text{H.7})$$

With Slice Sampling

$$\begin{aligned} & O(rh^3) + O(rO^3) + O \left(\sum_{j=1}^k (L_j - 1) \cdot r \cdot O \cdot hO \right) + O \left(\sum_{j=1}^k (L_j - 1) \cdot r \cdot O^2 \right) \\ &= O \left(r \left[h^3 + O^3 + \sum_{j=1}^k (L_j - 1) \cdot hO^2 \right] \right) \end{aligned} \quad (\text{H.8})$$

H.3 Posterior Sampling Computational Acceleration Brought About by Our Sequential Updating Methods in Section 4.4 (with spatial NNGP)

Suppose we have a large m . Recall that $1 \leq L$ or L_j 's $\leq m$ and that we have assumed $O, h, k \ll m$. When slice sampling (Section 3) is adopted without our sequential updating method, rejection sampling from a high-dimensional truncated mO -variate normal distribution (Equation (4.7)) gets unbearably slow for feasible computation when m gets large, as a very small acceptance rate leads to a huge number $n_{jl_j} \in \mathbb{N}$ of draws from $N_{mO}(\mathbf{0}, \tilde{F}(\rho) \otimes \kappa)$ required per sample of α_{jl_j} for each (j, l_j) . When m is large, we typically have $n_{jl_j}(m) \gg m$ for any (j, l_j) . With our spatial NNGP prior coupled with sequential updates, rejection sampling from low-dimensional truncated O -variate normal distributions would have adequate acceptance rates and thus small required numbers $n_{jl_j}^*$'s of draws from $N_O(V_{\mathbf{s}_i} \boldsymbol{\mu}_{jl_j, \mathbf{s}_i}, V_{\mathbf{s}_i})$'s (Equation (4.9) in Section 4.4) per sample of $\alpha_{jl_j}(\mathbf{s}_i)$'s. If $\max_{j \in \{1, \dots, k\}} L_j \ll m$ and $\max_{(j, l_j, i)} n_{jl_j}^* \ll m$, then

$$O \left(\sum_{j=1}^k [(L_j - 1) \cdot m(h^3 + O^3 + h^2 O^2) + \sum_{l_j=1}^{L_j-1} \sum_{i=1}^m n_{jl_j i}^* \cdot O^2] \right) = O(m).$$

Place of Scalability Improvements		Computational Acceleration for the Posterior Sampling Step of $\alpha_{j_l_j}$'s for all (j, l_j)	
		Without Slice Sampling (available for simulation comparisons)	With Slice Sampling
Key Quantities Concerned		$[L_{mO} + \tilde{F}(\rho)^{-1} \otimes \kappa^{-1}]^{-1}$, $\text{Chol}([L_{mO} + \tilde{F}(\rho)^{-1} \otimes \kappa^{-1}]^{-1})$	$\text{Chol}(\tilde{F}(\rho) \otimes \kappa)$ and $n_{j_l_j}$'s for mO -variate rejection sampling
Overall Order of Standard Computational Complexity	Before	$O(m^3) + O(k(L-1) \cdot (mO)^2) = O(m^3)$	$O(m^3) + O\left(\sum_{j=1}^k \sum_{l_j=1}^{L_j-1} n_{j_l_j} \cdot m^2\right) > O(m^3)$
	After	$O(mk(L-1)(h^3 + O^3 + h^2O^2)) = O(m)$ if $L \ll m$	$O\left(\sum_{j=1}^k [(L_j-1) \cdot m(h^3 + O^3 + h^2O^2) + \sum_{l_j=1}^{L_j-1} \sum_{i=1}^m n_{j_l_j}^* \cdot O^2]\right)$
References	Section(s)	Section 4.4	
	Equations	Equations (4.6) and (4.8)	Equations (4.7) and (4.9)

Table 7: A theoretical summary table of posterior sampling computation acceleration further brought about by our sequential updating methods in Section 4.4 on top of imposing our spatial NNGP prior (Section 4) with or without adopting slice sampling (Section 3). Our simulation experiments comparing the models NNGPblockFixedL and NNGPsequenFixedL should lead to results corresponding well to the table in terms of main model fitting time for $\alpha_{j_l_j}$'s.

H.4 An Overall Scalability Improvements Summary for Our Three Novelties

Suppose we have a large m . Recall that $1 \leq L$ or L_j 's $\leq m$ and that we have assumed $O, h, k, p \ll m$. We also assume $r < m$ for spatial prediction at $r \in \mathbb{N}$ new locations $\mathbf{s}_{(m+1):(m+r)}$. Let $N \in \mathbb{N}$ be the number of kept post-burn-in MCMC iterations. We denote the corresponding estimated number(s) of spatial mixture components as $L^{(t_i)}$ or $L_j^{(t_i)}$'s, $j \in \{1, \dots, k\}$, $i \in \{1, \dots, N\}$. In Table 8, storage requirements for spatial prediction and clustering correspond to all kept MCMC iterations, whereas computational complexity orders are only for one typical MCMC iteration.

Simulation Model	fullGPFixedL	NNGPblockFixedL	NNGPsequenFixedL	NNGPsequenVaryLj
Spatial NNGP Prior	No	Yes	Yes	Yes
Sequential Updating Methods	No	No	Yes	Yes
Slice Sampling Approach	No	No	No	Yes
Spatial Prediction Speed for $\hat{\alpha}_{j_l_j}(\mathbf{s}_{(m+1):(m+r)}) \alpha_{j_l_j}(\mathbf{s}_{1:m}), \kappa, \rho$'s	$O(m^3)$	$O(r[h^3 + O^3 + k(L-1)hO^2])$		$O\left(r[h^3 + O^3 + \sum_{j=1}^k (L_j-1) \cdot hO^2]\right)$
Posterior Sampling Speed for	ρ and $\kappa_{O \times O}$	$O(m^3)$	$O(k(L-1)O^2m^2)$	$O\left(\sum_{j=1}^k (L_j-1) \cdot O^2m^2\right)$
	$\alpha_{j_l_j}(\mathbf{s}_{1:m})$'s	$O(m^3)$	$O(mk(L-1)(h^3 + O^3 + h^2O^2))$	$O\left(\sum_{j=1}^k [(L_j-1)m \cdot (h^3 + O^3 + h^2O^2) + \sum_{l_j=1}^{L_j-1} \sum_{i=1}^m n_{j_l_j}^* \cdot O^2]\right)$
	$z_{j_l}(\mathbf{s}_{i,o})$'s or $u_j(\mathbf{s}_{i,o})$'s	$O(kLmO)$		$O(kmO)$
	$\delta_{1:k}, \theta_{j_l_j}$'s, and $\xi_j(\mathbf{s}_{i,o})$'s	$O(kLmOT(p+k))$ (absolute highest order from $\xi_j(\mathbf{s}_{i,o})$'s)		$O\left(\sum_{j=1}^k L_j \cdot mOT(p+k)\right)$ (absolute highest order from $\xi_j(\mathbf{s}_{i,o})$'s)
Storage Requirements for	$F(\rho)$ and $F(\rho)^{-1}$	$O(m^2)$	$O(m)$	
	Spatial Prediction	$O\left(mOk \sum_{i=1}^N L^{(t_i)}\right)$		$O\left(mO \sum_{i=1}^N \sum_{j=1}^k L_j^{(t_i)}\right)$
	Spatial Clustering			

Table 8: An overall theoretical summary table of scalability improvements brought about by our 3 novelties. For each of the four models implemented in our simulation experiments, we list its computational complexity orders for involved Gibbs sampler steps in posterior sampling and a major spatial prediction procedure. We also present memory requirements for two key quantities and spatial prediction & clustering under our four models.

With our slicing sampling approach (Section 3) adopted on top of our spatial NNGP prior (Section 4) coupled with sequential updates (Section 4.4), rejection sampling from low-dimensional truncated O -variate normal distributions would have adequate acceptance rates and thus small required numbers $n_{j_l_j}^*$'s of draws from $N_O(V_{s_i} \boldsymbol{\mu}_{j_l_j, s_i}, V_{s_i})$'s (Equation (4.9) in

Section 4.4) per sample of $\alpha_{jl_j}(\mathbf{s}_i)$'s. If $\max_{j \in \{1, \dots, k\}} L_j \ll m$ and $\max_{(j, l_j, i)} n_{jl_j i}^* \ll m$, then

$$O \left(\sum_{j=1}^k [(L_j - 1) \cdot m(h^3 + O^3 + h^2 O^2) + \sum_{l_j=1}^{L_j-1} \sum_{i=1}^m n_{jl_j i}^* \cdot O^2] \right) = O(m).$$

I Extension to Three Non-Gaussian Observed Data Types

Earlier on, we have only considered Gaussian observed data under all our three modeling frameworks (Sections 2 and 3). As we shall see in this section, our models can be conveniently extended to accommodate three non-normal observed data types – ‘**tobit**’, ‘**probit**’, and ‘**binomial**’, which can all still lead to Gaussian kernels. All we need to add is an extra `SampleY()` step sampling transformed normal response variables from our original observed non-normal data and based on our current posterior parameter estimates at the start of each MCMC iteration in the Gibbs samplers (Appendix A). After obtaining a model fit object, we shall also modify the corresponding portions calculating our diagnostics metrics and making both in-sample and out-of-sample predictions, which all turn out to be quite straightforward.

The first two non-Gaussian observed data types are simply defined based on some original normal distributions. A ‘**tobit**’ variable is obtained from a normally distributed instance that is set to 0 if negative and kept as it is otherwise. A ‘**probit**’ instance is set to 0 if the original normal value is non-positive and set to 1 otherwise. The `SampleY()` steps corresponding to these two data types are hence quite straightforward. For an observed value of 0 corresponding to either data type and for a ‘**probit**’ observed value of 1, we sample a transformed response variable from the truncated normal distribution with our current mean and variance posterior estimates left-censored and right-censored at 0 respectively. When making predictions for a certain outcome variable based on a fitted model, we first obtain a predicted transformed response as in the baseline ‘**normal**’ case and then set the counterpart predicted original response to be 0 or 1 if needed. When calculating log likelihoods for certain diagnostics metrics, we take note that the ‘**tobit**’ distribution is a rectified Gaussian distribution (a half-half mixture of a point mass at 0 and the positive portion of a normal distribution, which is neither discrete nor continuous), and that ‘**probit**’ is a discrete distribution with discontinuity points 0 and 1.

We now consider binomial observed data $y_t(\mathbf{s}_{i,o}) \sim \text{Binomial}(n_t(\mathbf{s}_{i,o}), \pi_t(\mathbf{s}_{i,o}))$, $(i, o, t) \in \{1, \dots, m\} \times \{1, \dots, O\} \times \{1, \dots, T\}$, where $n_t(\mathbf{s}_{i,o})$'s are the pre-specified numbers of trials. Following Berchuck et al. 2022's idea, we accommodate the binomial likelihood by extending Equation (2.1) to the general modeling framework³

$$y_t(\mathbf{s}_{i,o}) | \vartheta_t(\mathbf{s}_{i,o}), \zeta_t(\mathbf{s}_{i,o}) \stackrel{\text{ind}}{\sim} f(y_t(\mathbf{s}_{i,o}); g^{-1}(\vartheta_t(\mathbf{s}_{i,o})), \zeta_t(\mathbf{s}_{i,o})) \quad (\text{I.1})$$

$$\vartheta_t(\mathbf{s}_{i,o}) = \mathbf{x}_t(\mathbf{s}_{i,o})^\top \boldsymbol{\beta} + \sum_{j=1}^k \lambda_j(\mathbf{s}_{i,o}) \eta_{tj}$$

$$\forall (i, o, t) \in \{1, \dots, m\} \times \{1, \dots, O\} \times \{1, \dots, T\},$$

³ Note that for the Gaussian specification, g is the identity link and f is Gaussian with mean $\mu_t(\mathbf{s}_{i,o}) = g^{-1}(\vartheta_t(\mathbf{s}_{i,o})) = \vartheta_t(\mathbf{s}_{i,o})$ and variance (nuisance) $\zeta_t(\mathbf{s}_{i,o}) = \sigma^2(\mathbf{s}_{i,o})$.

where g is the logit link ($\zeta_t(\mathbf{s}_{i,o})$ is null) and f is binomial with probability $\pi_t(\mathbf{s}_{i,o}) = g^{-1}(\vartheta_t(\mathbf{s}_{i,o})) = \frac{e^{\vartheta_t(\mathbf{s}_{i,o})}}{1+e^{\vartheta_t(\mathbf{s}_{i,o})}} \in (0, 1)$. Our joint data likelihood is hence

$$\begin{aligned} f(\mathbf{y}|\boldsymbol{\vartheta}, \mathbf{n}) &= \prod_{t=1}^T \prod_{o=1}^O \prod_{i=1}^m \left(\frac{e^{\vartheta_t(\mathbf{s}_{i,o})}}{1+e^{\vartheta_t(\mathbf{s}_{i,o})}} \right)^{y_t(\mathbf{s}_{i,o})} \left(\frac{1}{1+e^{\vartheta_t(\mathbf{s}_{i,o})}} \right)^{n_t(\mathbf{s}_{i,o})-y_t(\mathbf{s}_{i,o})} \\ &= \prod_{t=1}^T \prod_{o=1}^O \prod_{i=1}^m \frac{\exp\{\vartheta_t(\mathbf{s}_{i,o})y_t(\mathbf{s}_{i,o})\}}{(1+\exp\{\vartheta_t(\mathbf{s}_{i,o})\})^{n_t(\mathbf{s}_{i,o})}}. \end{aligned} \quad (\text{I.2})$$

Directly proceeding with Equation (I.2), however, would be computationally prohibitive due to most parameters' loss of conjugacy. Hence, Berchuck et al. (2022) introduced Pólya-Gamma (PG) augmented parameters $\omega_t(\mathbf{s}_{i,o}) \stackrel{\text{ind}}{\sim} \text{PG}(n_t(\mathbf{s}_{i,o}), 0)$ so that

$$f(\mathbf{y}, \boldsymbol{\omega}|\boldsymbol{\vartheta}, \mathbf{n}) = \prod_{t=1}^T \prod_{o=1}^O \prod_{i=1}^m \left[\frac{\exp\{\vartheta_t(\mathbf{s}_{i,o})y_t(\mathbf{s}_{i,o})\}}{(1+\exp\{\vartheta_t(\mathbf{s}_{i,o})\})^{n_t(\mathbf{s}_{i,o})}} \right] \times f(\omega_t(\mathbf{s}_{i,o})|\vartheta_t(\mathbf{s}_{i,o}), n_t(\mathbf{s}_{i,o})) \quad (\text{I.3})$$

$$\begin{aligned} &\propto \prod_{t=1}^T \prod_{o=1}^O \prod_{i=1}^m \left[\frac{\exp\{\vartheta_t(\mathbf{s}_{i,o})y_t(\mathbf{s}_{i,o})\}}{(1+\exp\{\vartheta_t(\mathbf{s}_{i,o})\})^{n_t(\mathbf{s}_{i,o})}} \right] \exp\left\{-\frac{\vartheta_t^2(\mathbf{s}_{i,o})\omega_t(\mathbf{s}_{i,o})}{2}\right\} \left(\frac{1+\exp\{\vartheta_t(\mathbf{s}_{i,o})\}}{2\exp\{\vartheta_t(\mathbf{s}_{i,o})/2\}}\right)^{n_t(\mathbf{s}_{i,o})} \\ &\propto \prod_{t=1}^T \prod_{o=1}^O \prod_{i=1}^m \exp\left\{-\frac{\omega_t(\mathbf{s}_{i,o})}{2} [y_t^*(\mathbf{s}_{i,o}) - \vartheta_t(\mathbf{s}_{i,o})]^2\right\}, \end{aligned} \quad (\text{I.4})$$

where $y_t^*(\mathbf{s}_{i,o}) = \frac{\chi_t(\mathbf{s}_{i,o})}{\omega_t(\mathbf{s}_{i,o})}$ with $\chi_t(\mathbf{s}_{i,o}) = y_t(\mathbf{s}_{i,o}) - \frac{n_t(\mathbf{s}_{i,o})}{2} \forall (i, o, t)$. This transformed kernel is now Gaussian and conjugacy has thus been introduced.

Equation (I.4) suggests that $\sigma^2(\mathbf{s}_{i,o})$'s are no longer needed and the corresponding Gibbs sampler step can thus be removed. Instead, we add at the beginning of each MCMC iteration a step sampling the augmented PG parameters $\omega_t(\mathbf{s}_{i,o})$'s from their full conditional distributions $\omega_t(\mathbf{s}_{i,o}) \sim \text{PG}\left(n_t(\mathbf{s}_{i,o}), \mathbf{x}_t(\mathbf{s}_{i,o})^\top \boldsymbol{\beta} + \sum_{j=1}^k \lambda_j(\mathbf{s}_{i,o})\eta_{tj}\right) \forall (i, o, t)$. $y_t(\mathbf{s}_{i,o})$'s can then be transformed to $y_t^*(\mathbf{s}_{i,o})$'s accordingly in the `SampleY()` step. We should also replace $\sigma^2(\mathbf{s}_{i,o})$'s by $\frac{1}{\omega_t(\mathbf{s}_{i,o})}$'s in all other concerned Gibbs sampler steps, i.e., the steps sampling $\boldsymbol{\eta}$'s, $\boldsymbol{\beta}$, and $\boldsymbol{\lambda}_j$'s or $\xi_j(\mathbf{s}_{i,o})$'s, θ_{jl} 's. When calculating a log likelihood for $y_t(\mathbf{s}_{i,o})$ or obtaining an in-sample prediction $\hat{y}_t(\mathbf{s}_{i,o})$ for any arbitrary $(i, o, t) \in \{1, \dots, m\} \times \{1, \dots, O\} \times \{1, \dots, T\}$ based on a fitted model, we first calculate $\hat{\pi}_t(\mathbf{s}_{i,o}) = \frac{e^{\hat{\vartheta}_t(\mathbf{s}_{i,o})}}{1+e^{\hat{\vartheta}_t(\mathbf{s}_{i,o})}} \in (0, 1)$ from our posterior mean estimate $\hat{\vartheta}_t(\mathbf{s}_{i,o})$ and then proceed according to $y_t(\mathbf{s}_{i,o})$'s distribution Binomial($n_t(\mathbf{s}_{i,o}), \hat{\pi}_t(\mathbf{s}_{i,o})$). Out-of-sample predictions are similar to in-sample predictions in this case.

References

- Berchuck, Samuel I., Mark Janko, Felipe A. Medeiros, William Pan, and Sayan Mukherjee (2022). "Bayesian Non-Parametric Factor Analysis for Longitudinal Spatial Surfaces". In: *Bayesian Analysis* 17.2, pp. 435–464. DOI: [10.1214/20-BA1253](https://doi.org/10.1214/20-BA1253). arXiv: [1911.04337](https://arxiv.org/abs/1911.04337).
- Bhattacharya, A. and D. B. Dunson (2011). "Sparse Bayesian infinite factor models". In: *Biometrika* 98.2, pp. 291–306. ISSN: 00063444. DOI: [10.1093/biomet/asr013](https://doi.org/10.1093/biomet/asr013).
- Christensen, W. F. and Y. Amemiya (2002). "Latent variable analysis of multivariate spatial data". In: *Journal of the American Statistical Association* 97.457, pp. 302–317. ISSN: 01621459. DOI: [10.1198/016214502753479437](https://doi.org/10.1198/016214502753479437).

- Datta, Abhirup, Sudipto Banerjee, Andrew O. Finley, and Alan E. Gelfand (2016). “Hierarchical Nearest-Neighbor Gaussian Process Models for Large Geostatistical Datasets”. In: *Journal of the American Statistical Association* 111.514, pp. 800–812. ISSN: 1537274X. DOI: [10.1080/01621459.2015.1044091](https://doi.org/10.1080/01621459.2015.1044091). arXiv: [1406.7343](https://arxiv.org/abs/1406.7343).
- De Iorio, Maria, Stefano Favaro, Alessandra Guglielmi, and Lifeng Ye (2023). “Bayesian non-parametric mixture modeling for temporal dynamics of gender stereotypes”. In: *Annals of Applied Statistics* 17.3, pp. 2256–2278. ISSN: 19417330. DOI: [10.1214/22-AOAS1717](https://doi.org/10.1214/22-AOAS1717).
- Finley, Andrew O., Abhirup Datta, and Sudipto Banerjee (2022). “spNNGP R Package for Nearest Neighbor Gaussian Process Models”. In: *Journal of Statistical Software* 103.5, pp. 1–40. ISSN: 15487660. DOI: [10.18637/jss.v103.i05](https://doi.org/10.18637/jss.v103.i05). arXiv: [2001.09111](https://arxiv.org/abs/2001.09111).
- Finley, Andrew O., Abhirup Datta, Bruce D. Cook, Douglas C. Morton, Hans E. Andersen, and Sudipto Banerjee (2019). “Efficient Algorithms for Bayesian Nearest Neighbor Gaussian Processes”. In: *Journal of Computational and Graphical Statistics* 28.2, pp. 401–414. ISSN: 15372715. DOI: [10.1080/10618600.2018.1537924](https://doi.org/10.1080/10618600.2018.1537924). arXiv: [1702.00434](https://arxiv.org/abs/1702.00434).
- Hu, Guanyu, Junxian Geng, Yishu Xue, and Huiyan Sang (2023). “Bayesian Spatial Homogeneity Pursuit of Functional Data: An Application to the U.S. Income Distribution”. In: *Bayesian Analysis* 18.2, pp. 579–605. ISSN: 19316690. DOI: [10.1214/22-BA1320](https://doi.org/10.1214/22-BA1320).
- Jensen, Mark J. and John M. Maheu (2013). “Bayesian semiparametric multivariate GARCH modeling”. In: *Journal of Econometrics* 176.1, pp. 3–17. ISSN: 03044076. DOI: [10.1016/j.jeconom.2013.03.009](https://doi.org/10.1016/j.jeconom.2013.03.009).
- Katzfuss, Matthias and Joseph Guinness (2021). “A General Framework for Vecchia Approximations of Gaussian Processes”. In: *Statistical Science* 36.1, pp. 124–141. ISSN: 21688745. DOI: [10.1214/19-STS755](https://doi.org/10.1214/19-STS755).
- Mozdzen, Alexander, Andrea Cremaschi, Annalisa Cadonna, Alessandra Guglielmi, and Gregor Kastner (2022). “Bayesian modeling and clustering for spatio-temporal areal data: An application to Italian unemployment”. In: *Spatial Statistics* 52. ISSN: 22116753. DOI: [10.1016/j.spasta.2022.100715](https://doi.org/10.1016/j.spasta.2022.100715).
- Ren, Qian and Sudipto Banerjee (2013). “Hierarchical Factor Models for Large Spatially Misaligned Data: A Low-Rank Predictive Process Approach”. In: *Biometrics* 69.1, pp. 19–30. ISSN: 0006341X. DOI: [10.1111/j.1541-0420.2012.01832.x](https://doi.org/10.1111/j.1541-0420.2012.01832.x).
- Rodríguez, Abel and David B. Dunson (2011). “Nonparametric Bayesian models through probit stick-breaking processes”. In: *Bayesian Analysis* 6.1. ISSN: 19360975. DOI: [10.1214/11-BA605](https://doi.org/10.1214/11-BA605).
- Sethuraman, J. (1994). “A constructive definition of Dirichlet priors”. In: *Statistica Sinica* 4.2, pp. 639–650. URL: <http://www.jstor.org/stable/24305538>.
- Spiegelhalter, David J., Nicola G. Best, Bradley P. Carlin, and Angelika Van Der Linde (2002). “Bayesian measures of model complexity and fit”. In: *Journal of the Royal Statistical Society. Series B: Statistical Methodology* 64.4. ISSN: 13697412. DOI: [10.1111/1467-9868.00353](https://doi.org/10.1111/1467-9868.00353).
- Vecchia, A. V. (1988). “Estimation and Model Identification for Continuous Spatial Processes”. In: *Journal of the Royal Statistical Society: Series B (Methodological)* 50.2, pp. 297–312. DOI: [10.1111/j.2517-6161.1988.tb01729.x](https://doi.org/10.1111/j.2517-6161.1988.tb01729.x).

- Vehtari, Aki, Andrew Gelman, and Jonah Gabry (2017). “Practical Bayesian model evaluation using leave-one-out cross-validation and WAIC”. In: *Statistics and Computing* 27.5. ISSN: 15731375. DOI: [10.1007/s11222-016-9696-4](https://doi.org/10.1007/s11222-016-9696-4).
- Virbickaite, Audrone, M. Concepción Ausín, and Pedro Galeano (2015). “Bayesian inference methods for univariate and multivariate garch models: A survey”. In: *Journal of Economic Surveys* 29.1, pp. 76–96. ISSN: 14676419. DOI: [10.1111/joes.12046](https://doi.org/10.1111/joes.12046). arXiv: [1402.0346](https://arxiv.org/abs/1402.0346).
- Walker, Stephen G. (2007). “Sampling the Dirichlet Mixture Model with Slices”. In: *Communications in Statistics: Simulation and Computation* 36.1, pp. 45–54. DOI: <https://doi.org/10.1080/03610910601096262>.
- Wall, Melanie M. and Xuan Liu (2009). “Spatial latent class analysis model for spatially distributed multivariate binary data”. In: *Computational Statistics and Data Analysis* 53.8, pp. 3057–3069. ISSN: 01679473. DOI: [10.1016/j.csda.2008.07.037](https://doi.org/10.1016/j.csda.2008.07.037).
- Yang, Daewon, Taeryon Choi, Eric Lavigne, and Yeonseung Chung (2022). “Non-parametric Bayesian covariate-dependent multivariate functional clustering: An application to time-series data for multiple air pollutants”. In: *Journal of the Royal Statistical Society. Series C: Applied Statistics* 71.5, pp. 1521–1542. ISSN: 14679876. DOI: [10.1111/rssc.12589](https://doi.org/10.1111/rssc.12589).
- Zhang, Bohai, Huiyan Sang, Zhao Tang Luo, and Hui Huang (2023). “Bayesian clustering of spatial functional data with application to a human mobility study during COVID-19”. In: *Annals of Applied Statistics* 17.1, pp. 583–605. ISSN: 19417330. DOI: [10.1214/22-AOAS1643](https://doi.org/10.1214/22-AOAS1643).